EPIGENETIC REGULATION IN CANCER AND DEVELOPMENT

by

THEODORE BUSBY III

QUAMARUL HASSAN, CHAIR
AMJAD JAVED
CHAD PETIT
THOMAS RYAN
RUI ZHAO

A DISSERTATION

Submitted to the graduate faculty of The University of Alabama at Birmingham
in partial fulfillment of the requirements for the degree of
Doctor of Philosophy

BIRMINGHAM, ALABAMA

2020

EPIGENETIC REGULATION IN CANCER AND DEVELOPMENT

THEODORE BUSBY III

BIOCHEMISTRY AND STRUCTURAL BIOLOGY

ABSTRACT

Feedback loops between cellular cues and changes in gene expression mediate the interactions between a multitude of regulatory events that promote development and cancer. Vesicular trafficking is an important process in carrying out signaling events by transporting receptors and ligands to and from the cell surface. GBF1 and BIG1 are large guanine-exchange factors (GEFs) that activate GTPase mediated shuttling of cargo through the Golgi apparatus. This dissertation demonstrates that GBF1 localizes to the cytoplasmic membrane in glioblastoma multiform cells to maintain cell shape and promote migration. Reports have shown that BIG1translocates to the nucleus is hepatocyte carcinoma cell lines in response to serum starvation. Evidence that BIG1 functions in the nucleus includes direct binding to Dpy30, a positive regulator of gene expression. Dpy30 is an integral subunit of the Set1-Mll Histone 3 Lysine 4 (H3K4) methyltransferase complex. Expression of Dpy30 and its binding partner Ash2l are both upregulated in cancer cells by the oncogenic transcription factor c-Myc. This dissertation dissects the role of Dpy30 hyperactivation in Myc-dependent cancers and identifies Dpy30 as a potential therapeutic target for certain cancers. Dpy30 inhibition leads to a decrease in chromatin accessibility around Myc target genes. This supports a mechanism for co-regulation between methyltransferase complexes and ATPase-dependent chromatin remodelers like the BAF complex. BAF complexes are large molecular machines comprised of 15 different subunits that have tissue and context specific

assemblies. This dissertation also shows that BAF45A, a subunit of the BAF complex, mediates chromatin accessibility and gene expression in mineralized tissues including osteoblasts of the bone and odontoblasts of the tooth. Collectively, this research draws a connection between multifactorial chromatin regulation and Golgi trafficking. In addition, these studies demonstrate the importance of dissecting novel cellular mechanisms for the purpose of developing efficient therapeutic strategies across different diseases.

Keywords: GBF1, Golgi apparatus, DPY30, H3K4me, BAF45A, chromatin remodeling

DEDICATION

This dissertation is dedicated to the Busby and Love family. I draw strength and perseverance from them to begin a tradition of raising leaders in STEM.

ACKNOWLEDGEMENTS

I would like to thank my mentor Quamarul Hassan. I appreciate your belief in me while giving me a chance to continue to grow and learn from you. I would not have been able to reach this accomplishment without you. I would also like to thank my lab members Tanner Godfrey, Benjamin Wildman, Yuechuan Chen, Ashlee Williams, and Delores Stacks. In addition, I thank previous lab members Mohammad Rehan, Parul Sarwalia, and Mahfujul Haq Khan. These have been excellent colleagues and have treated me like family while working closely with me to complete me graduate training. I would also like to thank Elizabeth Sztul and Hao Jiang for their mentorship and training that helped me to become the scientist that I am today. I would like to also thank for all their help and contributions for the GBF1 story Jay Batt, Justyna Meissner, and Eunjoo Lee. For the DPY30 story, a giant thanks to Ying Tusing, Wei Li, Kushani Shah, Zhenhua Zhang, and Jing Hu for all of their contributions and for pushing me to be the best that I could be. I would like to acknowledge all of our collaborators. First I would like to thank our collaborators for the BAF45A story: Amjad Javed, Burthia Booker, Harunur Rashid from UAB who provided help and guidance with in vivo and in vitro assays; Maria Johnson and Tim Nagy from the UAB Small Animal Phenotyping Core for the uCT analysis; Shon Soosman and the analysis team at Novogene for RNA-seq analysis; David Crossman from the Heflin Center for Genomic Sciences for help with ATAC-seq analysis. I would also like to thank collaborators for the Ash2l peptide story William Placzek, Robert Whitaker, Hayley Widden, and Ivis Chapel for peptide generation and

help in the small molecule screen; Maaike Everts from Alabama Drug Discovery Alliance (ADDA) as well as Mark Suto, Robert Bostwick, and Larry Ross from Southern Research Institute for the library of small molecule inhibitors and performing the primary screening assays. I would like to thank Rameeza Allie for helping me with flow cytometry. I would also like to acknowledge my committee members Chad Petit, Rui Zhao, Thomas Ryan, and Amjad Javed for their guidance and advice throughout my graduate training. A very special gratitude to Nicquet Blake, Debra Murray, Michael Bender, and Tracie Gibson for their mentorship, encouragement, and for being a foundation for me through all of the trials of becoming a scientist. I hope to be able to pay forward at least a fraction of what you all have done for young scientists like me.

I would like to most of all give thanks to my friends and family, new and old, for their support throughout the years. I thank my parents Theodore Busby Jr. and Shaneequa Busby; my brothers Thaddeus and Theloneas Busby; Andrea Howland and family; the Chisolm family Eugene, Ophelia, Eugenia, Yolanda, and Damian Chisolm; and as special thanks my best friend Danielle Chisolm.

TABLE OF CONTENTS

Page

LIST OF FIGURES

Figure Page

ALTERNATIVE FUNCTIONS OF LARGE VESICULAR TRAFFICKING PROTEINS OF THE GOLGI APPARATUS

THE ARF ACTIVATOR GBF1 LOCALIZES TO PLASMA MEMBRANE SITES INVOLVED IN CELL ADHESION AND MOTILITY

GBF1 REGULATES CELL SHAPE IN GBM CELLS

FUNCTIONAL ROLE OF DPY30 IN MYC-DRIVEN TUMORIGENESIS

LIST OF ABBREVIATIONS

AKAP	A-kinase anchoring protein 1
Ambn	ameloblastin
AMPK	AMP-activated protein kinase
ARF	ADP-ribosylation factor
Ash2l	absent, small, or homeotic 2-like
ATAC	assay for transposase accessible chromatin
Atf4	activating transcription factor 4
BFA	brefeldin A
BAF	BRG1 or BRM-associated factor
BET	Bromodomain and extra-terminal
BIG1	Brefeldin A-inhibited guanine nucleotide-exchange protein 1
Bre2	yeast homolog of Ash2l
CDK1	cyclin dependent kinase 1
ChIP	Chromatin immunoprecipitation
Co-IP	co-immunoprecipitation
COMPASS	Set1-Mll complex
DCB	dimerization and cyclophilin binding
Dmp1	dentin matrix acidic phosphoprotein 1

Dspp	dentin sialophosphoprotein
EGFR	epidermal growth factor receptor
Enam	enamelin
ER	endoplastic reticulum
EZH2	enhancer of zeste homolog 2
FPA	fluorescence polarization assay
GAP	GTPase-activating proteins
GBF1	golgi brefeldin A Resistant guanine nucleotide exchange factor 1
GEF	guanine nucleotide exchange factors
GPCR	G protein-coupled receptor
H3K4me	histone 3 lysine 4 methylation
H3K9ac	histone 3 lysine 9 acetylation
H3K9me	histone H3 lysine 9 methylation
H3K27ac	histone 3 lysine 27 acetylation
H3K27me	histone 3 lysine 27 methylation
Hox	homeobox
HUS	homology upstream of Sec7
IgH	immunoglobulin heavy locus
Klf4	Kruppel-like factor 4
MEF	mouse embryonic fibroblasts
MLL	mixed lineage leukemia
NURF	Nucleosome remodeling factor
Phf10	PHD finger protein 10

PIP	phosphatidylinositol phosphate
PRC2	polycomb repressive complex 2
qPCR	quantitative polymerase chain reaction
RbBP5	retinoblastoma-binding protein 5
RTK	receptor tyrosine kinase
Runx2	runt-related transcription factor 2
Sdc1	yeast homolog of Dpy30
SDI	Sdc interaction domain
Swi/Snf	switch/sucrose non-fermentable
Trr	trithorax-related
Trx	trithorax
Wdr5	WD repeat domain 5

CHAPTER 1

INTRODUCTION

Cellular cues converge to promote tissue specific gene expression and protein activity [1]. Differences in gene expression profiles from one cell type to the next are driven in part by the combined balance between activating and repressive histone modulators, transcription factors, and non-coding RNAs [2]. At the chromatin level, readers associate with epigenetic marks, writers post-translationally modify the histones, and erasers remove these histone marks [3-10]. To induce gene activation, chromatin remodelers loosen the DNA around histones, causing genes to be open and accessible to transcriptional machinery [2, 4, 11-14]. Many of these chromatin modulators, of each class, share overlapping functions but differ in their cell type and gene specific assembly of homologs. Although we understand that dynamic changes in gene expression and protein activity are important steps during differentiation and are corrupted during tumor formation, more nuanced mechanism have not been characterized in detail [15]. Examination of these specific mechanisms have been the focus of recent studies to develop novel therapeutics to a wide range of diseases [16].

BAF Chromatin Remodeling in Specific Tissue Types

Tissue development requires specific assemblies of chromatin modulators that undergo class switching at sequential stages of differentiation [2, 14]. The Brg1-associated factor (BAF), or mammalian Swi/Snf, chromatin remodeling complex is an ATPase-dependent epigenetic modulator that promotes active gene expression by sliding nucleosomes into an open confirmation around promoters [11-13]. Cell specific regulation by the BAF complex is mediated by the exact assembly of subunits [11, 12, 17]. This 2 MDa complex is comprised of 15 different subunits encoded by 29 different homologs [11, 12, 17]. Studies in neurons, immune cells, and embryonic stem cells highlight the importance of tissue specific BAF complex assemblies [11, 12, 18-21]. However, in-depth analysis of chromatin remodeling in tissue types derived from the mesenchyme like osteoblasts have been understudied [22-26]. Furthermore, mutations in BAF subunits have been associated with tumorigenesis, similar to what has been observed for other chromatin modulators.

SET1/MLL Histone Methyltransferase in Cancer

As with the BAF complex, the Set1-Mll complex is a chromatin modulator that promotes active gene expression by binding to the promoter region of genes to be transcribed. Set1-Mll complexes are the major H3K4 methylation enzymes in mammals [27-29]. Histone H3K4 methylation is a prominent epigenetic mark associated with active or poised transcription [29, 30] . Specific Set1-Mll complex subunit assemblies regulate different regions of the genome, similar to regulation by the BAF complex. Among these

subunits, the catalytic methyltransferase subunits have been found to be mutated in cancers. Malignancies of the hematopoietic system have been associated with chromosomal translocation between Mll genes and other transcriptional activators, resulting in Mll-rearranged leukemias. Mll-fusion proteins promote gene expression profiles conducive to growth and proliferation, which require the activity of fully functional intact Set1-Mll complexes. This has prompted investigations to determine how the wild type function of this methyltransferase complex becomes compromised during tumorigenesis. However, alteration of canonical protein activity in cancer cells is not restricted to gene regulators.

Golgi Associated Factors Respond to Specific Stimuli in Cancer

The Set1-Mll complex directly interacts with the Golgi associated protein BIG1 [31]. Previous research has shown that BIG1 translocates from the cytoplasm to the nucleus in hepatocyte carcinoma cells as a result of serum starvation [32, 33]. However, the connection between BIG1 and gene expression remains unidentified. BIG1 typically functions at the Golgi apparatus as an activating guanine-exchange factor (GEF) of the ARF family of Ras-GTPases in order to facility cargo trafficking through the secretory pathway [30, 34, 35]. GBF1 is another ARF-GEF that functions at the Golgi apparatus. In leukemia cells, GBF1 has been shown to translocate to the cytoplasmic membrane at the leading edge of migration during chemotaxis [36]. Although both GBF1 and BIG1 perform non-canonical activities in response to specific stimuli in cancer cells, they each must maintain function at the Golgi apparatus. Inhibition of either GEF leads to the collapse of the stacked structure of the Golgi into dispersed vesicles that begin to fuse

with the endoplasmic reticulum [37-39]. Although chemical inhibition of GBF1 and BIG is reversible with removal of inhibitors, sustained inhibition leads to cell death [37-39]. Thus, understanding cancer specific, non-canonical functions of proteins opens the door for discovering new therapeutic targets that may efficiently inhibit cancer cells in combination with previously established anti-cancer therapeutics.

Summary

This dissertation discusses ubiquitously expressed proteins that have well defined functions that exhibit cancer specific alternative function. Furthermore, this research examines chromatin regulation by non-catalytic subunits of large gene activating complexes. Chapters 2, 3, and 4 of this dissertation will show that the Golgi associated factor GBF1 localize to the leading edge cytoplasmic membrane of glioblastoma multiform cells and is important for maintaining cell shape. Chapters 5, 6, and 7 will cover the relationship between the SET1-MLL complex and the oncogenic transcription factor c-Myc during tumor formation. This study further showed that the SET1-MLL complex is a druggable target in Myc-dependent cancer cells. Chapters 8 and 9 will highlight a current story characterizing the importance of a BAF complex subunit that regulates gene expression in mineralized tissue.

CHAPTER 2

ALTERNATIVE FUNCTIONS OF LARGE VESICULAR TRAFFICKING PROTEINS OF THE GOLGI APPARATUS

Vesicle Trafficking Machinery of The Golgi Apparatus.

Secreted proteins undergo a maturation process in the lumen of the endoplasmic reticulum (ER) before being packaged into vesicles and transported from ER exit sites to be further processed in the lumen of the Golgi apparatus for trafficking to the endosomes [39-43]. Misfolded proteins and ER resident transport chaperones must also be packaged into vesicles to be trafficked back to the ER from the early Golgi [40]. ADP-Ribosylation Factor (ARF) GTPases, members of the Ras-family of small GTPases, are critical factors in vesicle formation, in addition to their roles as signal cascade intermediates [44]. These ARFs include Class 1 (Arf1 and Arf3), Class 2 (Arf4 and Arf5), Class 3 (Arf6), and over 20 ARF-like proteins, which have both overlapping and context specific functions [45, 46]. In addition to Golgi trafficking, ARFs are also important for shuttling vesicles between endosomal compartments and the cytoplasmic membrane [47]. ARF activity, like other GTPases, is regulated by activating guanine-nucleotide exchange factors (GEFs) and inactivating GTPase activating proteins (GAPs) [44-47]. Research in this dissertation focuses on the activating GEFs of these molecular switches.

Large ARF GEFs

The Sec7 domain family of ARF-GEF proteins stimulate the expulsion of GDP from inactive ARFs to allow ARFs to bind GTP in an active confirmation (Figure 1) [39, 41, 42, 48-50]. These activating GEFs are divided into two main classes, the 200kDa large GEFs (GBF1, BIG1, and BIG2) and the small GEFs (Cytohesin1-4, BRAG1-3, EFA6A-D, and FBX8) [51]. The large GEFs of not primarily function at the Golgi apparatus.

Brefeldin A-Inhibited Guanine Nucleotide-Exchange Proteins (BIGs) Function at The Trans-Golgi And in The Nucleus

BIG1 and BIG2 regulate vesicular trafficking between the Trans-Golgi Network (TGN) and the endosomal compartments (Figure 1) [34]. These GEFs facilitate vesicle formation by activating Arf4 and Arf5 (Figure 1 and Figure 2) [34, 44, 46]. Glutamic Acid and Alanine residues within the BIG1 and BIG2 Sec7 domain eject guanosine diphosphate (GDP) from inactive Arf4 and Arf5 to allow binding of guanosine triphosphate (GTP), subsequently activating the ARFs [34, 44, 46]. Additionally, BIG1 and BIG2 contain N-terminal DCB and HUS domains to mediate protein-protein interactions and four C-terminal HDS domains which facilitate membrane association (Figure 2) [32, 33, 51]. Signaling through protein kinase A (PKA) dependent pathways has been demonstrated to regulate BIG1 function and cellular localization [32, 33, 51]. However, there remains much to be learned about the mechanistic function of signal pathway integration to regulate BIG1 and BIG2 mediated trafficking. Previous studies

have shown that serum starvation of HepG2 hepatocyte carcinoma cells and activation of c-AMP dependent kinase (AMPK) pathways lead to translocation of BIG1 from the cytoplasm to the nucleus [32, 33, 51]. Furthermore, BIG1 has also been identified to interact with chromatin modulating complexes that localize to the nucleus [31]. Thus, BIG1 may function in the nucleus to regulate gene expression.

Golgi-Specific Brefeldin A-Resistance Guanine Nucleotide Exchange Factor 1 (GBF1) Mediates Trafficking at The Cis-Golgi

GBF1 is another member of the large Sec7d ARF-GEFs that predominantly localizes to the early Golgi compartments (Figure 1) [39, 41, 42]. At the early, cis-Golgi cisternae, GBF1 activation of Arf1 leads to the direct recruitment of COPI coatomers to nascent, cargo carrying vesicles to be trafficked in a retrograde direction to the ER (Figure 1) [39, 41, 42]. GBF1 also activates Arf4 and Arf5 at the late trans-Golgi network (TGN) to recruit BIG1 and BIG2 [34]. Another function of GBF1 is to maintain the dynamic, stacked structure of the Golgi apparatus [34]. The integrity of the Golgi structure is disrupted if GBF1 is inhibited by either RNAi, GolgicideA, or the fungal metabolite BrefeldinA (BFA) (Figure 3) [39, 41, 42, 52, 53]. Collapse of the Golgi was also observed when a dominant negative mutant of GBF1 is expressed in HeLa cells [51]. While GBF1 function has been extensively studied, the mechanisms that regulate GBF1 activation and inactivation are not well understood.

The large ARF-GEFs share structural homology. Similar to BIG1 and BIG2, GBF1 activates ARFs through the Sec7 domain (Figure 2) [39, 41, 42, 52, 53] [51].

Recent studies have shown that mutating Lysine 91 and Glutamic Acid 130 both to Alanine residues (K91A/E130A) within the DCB domain disrupts dimerization [51]. Unlike pharmacological inhibition, monomerization of GBF1 had no effect on the stability of the stacked nature of the Golgi apparatus [51]. Furthermore, monomeric GBF1 maintains the ability to localize to the Golgi membrane with increased affinity [51].

This information prompted investigation of the relationship between dimerization of GBF1 and its ability to activate ARFs [51]. Mutation of Glutamic Acid 794 to a Lysine (E794K) residue within the GBF1 Sec7 domain stabilizes GBF1 in an inactive confirmation with GDP-bound Arfs (Figure 3) [51]. As with BFA or GCA treatment, GBF1-E794K becomes locked onto the Golgi membrane causing the dynamic stacks to collapse into small vesicles (Figure 3) [51]. A triple mutant to block dimerization and trafficking (K91A/E130A/E794K) also caused the Golgi to disperse [51].

Monomerization of GBF1 does not rescue trafficking defects of the E794K mutant [51]. However, mutating the adjacent Alanine 795 to Glutamic acid (A795E) confers resistance to inhibition by BFA. Albeit moderate, monomerization of the BFA resistant GBF1 (K91A/E130A/A795E) demonstrated reduced function compared to BFA resistant GBF1 alone (795) [51]. This was in part due to a reduction in GBF1 protein stability [51]. Continued studies aim to understand the full range of GBF1 function at the Golgi membrane.

GBF1 Regulates Migration in Cancer Cells

Cancer cell survival and invasiveness are promoted by dysregulation of signal cascades that have also been shown to impact the activity of GBF1-substrate ARFs. For example, Arf4 is upregulated by the transcription factor CREB3 to promote breast cancer cell migration [54]. Arf4 also mediates migration in ovarian cancer cells by inducing endosomal traffic of alpha5beta1 integrins [47]. Though its activation is required for migration in certain cell types, Arf4 is inactivated at the gene level in migratory lymphoma B cells [55]. GBF1 also plays a role in cell motility in HeLa, D54 glioblastoma, and HL-60 leukemia cells [39, 41]. Chemotaxis in the leukemia cells leads to the recruitment of GBF1 to the leading-edge plasma membrane where it activates Arf1 (Figure 4) [36]. GBF1 associates with the plasma membrane by binding to PIP3 produced by PI3K in response to GPCR chemoreceptor activity [36]. Blocking GBF1 from binding to PIP3 at the plasma membrane impairs chemotaxis but does not affect GBF1 localization to the Golgi apparatus [36]. These studies suggest that specific stimuli promote non-canonical GBF1-dependent mechanisms.

Glioblastoma multiform (GBM) is the most common form of malignant brain cancer in adults with a median survival rate of one year [56]. These tumor cells metastasize by migrating on blood vessels to other regions of the brain [57]. One driver of invasive GBM is the epidermal growth factor receptor (EGFR) with a deletion of exons 2-7 (EGFRvIII) which leads to constitutive activation of EGF signaling [56, 57]. Furthermore, GBF1 depletion inhibits glioblastoma migration [39]. Thus, specific signaling events potentially drive different GBF1 mechanisms simultaneously to promote malignancies.

Signal Transduction and Regulation of Golgi Associated Factors

Growth factor-stimulated signal cascades have been shown to regulate GEFs through phosphorylation in order to modulate the activity of small GTPases. For example, the Rab8 activating GEF Rabin8 is phosphorylated by ERK1/2 in response to EGF stimulation [58]. Erk1/2 phosphorylation activates Rabin8 GEF function by releasing it from an auto-inhibitory confirmation to promote Rab8 mediated trafficking of vesicles to the cell surface via exocytosis. Related to this, GBF1 activity has been shown to be modified via kinase regulated events such as progression through the cell cycle and cellular stress. GBF1 has been shown to be phosphorylated by AMP-activated protein kinase (AMPK) at Threonine 1337, which leads to the disruption of the Golgi cisternae in the presence of AMPK activators [52, 59]. In addition, CDK1 phosphorylates GBF1 in mitosis, also causing disruption of the Golgi [53]. EGF-stimulation modulates the activity of the GBF1 substrate Arf4 to induce PLD2 activation and AP1-dependent transcription [60]. EGF-stimulation also leads to Arf1 activity to promote breast cancer cell migration [61]. For both Arf1 and Arf4, EGF-stimulation leads to the recruitment of these GTPases to the plasma membrane [60, 61]. However, the intermediate activating GEF for ARF1 and ARF4 in response to EGF-dependent activation is unknown. EGF-dependent signaling, like that of GPCR activation in leukemia cells, also activates PI3K and has been identified as an inducer of GBF1 hyper-phosphorylation [36]. Therefore, it is possible that GBF1 is phosphorylated by an EGF-dependent pathway kinase to facilitate PIP3 binding at the plasma membrane. We hypothesized a model in which EGF-signaling activates PI3K to produce PIP3 for GBF1 docking at the plasma membrane (Figure 4). It is possible that EGF-signaling also activates a protein kinase that

phosphorylates GBF1 in order to facilitate PIP3 docking and activation of Arf-GTPases at the plasma membrane (Figure 4). The answers to these questions would expand our mechanistic knowledge of these large Arf activating GEFs.

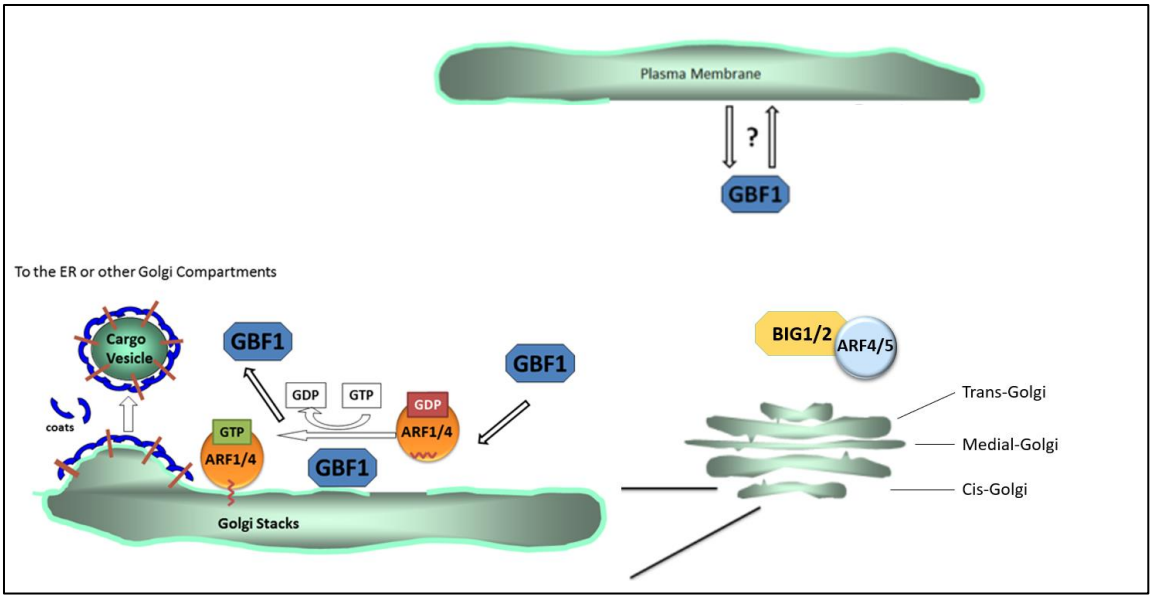

Figure 1. GBF1 catalyzes the nucleotide exchange of Arf-GTPases to facilitate vesicular traffic at the Golgi membrane. GBF1 dynamic association with the Golgi membrane recruits coat proteins to nascent vesicles formed at the cis-Golgi. At the Trans-Golgi, GBF1 recruits Arf4 and Arf5 with BIG1 and BIG2. GBF1 also localizes to the cytoplasmic membrane.

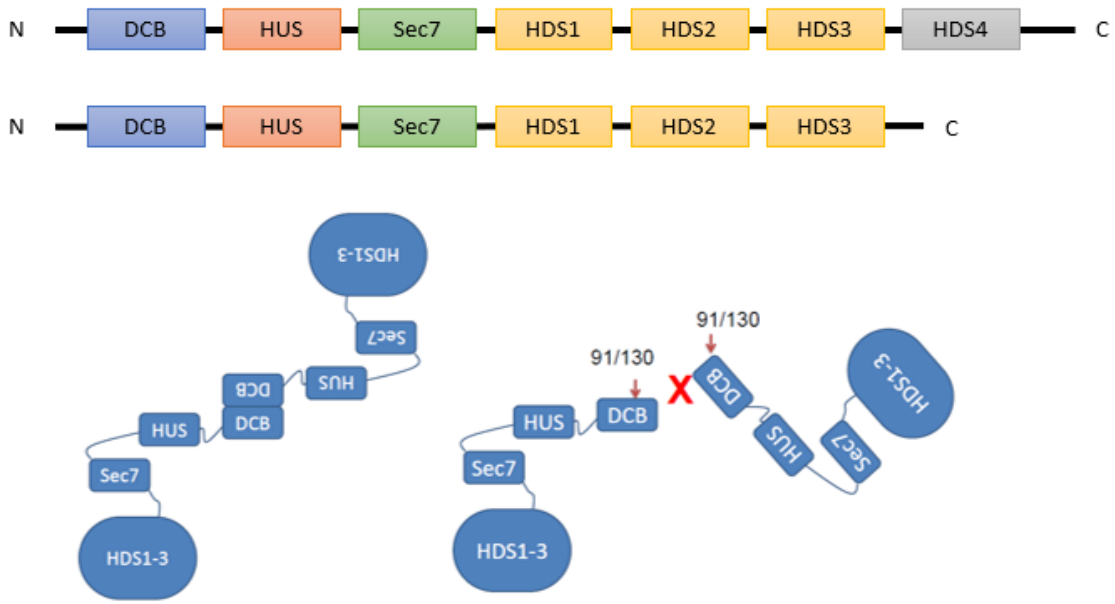

Figure 2. (A.) Domain layout of the large ARF activating GEFs BIG1, BIG2 and GBF1. (B.) The N-terminal DCB domain of GBF1 is responsible for dimerization. Wild-type and monomeric K91A/E130A mutant were analyzed on blue native gels. 91/130 migrates as a monomer and wt GBF1 as a dimer.

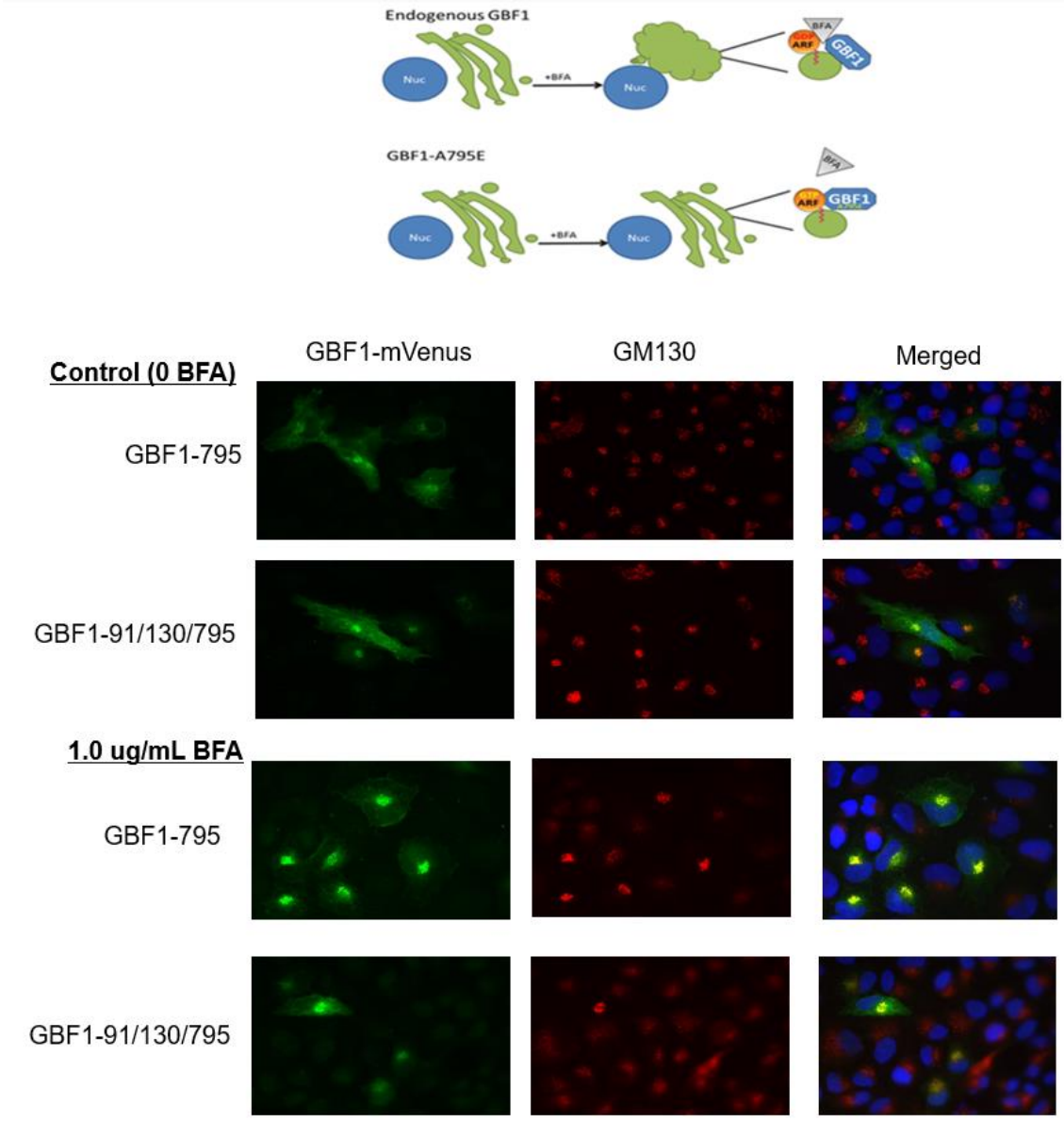

Figure 3. (A.)The fungal metabolite Brefeldin A (BFA) locks GBF1 in an inactive complex with Arf-GDP on the Golgi membrane leading to the dispersion of the Golgi stacks. (B.)The BFA resistant GBF1 A795E mutation rescues the Golgi structure.

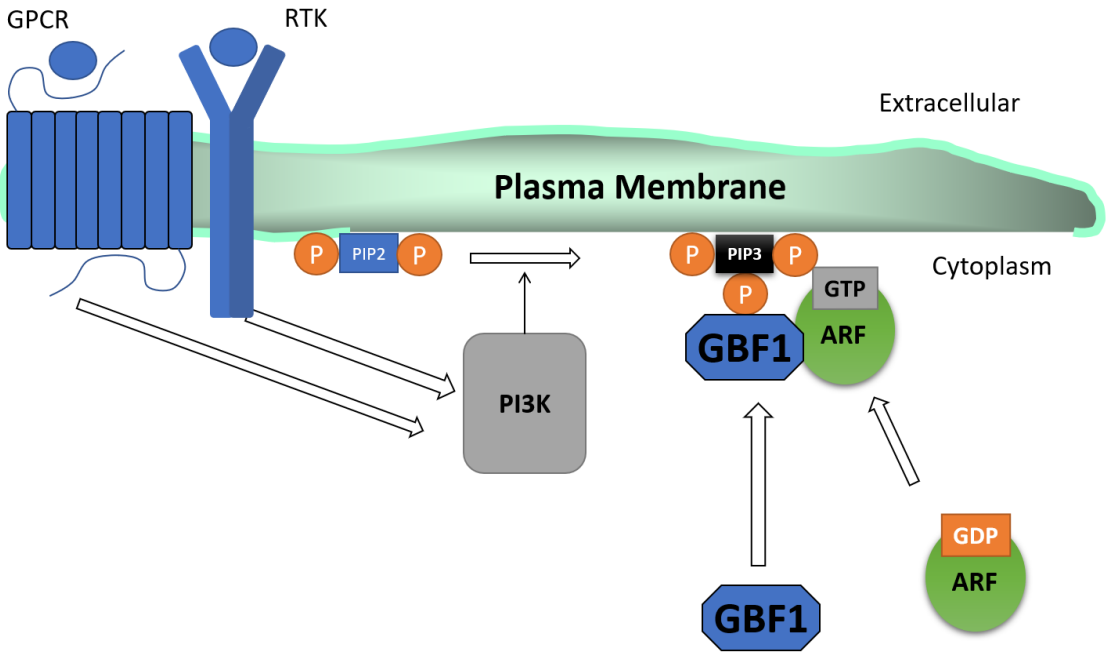

Figure 4. Chemotactic factors induce GBF1 activation of Arf-GTPases at the plasma membrane in glioblastoma cells .

THE ARF ACTIVATOR GBF1 LOCALIZES TO PLASMA MEMBRANE SITES INVOLVED IN CELL ADHESION AND MOTILITY

by

THEODORE BUSBY, JUSTYNA M. MEISSNER, MELANIE L. STYERS, JAY BHATT, AKHIL KAUSHIK, ANITA B. HJELMELAND & ELIZABETH SZTUL

Cellular Logistics Theodore Busby, Justyna M. Meissner, Melanie L. Styers, Jay Bhatt, Akhil Kaushik, Anita B. Hjelmeland & Elizabeth Sztul. The Arf activator GBF1 localizes to plasma membrane sites involved in cell adhesion and motility. *Cellular Logistics*. 2: p. e1308900, 2017.

CHAPTER 3

THE ARF ACTIVATOR GBF1 LOCALIZES TO PLASMA MEMBRANE SITES INVOLVED IN CELL ADHESION AND MOTILITY.

Introduction

GBF1 is ubiquitously expressed in eukaryotic cells and is essential for cellular and organismal life. Depletion of GBF1 from cultured cells induces apoptosis, while mouse GBF1 knockout and *D. melanogaster* knockout of GARZ (the fly GBF1 ortholog) cause embryonic lethality [1,2]. Silencing GARZ in only the salivary glands leads to severely stunted and disorganized glands, with disorganized lumens and dramatic disorganization of the actin cytoskeleton of the epithelial salivary cells [3].

GBF1 belongs to a sub-family of 3 large guanine-exchange factors (GEFs), 200 kDa each, within a 15-member family of ARF-GTPase activators [4,5]. The large GEFs, that include GBF1, BIG1 and BIG2, are only encoded in eukaryotic genomes, consistent with their fundamental roles in organellogenesis and membrane trafficking. All large GEFs are inhibited by the fungal metabolite Brefeldin A (BFA), a feature that distinguishes them from the other ARF GEFs.

GBF1 regulates membrane trafficking at the ER-Golgi interface and is the only GEF capable of sustaining ARF activation required for the recruitment of the COPI coat [6-11]. Inactivation of GBF1 through mutation of the catalytic Sec 7-domain or BFA treatment leads to the dissociation of COPI from membranes, the collapse of the Golgi

into the ER, and inhibition of trafficking through the secretory pathway. Previous research from our group and others have shown that in fibroblastic cells such as HeLa, GBF1 is mostly (~90%) cytosolic, with the remaining ~10% localized to the Golgi complex [9,12]. The 2 populations exist in equilibrium and GBF1 cycles between cytosol and Golgi membranes with rapid turnover [12,13]. Immunofluorescence and electron microscopy Immunogold analyses of cells in culture and tissues indicate that GBF1 is concentrated at the Golgi complex, with a preferred localization to the cis- face of the Golgi stack [14].

In addition to the well-documented localization and function of GBF1 at the Golgi, GBF1 was also detected within ~100 nm proximity to the plasma membrane in *D. melanogaster* S2RC cells, and was essential for constitutive fluid-phase endocytosis from the cell surface in a process that is dependent on active Actin remodeling [15]. Furthermore, GBF1 has been detected at the leading edge in HL60 neutrophils stimulated with N-formyl-methionyl-leucyl-phenylalanine (fMLP) [16]. Specifically, fMLP binding to G-Protein Coupled Receptors (GPCRs) leads to the recruitment and stimulation of Phosphatidyl Inositol 3-Kinase g (PI3Kg). The PI3Kg–mediated production of Phosphatidyl Inositol 3-Phosphates (PIP3s) at the leading edge then facilitates GBF1 recruitment. PI3Kg activity is essential for GBF1 recruitment as inactivation of PI3Kg either with the drug AS-604850 or by siRNA-mediated knockdown blocked fMLP-induced GBF1 localization to the leading edge. Importantly, the plasma membrane recruitment of GBF1 was observed only in HL60 cells stimulated with fMLP, while GBF1 was found exclusively at the Golgi in non-stimulated cells.

One of the key characteristics of stimulated HL60 cells is the establishment of directional polarity, suggesting that GBF1 recruitment to the plasma membrane may occur in other cells that exhibit directional motility or extrude directional processes. This model predicts that in cells that exhibit strong polarized architecture, GBF1 might localize to plasma membrane domains independent of acute chemotactic stimulation. Thus, we examined GBF1 localization in cell lines derived from human glioblastomas (GBM), focusing on the possible recruitment of GBF1 to the plasma membrane regions specialized for adhesion and/or migration.

Results

Endogenous GBF1 Localizes to The Golgi And Cell Protrusions in GBM Cells

We used immunofluorescence to compare the localization of endogenous GBF1 in HeLa cells and in three cell lines derived from human glioblastomas (WHO grade IV astrocytoma), specifically D54, U87 and U251. Previous research has shown GBF1 localization at the Golgi in all cells examined to date [6-8,17]. Consistent with these findings, we detected GBF1 in a peri-nuclear region where it co-localized with the cis-Golgi marker GM130 in HeLa (Fig. 1A) and U87 (Fig. 1B) cells. In U87 cells, GBF1 staining was also evident at the plasma membrane (PM), specifically at the tips of extensions (Fig. 1B, arrows). In contrast, GM130 was not detected at the PM, suggesting that GBF1 location is specific for this cellular component and does not represent a general relocation of Golgi proteins.

To determine if GBF1 localization to the PM was specific to the U87 cell line, we also examined GBF1 distribution in D54 and U251 cells. As shown in Fig. 1C, GBF1 was readily detected in a peri-nuclear region consistent with Golgi localization in all cells. However, GBF1 was also visible at tips of cellular extensions in cells with spindle-like architecture or containing multiple long extensions, and at the leading edge in cells with more compact architecture (arrows). All cells with clearly extended protrusions contained GBF1 at the tips of such extensions, confirming the generality of this observation. These cells were grown in normal culture medium and were not treated with chemotactic stimuli, suggesting that GBF1 may be recruited to the PM in response to growth factors from the medium or in response to cell secreted signaling molecules.

The same Golgi and peripheral staining were observed with polyclonal anti-GBF1 antibodies raised in rabbits (Fig. 1B), as with monoclonal affinity-purified anti-GBF1 antibodies raised in mice (Fig. 1C). To further ascertain the specificity of the GBF1 signal, we performed an antigen-inhibition study. His-tagged full length GBF1 was expressed in HEK293 cells and purified by affinity adsorption on Ni-Agarose beads. The isolation protocol generated an enriched fraction of GBF1, as evident by Coomassie Blue staining of an SDS-PAGE gel (Fig. 2A, lane 4). As a control, analogous purification protocol was performed from cells not transfected with His-GBF1, and the material eluted from the Ni-agarose beads represents the control eluate (lane 8). Purified GBF1 or the control eluate were preincubated with monoclonal anti-GBF1 antibodies, and such antibodies were subsequently used for IF on U87 cells. While a GBF1 signal was detected at the Golgi and at the tips of cellular extensions when IF was done with antibodies pre-incubated with the control eluate (Fig. 2B), no visible Golgi or peripheral

signal was detected when IF was done with antibodies presorbed with purified GBF1 (Fig. 2C). Antigen competition results strongly suggest that the IF signal observed with the anti-GBF1 antibodies is specific.

Endogenous GBF1 Co-Localizes With Cellular Adhesion Proteins

Tips of cellular protrusions and the leading edge are areas of substrate adhesion that allow cells to extend processes by tethering their PM to components of the extracellular matrix. Migration and extension of cellular processes occurs in response to extracellular signals and is mediated by localized actin polymerization. This propels the extension of lamellipodia and necessitates the formation of focal adhesions to anchor the newly formed protrusions. Focal adhesions are foci of functional linkage between the extracellular matrix and the actin cytoskeleton. The bridging function is provided by integrins, heterodimeric transmembrane proteins that bind matrix components through their extracellular domains and interact with cytosolic focal adhesion proteins through their cytoplasmic tails [18-20] One of the key components of focal adhesions is Alpha-actinin, which binds both integrins and actin filaments to directly link the cytoplasmic tails of integrins to the actin cytoskeleton [21]. Alpha-actinin is a homodimer that bundles Actin filaments to increase the stiffness of stress fibers originating from focal adhesions. Focal adhesions are also enriched with Paxillin that directly binds to integrins and recruits Vinculin, which in turn, directly interacts with Actin filaments to facilitate the stabilization of focal adhesions.

Thus, we examined whether the surface localized GBF1 colocalized with these adhesion proteins. As shown in Fig. 3, endogenous GBF1 was concentrated at regions

enriched in alpha-actinin (A) and vinculin (B) and was largely absent from other domains of the cell surface (arrows). Focal adhesions and the leading edge of cells are enriched in actin filaments that can be selectively visualized with phalloidin, a bicyclic heptapeptide that binds and stabilizes filamentous actin (F-actin) and prevents the depolymerization of actin fibers [22,23]. As shown in Fig. 3C, endogenous GBF1 was concentrated at the leading edge as determined by enriched phalloidin staining (arrows).

Exogenously Expressed GBF1 is Recruited to Adhesion Sites

As GBF1 localization to adhesion sites has not been described previously to our knowledge, we sought to further ensure that the staining was not an artifact of antibody cross-reactivity. We therefore transfected glioblastoma cells with GFP-tagged GBF1 and assessed the localization of the construct with anti-GFP antibodies. In agreement with Golgi localization of endogenous GBF1 in all cells, GFP-GBF1 co-localized with the Golgi marker GM130 in D54 cells (Fig. 4A). In addition, and confirming results evaluating the localization of endogenous GBF1, the exogenously expressed GFP-GBF1 was detected at the tips of cellular extensions (arrows). Echoing the localization of endogenous GBF1 to protrusions in all examined cells, GFP-GBF1 also was detected at tips of protrusions in all transfected cells. These GBF1-containing foci represent adhesion sites, as shown by the co-localization of GFP-GBF1 with paxillin, a protein found in focal adhesions and other actin-rich structures such as peripheral ruffles, dorsal ruffles and invadopodia/podosomes (Fig. 4B). Analogous results were obtained in U87 cells expressing GFP-GBF1: the construct was detected at the Golgi where it co-localized with GM130 and also at the tips of cellular projections (Fig. 4C). The cell surface centers of

GFP-GBF1 represent adhesion sites as shown by their content of paxillin (Fig. 4D). Furthermore, we only observed staining at the Golgi and at the tips of cellular extensions in cells expressing GFP-GBF1, while untransfected cells had no visible signal. This indicates that the primary and secondary antibodies used in these IFs do not recognize any endogenous antigen that could generate a non-specific signal.

Taken together, our data show that both endogenous and exogenously expressed GBF1 show dual localization within glioblastoma cells, with a pool of GBF1 concentrated at the Golgi complex and another pool localized to cellular adhesion sites at the tips of PM protrusions and the leading edge.

Discussion

GBF1 and its orthologues have been shown to localize to the Golgi complex in all examined cells ranging from mammalian to *D. melanogaster* and *S. cerevisiae* [7, 8, 17, 24]. The Golgi localization is consistent with the well characterized role of GBF1 in COPI recruitment to membranes, a process essential for the formation of COPI vesicles and ER-Golgi traffic. The essential Golgi function of GBF1 is underscored by the collapse and disassembly of the Golgi and inhibition in membrane traffic when GBF1 is inactivated or depleted [10,24,25].

However, in the HL60 neutrophil cell line acutely stimulated with fMLP, GBF1 was recruited to the leading edge oriented toward the chemotactic stimulus and was required for directional motility [16]. Importantly, GBF1 was not detected at the plasma membrane in unstimulated HL60 cells, suggesting that only acute activation of surface

GPCRs results in GBF1 relocation. These data also suggested that GBF1 recruitment to the plasma membrane may be regulated by specific chemotactic stimuli.

In this dissertation chapter, we report that GBF1 is found at the leading edge and in adhesion sites in several human GBM cell lines. This supports previous research that has demonstrated that GBF1 localizes to the cell surface in migrating cancer cells [16]. Furthermore, this is in agreement with data in *Drosophila*, where GARZ (the fly GBF1) has been detected close to the cell surface (within ~100 nm) and facilitated fluid-phase pinocytosis in S2RC cells [15].

The potential functional relevance of GBF1 recruitment to adhesion sites in GBM cells remains to be determined, but it is possible that GBF1 directly or indirectly affects cell motility. This is consistent with our earlier finding that siRNA-mediated depletion of GBF1 from D54 cells inhibited the migratory potential of these cells [10]. However, in those experiments, depletion of GBF1 would affect GBF1 functions throughout the cell (at the Golgi and at adhesions) making it impossible to assign the motility defect as inhibition of GBF1 function in the cell periphery. GBF1 is a large multi-domain protein and could impact motility directly by providing a scaffolding function to organize proteins that regulate actin dynamics. Alternatively, GBF1 could function indirectly, by activating ARF, which then could directly impact motility. Activated ARF1 has been shown to recruit the RhoGap domain-containing protein, ARHGAP10, which modulates Cdc42 dynamics at the cell surface [26]. The exact role that GBF1 plays at the periphery of GBM cells and how GBF1 activity may contribute to GBM invasiveness remain to be determined.

GBF1 may affect actin dynamics and assembly, as suggested by our previous report that depletion of GARZ in salivary glands of *D. melanogaster* causes marked disruption of the actin network [3]. A putative function for GBF1 in actin dynamics is also supported by the described previously links between GEA1 and GEA2 (yeast orthologs of GBF1) and actin architecture in *S. cerevisiae* [27]. First, GEA1 and GEA2 were identified as multicopy suppressors of Profilin deletion that could rescue the disassembly of actin cables and the lack of polarized actin cortical patches in *S. cerevisiae* lacking Profilin. Second, cells deleted of GEA2 and expressing inactive mutant alleles of GEA1 were defective in actin cytoskeleton and budding (an actin-dependent process). Third, overexpression of GEA1 or GEA2 in wild-type cells increased the appearance of actin cable-like structures. However, the mechanisms through which GEA1 and GEA2 influence actin dynamics remain to be determined.

Precise regulation of actin and focal adhesion dynamics is required for cell migration during normal physiological processes such as developmental morphogenesis, but it also contributes to pathologies by increasing the invasive potential of cancer cells. Glioblastoma multiform is the most common and aggressive primary brain cancer in adults. Glioblastoma multiform remains a lethal disease due in part to the ability of these cells to infiltrate healthy brain tissue making surgical removal of all tumor cells impossible. GBM cells form PM protrusions and invadopodia to facilitate cell-cell interactions and motility. Our finding that GBF1 is concentrated at adhesion sites in GBM cells raises the possibility that it might be involved in processes regulating actin dynamics at those sites and, consequently, may be fundamentally involved in the invasive capacity of GBM cells.

GBF1 joins an ever-increasing number of proteins with multiple cellular localizations and functions. Such "moonlighting" proteins are exemplified by ARF-like 2 (ARL2), which regulates both mitochondrial fusion and microtubule dynamics [28-30]. Orc6 which participates in DNA replication and cytokinesis [31-34] and the Exocyst complex which facilitates polarized deliver of secretory cargoes as well as regulates actin dynamics [35-37]. It is likely that such functional duality reflects the cellular need for coordination since the utilization of a single protein in multiple processes provides a mechanism for cross-talk and coordination of distinct cellular responses.

Materials and Methods

Antibodies

The following antibodies were commercially obtained: rabbit polyclonal anti-GFP (Abcam, Ab290), mouse monoclonal affinity- purified anti-GBF1 (BD Bioscience, 612116; this antibody detected a single band on Western blots), mouse monoclonal affinity purified anti-GM130 (BD Transduction Laboratories, 610823), mouse monoclonal anti-paxillin (ThermoFisher, AHO0492), mouse monoclonal anti-vinculin (Abcam, Ab18058) and mouse monoclonal anti-a-actinin (Abcam, Ab18061). Polyclonal anti GM130 were raised in a rabbit and have been described previously [38]. Secondary anti-rabbit or anti-mouse antibodies conjugated with Alexa 488 or Alexa 594 were obtained from Invitrogen (A11001, A11034, A11037, A11032). Phalloidin conjugated with Alexa 594 was purchased from Invitrogen (A12381). In some experiments, monoclonal anti-GBF1 antibodies (0.05mg) were incubated with 0.3mg of purified GBF1 or with equivalent volume of control eluate (material from a control purification; see below) for 2 hours at 4^{o}C before being used in IF.

Plasmids

N-terminally GFP-tagged GBF1 (GFP-GBF1) was constructed by sub-cloning human GBF1 into the pEGFP vector using XhoI and Xmas restriction enzymes and has been described in [12]. C-teminally his-tagged GBF1 was generated by subcloning human GBF1 into the pcDNA4-myc-His B vector using EcoRI and XhoI restriction enzymes.

Cell Culture and Transfection

D54 cells originated from a surgical resection from a GBM patient. D54 is a commonly studied cell line that has been extensively characterized. U-87 cell line is also derived from a grade 4 patient. Similarly, U-251 is derived from a human malignant glioblastoma multiforme isolated from a patient with grade III-IV malignant tumor by explant technique. D54, U87 and U251 cells were grown in cell culture dishes, some containing glass coverslips (diameter =12mm), in Dulbecco's Modified Eagle's Medium, supplemented with L-glutamine (10–090-CV), 20% fetal bovine serum (35–010 CV), 100 units/mL penicillin/streptomycin (30–001-CI). All these reagents were purchased from Corning. Cells were grown at 37^{o}C in 5% CO2 **until ~75%** confluent and were transfected

with Mirus TransIT-X2 Transfection Reagent (Mirus Bio Corporation, MIR6004), according to the manufacturer's instructions. After transfection, cells were incubated for 24 hours and processed for immunofluorescence. HEK (GripTiteTM 293 MSR, R79507) cells were purchased from ThermoFisher scientific, NY, USA. Cells were cultured in vitro in DMEM Eagle medium (Cellgro, Manassas, VA) supplemented with L-

glutamine, 10% fetal bovine serum, 100/units/ml penicillin, 100 mg/ml streptomycin, and 1 mM sodium pyruvate (Cellgro, Manassas, VA) at 37°C in humidified atmosphere and transfected with Mirus TransIT-LT1 Transfection Reagent (Mirus Bio Corporation, Madison, WI), according to the manufacturer's instructions.

GBF1 Purification

His-GBF1 was purified from HEK293 cells 48 hours after transfection. Cells were lysed in 50 mM HEPES (pH 7.4), 100 mM NaCl, protease inhibitor, scraped and lysed by passage 5 times through 21G needles (BD Bioscience, CA, USA) and twice through 27G needles (BD Bioscience, CA, USA). Cell debris was removed by centrifugation at 14 000 rpm for 15 min at 4°C. Supernatants were pre-cleaned using Pierce Glutatione Agarose (Thermo Scientific, IL, USA); at 4°C for 1 hour and centrifuged 1 000 rpm for 2 mins. Proteins were purified using Ni-NTA Agarose beads (Qiagen, CA, USA) for 3 hours at 4°C. Beads were recovered by centrifugation at 1000 rpm for 1 min and washed with 20mM HEPES (pH 7.4), 100mM NaCl, 20mM imidazole buffer 5 times 5 min at 4°C, then centrifuged at 1 000 rpm for 2 min. Proteins were eluted from the beads with 25 mM HEPES (pH 7.4), 100 mM NaCl, 250 mM imidazole, 3 times 5 mins at 4°C and centrifuged 2000rpm for 1 min. The same protocol was used to prepare "control eluate" sample from cells not transfected with GBF1. Purified proteins were stored at -80°C. For antigen competition analysis, 0.05 mg monoclonal anti-GBF1 antibodies were incubated with 0.3 mg of purified GBF1 (> 4-fold molar excess) or with equivalent volume of eluate from mock-transfected cells. The mixtures were incubated at 4°C for 1 hour and then used for IF as described below.

SDS-PAGE

Proteins were resolved on 8% SDS-PAGE as described previously [39]

Immunofluorescence and Confocal Microscopy

Cells were processed for IF as described in [8]: cells on coverslips were washed 3 times in PBS, fixed in 3% paraformaldehyde in PBS for 10 minutes and quenched with 10mM ammonium chloride in PBS for another 10 min. Subsequently cells were washed 3 times with PBS. Cells were then permeabilized in 0.1% Triton X-100 in PBS for 7 min. The coverslips were then washed in PBS, blocked in PBS containing 2.5% goat serum and 0.2% Tween 20 for 5 min, and in PBS, 0.4% fish skin gelatin, 0.2% Tween-20 for another 5 min. Cells were incubated with primary antibody diluted in 0.4% fish skin gelatin for 1 hour at room temperature, washed in PBS 0.2% Tween-20, and blocked like described above. Subsequently cells were incubated with secondary antibodies diluted in 2.5% goat serum for 45 minutes at room temperature. For coverslips processed with phalloidin, the phalloidin was diluted in 2.5% goat serum and cells were incubated with this phalloidin for 15 minutes at room temperature. Nuclei were stained using Hoechst; coverslips were washed with PBS-0.2% Tween-20 and mounted on slides in ProLong Gold antifade reagent (Invitrogen, P36930). Fluorescence was visualized with a Leitz Orthoplan epifluorescence microscope (Wetzlar, Germany). Images were captured with a 12-bit CCD camera from Q imaging using iVision-Mac software. Confocal imaging studies were performed using a Perkin Elmer Ultraview ERS 6FE spinning disk confocal attached to a Nikon TE 2000-U microscope equipped with laser and filter sets for FITC,

TRITC and DAPI fluorescence. Images were captured using a Hamamatsu C9100–50 EM-CCD camera (Hamamatsu Photonics K.K) and 60X or 100X Plan APO oil immersion objectives. The imaging system was controlled by Velocity 6.2 software (Perkin Elmer).

Disclosure of Potential Conflicts of Interest

No potential conflicts of interest were disclosed.

Acknowledgments

We thank Dr. Susan Nozell for the gift of D54, U87 and U251 cells and her invaluable advice on cell culture and transfection of these cells.

Funding

This work was supported by MCB0744471 to ES and 1R21NS096531 to ABH.

ORCID

Melanie L. Styers http://orcid.org/0000-0002-8234-6704

Akhil Kaushik http://orcid.org/0000-0002-9154-6337

Anita B. Hjelmeland http://orcid.org/0000-0003-2200-3248

References

[1] Wang S, Meyer H, Ochoa-Espinosa A, Buchwald U, Onel S, Altenhein B, Heinisch JJ, Affolter M, Paululat A. GBF1 (Gartenzwerg)- dependent secretion is required for

Drosophila tubulogenesis. J Cell Sci 2012; 125:461-72; PMID:22302994; http://dx.doi.org/10.1242/jcs.092551

[2] Armbruster K, Luschnig S. The Drosophila Sec 7 domain guanine nucleotide exchange factor protein Gartenzwerg localizes at the cis-Golgi and is essential for epithelial tube expansion. J Cell Sci 2012; 125:1318-28; PMID:22349697; http://dx.doi.org/10.1242/jcs.096263

[3] Szul T, Burgess J, Jeon M, Zinn K, Marques G, Brill JA, Sztul E. The Garz Sec 7 domain guanine nucleotide exchange factor for Arf regulates salivary gland development in Drosophila. Cell Logist 2011; 1:69-76; PMID:21686256; http://dx.doi.org/10.4161/cl.1.2.15512

[4] Wright J, Kahn RA, Sztul E. Regulating the large Sec 7 ARF guanine nucleotide exchange factors: the when, where and how of activation. Cell Mol Life Sci 2014; 71:3419-38; PMID:24728583; http://dx.doi. org/10.1007/s00018-014-1602-7

[5] Bui QT, Golinelli-Cohen MP, Jackson CL. Large Arf1 guanine nucleotide exchange factors: evolution, domain structure, and roles in membrane trafficking and human disease. Mol Genet Genomics 2009; 282:329-50; PMID:19669794; http://dx.doi.org/ 10.1007/s00438-009-0473-3

[6] Claude A, Zhao BP, Kuziemsky CE, Dahan S, Berger SJ, Yan JP, Armold AD, Sullivan EM, Melancon P. GBF1: A novel Golgi-associated BFA-resistant guanine nucleotide exchange factor that displays specificity for ADP-ribosylation factor 5. J Cell Biol 1999; 146:71-84; PMID:10402461

[7] Kawamoto K, Yoshida Y, Tamaki H, Torii S, Shinotsuka C, Yamashina S, Nakayama K. GBF1, a guanine nucleotide exchange factor for ADP-ribosylation factors, is localized to the cis-Golgi and involved in membrane association of the COPI coat. Traffic 2002; 3:483-95; PMID:12047556; http://dx.doi.org/10.1034/j.1600-0854.2002.30705.x

[8] Garcia-Mata R, Szul T, Alvarez C, Sztul E. ADP-ribosylation factor/COPI-dependent events at the endoplasmic reticulum-Golgi interfaceare regulated by the guanine nucleotide exchange factor GBF1. Mol Biol Cell 2003; 14:2250-61; PMID:12808027

[9] Zhao X, Claude A, Chun J, Shields DJ, Presley JF, Melancon P. GBF1, a cis-Golgi and VTCs-localized ARF-GEF, is implicated in ER-to-Golgi protein traffic. J Cell Sci 2006; 119:3743-53; PMID:16926190; http://dx.doi.org/10.1242/jcs.03173

[10] Szul T, Grabski R, Lyons S, Morohashi Y, Shestopal S, Lowe M, Sztul E. Dissecting the role of the ARF guanine nucleotide exchange factor GBF1 in Golgi biogenesis and protein trafficking. J Cell Sci 2007; 120:3929-40; PMID:17956946; http://dx.doi.org/10.1242/jcs.010769

[11] Saenz JB, Sun WJ, Chang JW, Li J, Bursulaya B, Gray NS, Haslam DB. Golgicide A reveals essential roles for GBF1 in Golgi assembly and function. Nat Chem Biol 2009; 5:157-65; PMID:19182783; http://dx.doi.org/10.1038/nchembio.144

[12] Szul T, Garcia-Mata R, Brandon E, Shestopal S, Alvarez C, Sztul E. Dissection of Membrane Dynamics of the ARF-Guanine Nucleotide Exchange Factor GBF1. Traffic 2005; 6:374-85; PMID:15813748; http://dx.doi.org/10.1111/j.1600-0854.2005.00282.x

[13] Niu TK, Pfeifer AC, Lippincott-Schwartz J, Jackson CL. Dynamics of GBF1, a Brefeldin A-Sensitive Arf1 Exchange Factor at the Golgi. Mol Biol Cell 2005; 16:1213-22; PMID:15616190; http://dx.doi.org/ 10.1091/mbc.E04-07-0599

[14] Lowery J, Szul T, Styers M, Holloway Z, Oorschot V, Klumperman J, Sztul E. The Sec 7 guanine nucleotide exchange factor GBF1 regulates membrane recruitment of BIG1 and BIG2 to the trans-Golgi network (TGN). J Biol Chem 2013; 288(16):11532-45; PMID:23386609; http://dx.doi.org/10.1074/jbc.M112.438481 doi:M112.438481 [pii]

[15] Gupta GD, SwethaMG, Kumari S, Lakshminarayan R, Dey G,Mayor S. Analysis of endocytic pathways in Drosophila cells reveals a conserved role for GBF1 in internalization via GEECs. PLoS One 2009; 4:e6768; PMID:19707569; http://dx.doi.org/10.1371/journal.pone.0006768

[16] Mazaki Y, Nishimura Y, Sabe H. GBF1 bears a novel phosphatidylinositol-phosphate binding module, BP3K, to link PI3Kgamma activity with Arf1 activation involved in GPCR-mediated neutrophil chemotaxis and superoxide production. Mol Biol Cell 2012; 23:2457-67; PMID:22573891; http://dx.doi.org/10.1091/mbc.E12-01-0062

[17] Zhao X, Lasell TK, Melancon P. Localization of large ADP-ribosylation factor-guanine nucleotide exchange factors to different Golgi compartments: evidence for distinct functions in protein traffic. Mol Biol Cell 2002; 13:119-33; PMID:11809827; http://dx.doi.org/10.1091/mbc.01-08-0420

[18] Li Z, Lee H, Zhu C. Molecular mechanisms of mechanotransduction in integrin-mediated cell-matrix adhesion. Exp Cell Res 2016; 349:85-94; PMID:27720950; http://dx.doi.org/10.1016/j.yexcr.2016.10.001

[19] Arnaout MA, Goodman SL, Xiong JP. Structure and mechanics of integrin-based cell adhesion. Curr Opin Cell Biol 2007; 19:495-507; PMID:17928215; http://dx.doi.org/10.1016/j.ceb.2007.08.002

[20] Critchley DR, Holt MR, Barry ST, Priddle H, Hemmings L, Norman J. Integrin-mediated cell adhesion: the cytoskeletal connection. Biochem Soc Symp 1999; 65:79-99; PMID:10320934

[21] Le Clainche C, Carlier MF. Regulation of actin assembly associated with protrusion and adhesion in cell migration. Physiol Rev 2008; 88:489-513; PMID:18391171; http://dx.doi.org/10.1152/physrev.00021.2007 CELLULAR LOGISTICS e1308900-7

[22] Chazotte B. Labeling cytoskeletal F-actin with rhodamine phalloidin or fluorescein phalloidin for imaging. Cold Spring Harb Protoc 2010; 2010:pdb prot4947

[23] VanBuren P, Begin K, Warshaw DM. Fluorescent phalloidin enables visualization of actin without effects on myosin's actin filament sliding velocity and hydrolytic properties in vitro. J Mol Cell Cardiol 1998; 30:2777-83; PMID:9990547; http://dx.doi.org/ 10.1006/jmcc.1998.0856

[24] Peyroche A, Courbeyrette R, Rambourg A, Jackson CL. The ARF exchange factors Gea1p and Gea2p regulate Golgi structure and function in yeast. J Cell Sci 2001; 114:2241-53; PMID:11493664

[25] Niu TK, Pfeifer AC, Lippincott-Schwartz J, Jackson CL. Dynamics of GBF1, a Brefeldin A-sensitive Arf1 Exchange Factor at the Golgi. Mol Biol Cell 2004; 16(3):1213-22; PMID:15616190

[26] Kumari S, Mayor S. ARF1 is directly involved in dynamin-independent endocytosis. Nat Cell Biol 2008; 10:30-41; PMID:18084285; http://dx.doi.org/10.1038/ncb1666

[27] Zakrzewska E, Perron M, Laroche A, Pallotta D. A role for GEA1 and GEA2 in the organization of the actin cytoskeleton in Saccharomyces cerevisiae. Genetics 2003; 165:985-95; PMID:14668359

[28] Zhou C, Cunningham L, Marcus AI, Li Y, Kahn RA. Arl2 and Arl3 regulate different microtubule-dependent processes. Mol Biol Cell 2006; 17:2476-87; PMID:16525022; http://dx.doi.org/10.1091/mbc. E05-10-0929

[29] Francis JW, Turn RE, Newman LE, Schiavon C, Kahn RA. Higher order signaling: ARL2 as regulator of both mitochondrial fusion and microtubule dynamics allows integration of 2 essential cell functions. Small GTPases 2016; 7(4):188-96; http://dx.doi.org/10.1080/ 21541248.2016.1211069

[30] Newman LE, Zhou CJ, Mudigonda S, Mattheyses AL, Paradies E, Marobbio CM, Kahn RA. The ARL2 GTPase is required for mitochondrial morphology, motility, and maintenance of ATP levels. PLoS One 2014; 9:e99270; PMID:24911211; http://dx.doi.org/ 10.1371/journal.pone.0099270

[31] Akhmetova K, Balasov M, Huijbregts RP, Chesnokov I. Functional insight into the role of Orc6 in septin complex filament formation in Drosophila. Mol Biol Cell 2015; 26:15-28; PMID:25355953; http://dx. doi.org/10.1091/mbc.E14-02-0734

[32] Huijbregts RP, Svitin A, Stinnett MW, Renfrow MB, Chesnokov I. Drosophila Orc6 facilitates GTPase activity and filament formation of the septin complex. Mol Biol Cell 2009; 20:270-81; PMID:18987337; http://dx.doi.org/10.1091/mbc.E08-07-0754

[33] BalasovM,Huijbregts RP,Chesnokov I. Role of theOrc6 protein in origin recognition complex-dependent DNA binding and replication in Drosophila melanogaster. Mol Cell Biol 2007; 27:3143-53; PMID:17283052; http://dx.doi.org/10.1128/MCB.02382-06

[34] Chesnokov IN, Chesnokova ON, Botchan M. A cytokinetic function of Drosophila ORC6 protein resides in a domain distinct from its replication activity. Proc Natl Acad Sci U S A 2003; 100:9150-55; PMID:12878722; http://dx.doi.org/10.1073/pnas.1633580100

[35] Biondini M, Sadou-Dubourgnoux A, Paul-Gilloteaux P, Zago G, Arslanhan MD, Waharte F, Formstecher E, Hertzog M, Yu J, Guerois R, Gautreau A, Scita G, Camonis J, Parrini MC. Direct interaction between exocyst and Wave complexes promotes cell protrusions and motility. J Cell Sci 2016; 129:3756-69; PMID:27591259; http://dx.doi.org/10.1242/jcs.187336

[36] Lizunov VA, Lisinski I, Stenkula K, Zimmerberg J, Cushman SW. Insulin regulates fusion of GLUT4 vesicles independent of Exo70-mediated tethering. J Biol Chem 2009; 284:7914-19; PMID:19155211; http://dx.doi.org/10.1074/jbc.M806460200

[37] Guo W, Roth D, Walch-Solimena C, Novick P. The exocyst is an effector for Sec 4p, targeting secretory vesicles to sites of exocytosis. EMBO J 1999; 18:1071-80; PMID:10022848; http://dx.doi.org/ 10.1093/emboj/18.4.1071

[38] Alvarez C, Garcia-Mata R, Hauri HP, Sztul E. The p115-interactive proteins GM130 and giantin participate in endoplasmic reticulum-Golgi traffic. J Biol Chem 2001; 276:2693-2700; PMID:11035033; http://dx.doi.org/10.1074/jbc.M007957200

[39] Gao YS, Alvarez C, Nelson DS, Sztul E. Molecular cloning, characterization, and dynamics of rat formiminotransferase cyclodeaminase, a Golgi-associated 58-kDa protein. J Biol Chem 1998; 273:33825-34; PMID:9837973; http://dx.doi.org/10.1074/jbc.273.50.33825

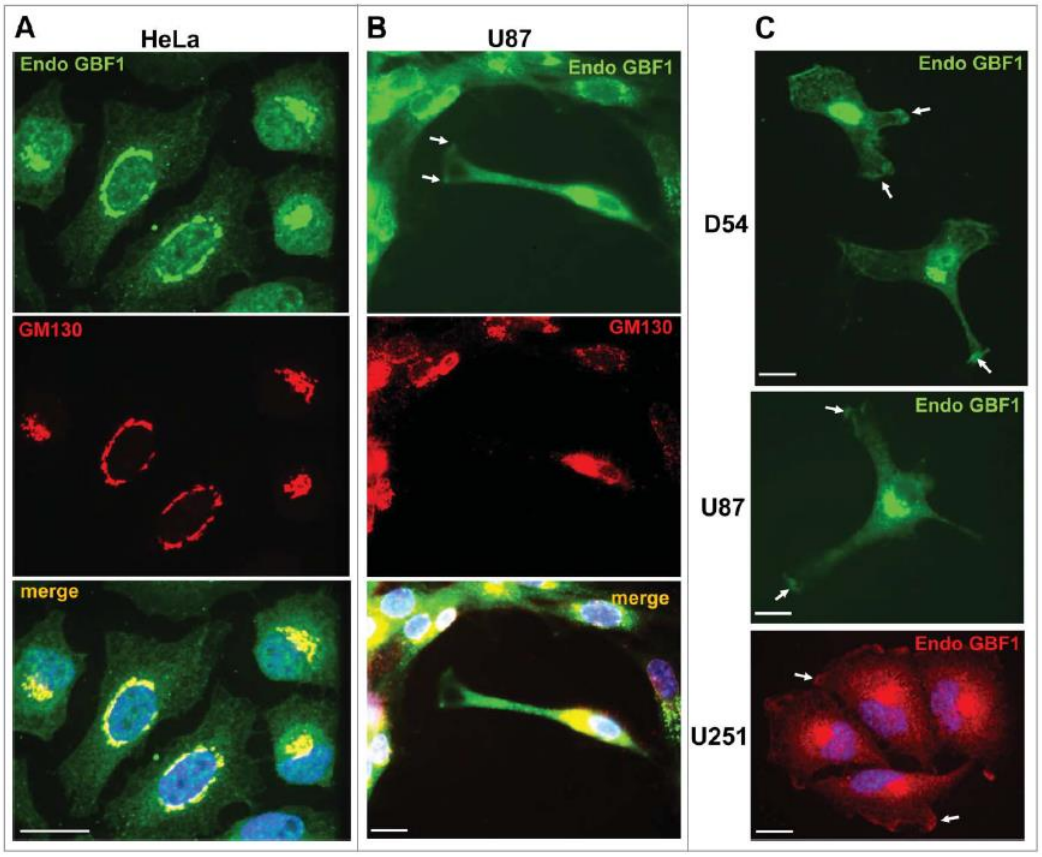

Figure 1. Dual Golgi and PM localization of GBF1 in GBM cells. HeLa (A) and U87 (B) cells were probed by double label IF with polyclonal rabbit anti-GBF1 and monoclonal mouse anti-GM130 antibodies. GBF1 co-localizes with GM130 to the Golgi, but is also present at tips of protrusions in U87 cells (arrows). (C) D54, U87 and U251 cells were processed for IF with monoclonal mouse anti-GBF1 antibodies. GBF1 localizes to the peri-nuclear Golgi and at tips of protrusions and the leading edge (arrows). Representative images from more than 3 independent experiments. Bar is 10 mm.

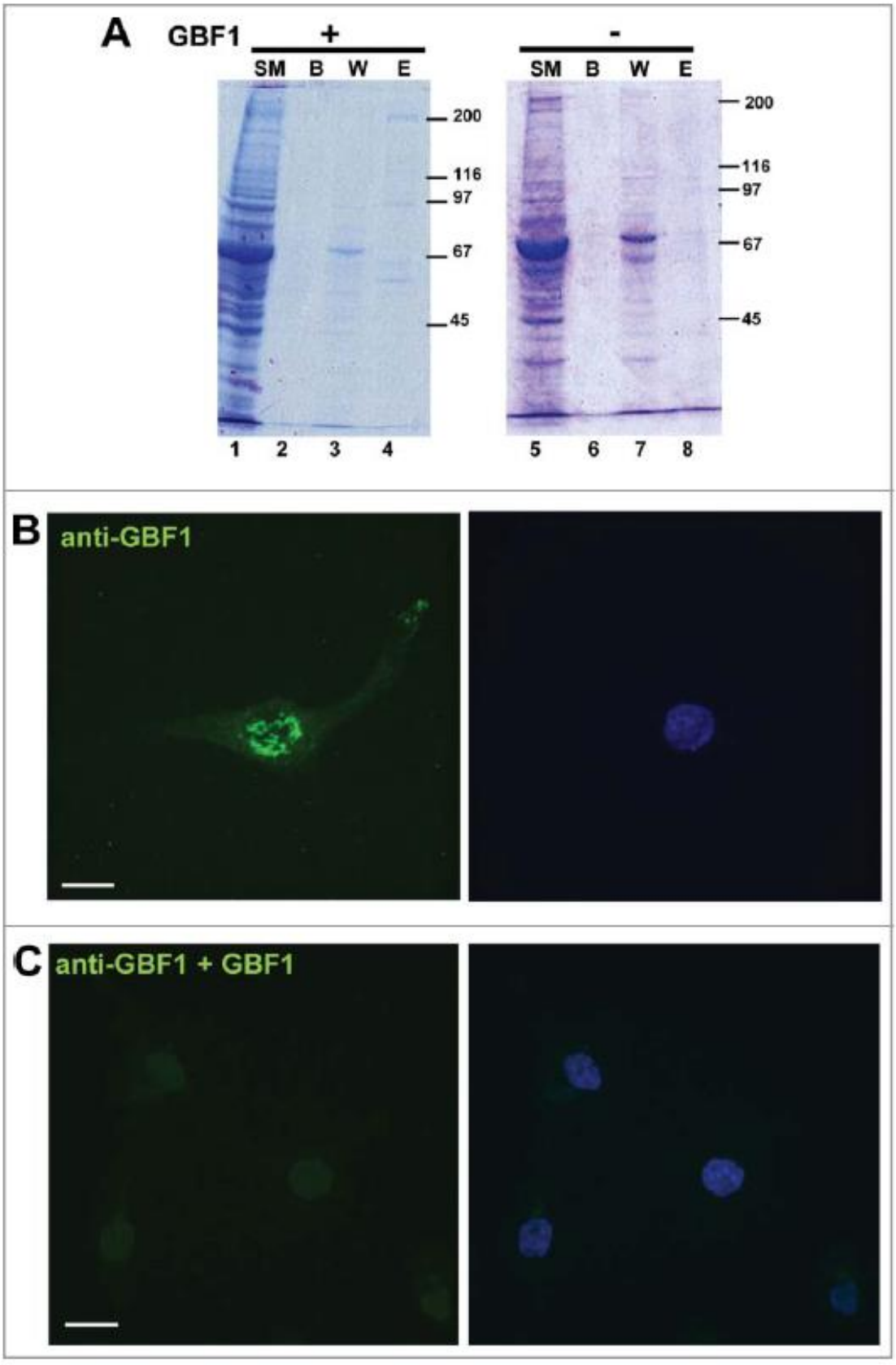
A
GBF1
+
-
SM B W E
SM B W E
200
116
97
67
45
200
116
97
67
45
1 2 3 4
5 6 7 8
B
anti-GBF1
C
anti-GBF1 + GBF1

Figure 2. Specificity of GBF1 antibodies person (A) HEK293 cells were transfected with His-tagged GBF1 (lanes 1–4) or mock-transfected (lanes 5–8), lysed 48 h later, and the lysates subject to Ni-agarose purification. Equivalent volume of indicated sample was processed by SDS-PAGE. (SM: starting material; B: beads after elution; W: wash E: elution. An »200 kD GBF1 band is visible in lane 4, but not in lane 8. (B) D54 cells were probed with monoclonal mouse anti-GBF1 antibodies that were pre-incubated with eluate from mock-transfected cells. (C) D54 cells were probed with monoclonal mouse anti-GBF1 antibodies that were pre-incubated with purified GBF1. Peri-nuclear Golgi staining and PM staining is evident in cells processed with antibodies pre-incubated with control eluate, but both signals are abrogated when the antibodies are pre-incubated with purified GBF1. Representative images from 2 independent experiments. Bar is 10 mm.

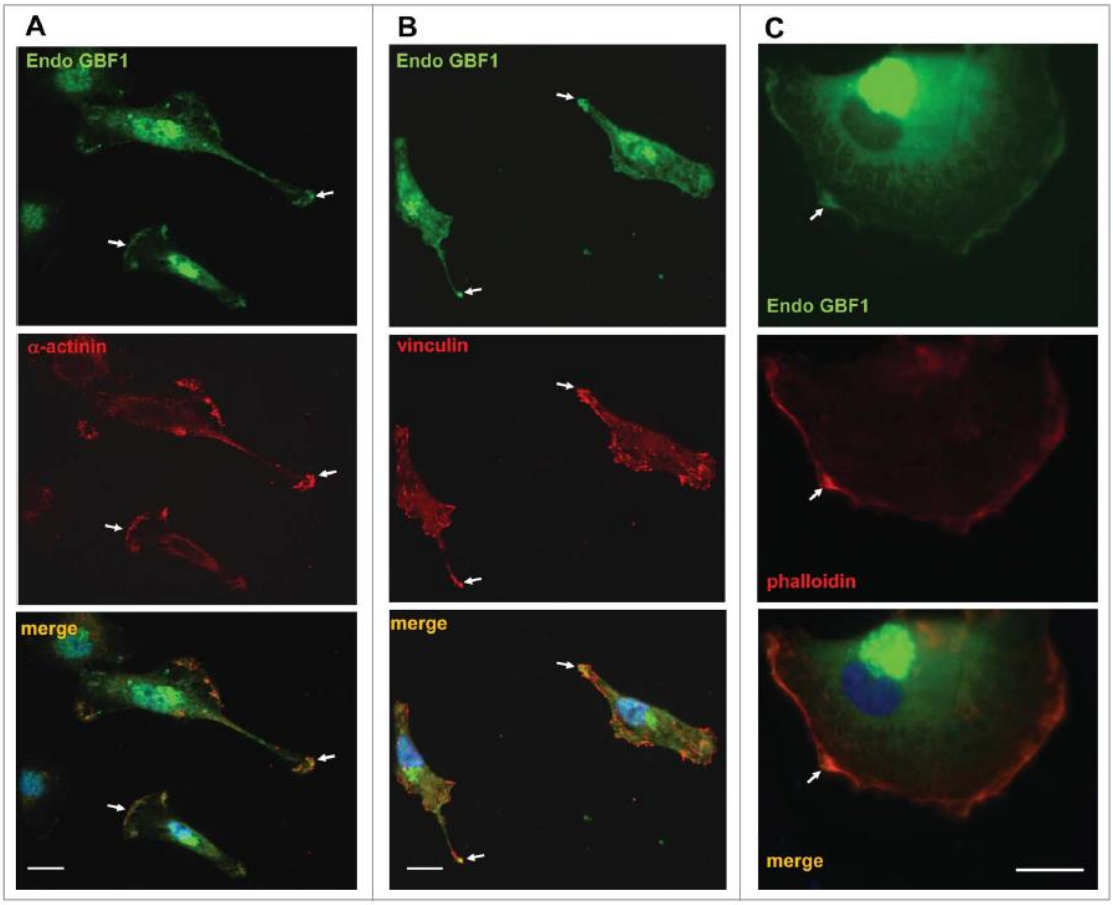

Figure 3. Co-localization of GBF1 with adhesion proteins in GBM cells person D54 cells were probed by double label IF with polyclonal anti-GBF1 and either monoclonal anti-a-actinin, monoclonal anti-vincullin or phalloidin staining. In addition to peri-nuclear Golgi staining, GBF1 localizes to focal adhesions and the leading edge containing adhesion proteins or actin-rich foci (arrows). Representative images from more than 2 independent experiments. Bar is 10 mm.

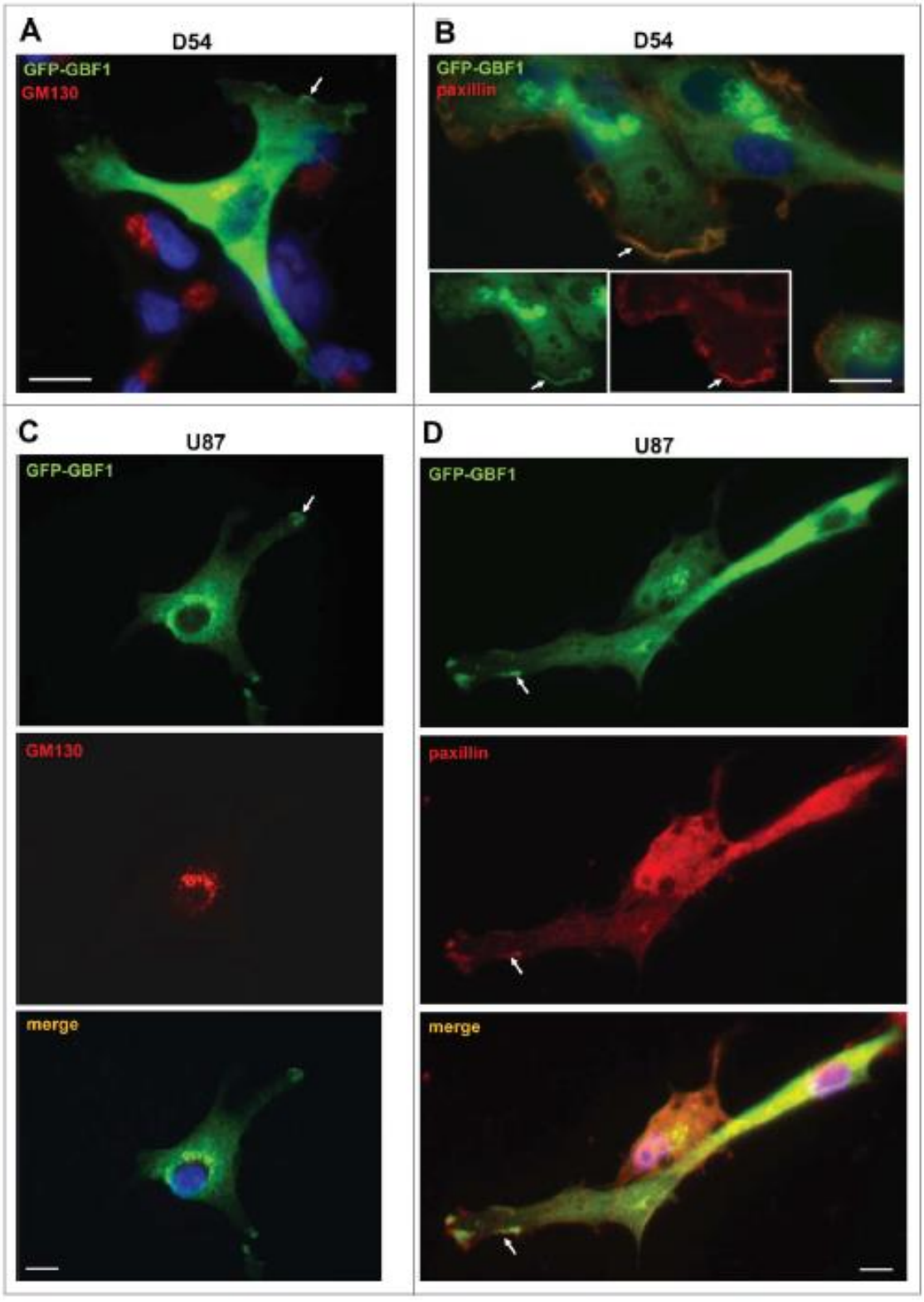
A
D54
GFP-GBF1
GM130
B
D54
GFP-GBF1
paxillin
C
U87
GFP-GBF1
GM130
merge
D
U87
GFP-GBF1
paxillin
merge

Figure 4. Golgi and PM localization of exogenously expressed GBF1 in GBM cells person D54 (A and B) and U87 (C and D) cells were transfected with GFP-tagged GBF1 and probed by double label IF with polyclonal anti-GFP and either monoclonal anti-GM130 (A and C) or monoclonal anti-paxillin antibodies (B and D). Exogenous GFPGFP1 co-localizes with GM130 at the Golgi and co-localizes with paxillin at tips of cellular protrusions and the leading edge (arrows). Representative images from more than 3 independent experiments. Bar is 10 mm.

CHAPTER 4

GBF1 REGULATES CELL SHAPE IN GBM CELLS

GBF1 mediates activation of Arf GTPases, cargo trafficking, and maintenance of the Golgi architecture [39, 42, 51, 62]. This large Sec7d guanosine exchange factor cycles between the cytoplasm and the cis-Golgi, as well as the plasma membrane [51, 63]. These studies illustrate that the N-terminal DCB and HUS domains are important for oligomerization and protein stability of GBF1 [51]. Key questions that continue to be researched include understanding the mechanisms through which GBF1 undergoes conformational changes to associate with membranes via the C-terminal HDS domains [64]. An extension of this is the need to decipher how multiple signaling events converge to mediate context specific function of GBF1.

GBF1 at the Plasma Membrane

GBF1 localizes to distant protrusions in glioblastoma cell lines [63]. We wanted to know if the localization of GBF1 to these processes was associated with ARF activation. Typically, in HeLa cells, overnight transfection of the GBF1-E794K, a dominant negative mutant, the Golgi stack will collapse into the ER, but there is no change in overall cell shape [51]. However, we found that expression of GBF1-E794K in U87 glioblastoma cells not only collapsed the Golgi apparatus, but it also caused the

entire cell shape to collapse. The cells changed from a long polar spindle shape to a tear drop shape (Figure 1) [51, 65]. After one hour of BFA treatment, the Golgi stacks had collapsed and GBF1 was no longer localized to the cytoplasmic space within the protrusion. However, at this early time in GBF1 inhibition, the cell shape had not collapsed. Perhaps, under specific stimuli, GBF1 works with focal adhesion complexes and cell surface receptors during GBM migration. To dig deeper into this mechanism, a combination of live image microscopy and mass/spec would identify specific signaling cues corresponding to GBF1 regulation of Arf-GTPases, cellular localization, and mechanisms during metastasis in GBM.

We hypothesized that GBF1 localization may be regulated by external cues. AMP-dependent Kinase has been reported to phosphorylate GBF1 at threonine 1337, located within a cluster of putative phosphorylation sites just c-terminal to the PIP3 binding domain (Figure 2) [36, 52, 59, 64]. EGF stimulation was also identified as an inducer of GBF1 phosphorylation at Serine1298 and Serine1318, C-terminal to the PIP3 binding domain (Figure 2) [66-68]. EGFR signaling results in kinase phosphorylation events that regulate the activity of GEFs and their substrate GTPases at the plasma membrane [58]. In addition, EGF stimulation has been reported to promote activation of GBF1-substrates ARF1 and ARF4 at the plasma membrane [60, 61]. Ongoing research continues to unravel the connections between pathways like EGF signaling and GBF1 function (Figure 2) [62].

BIG1 Potential in Gene Regulation

BIG1 is also a curious figure in all of this. Previous studies have focused on the cycling of BIG1 between the trans-Golgi-Network and the endosomal compartments [34]. However, the stimuli induced localization of BIG1 to the nucleus goes understudied [32, 33]. Evidence that demonstrates potential function of this phenomenon comes from studies of chromatin regulators [31]. BIG1 binds directly to the chromatin modulator Dpy30, a core subunit of the SET1-MLL histone methylation complex [31]. This demonstrates that there may be many molecular functions waiting to be identified that depend on specific signaling events. We also hypothesize that BIG1 acts not only as a scaffold protein in the nucleus, it may also function in regulating gene expression [35]. This demonstrates that signal specific events may reveal previously unidentified protein mechanisms. Examining these functions would help us better understand the spatiotemporal messaging between extracellular cues, signal cascades, and gene expression.

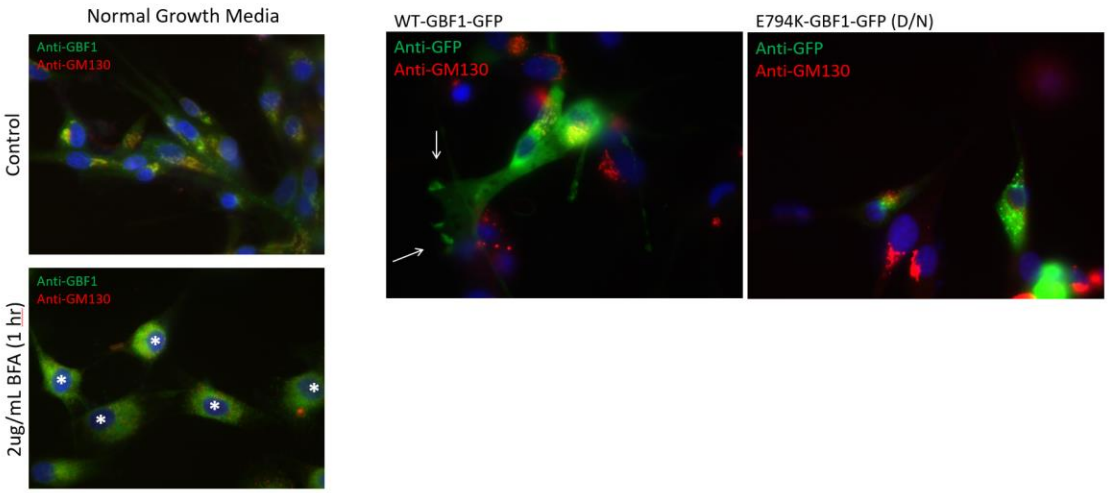

Figure 1. (A.) GBM cells retract leading processes in the presence of the GBF1 inhibitor BrefeldinA (BFA). (B.) Inhibition of GBF1 by overexpressing the dominant negative GBF1 mutant (E794K) induces a morphological change in GBM processes.

Inhibited kinase	Stimulated Kinase	Residue
MAPK/ p38MAPK/CKII	**EGFR**	Ser1298
?	?	**Tyr1316**
Src/CHK1/CHK2	?	Thr1317
MAPK/ p38MAPK/CKII	**EGFR**	Ser1318
Cdc2	?	Ser1320
MEK	?	**Tyr1323**
Src/Cdc2	?	Ser1335
?	**AMPK**	Thr1337

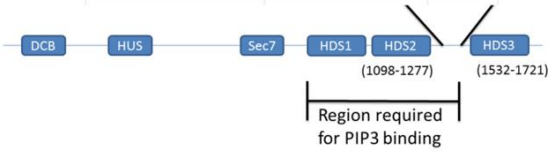

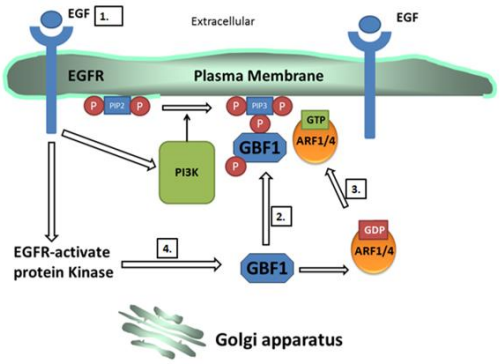

Figure 2. (A.) Phosphorylated GBF1 residues. The HDS2/3 inter-domain linker region is a highly phosphorylated region of GBF1 as determined by high throughput mass spectrometry screens. Phosphorylation of each site was validated across multiple studies. **B.** Potential model for EGF-stimulated signaling: EGF stimulation recruits GBF1 to the plasma membrane (**1**.) where GBF1 bind to PIP3 (**2**.) and recruits its substrate Arf (**3**.) mediated by phosphorylation of GBF1 by an EGF-singaling kinase event (**4**.).

CHAPTER 5

TARGETING THE SET1-MLL CORE COMPLEX IN CANCER

Cancer cell pathogenesis is driven in part by deregulation of specific factors leading to the activation of oncogenes, inactivation of tumor suppressor genes, and an elevated need for non-oncogenic factors [4, 69-73]. Many histone modifiers represent at least one of these categories suggesting that epigenetic regulation is key in promoting cancer [4]. Perturbation of epigenetic modulators can be preferentially catastrophic in certain cancer cells while having little to no effect on their normal cell counterparts, suggesting that chromatin regulation is a point of vulnerability in cancer cells [4]. Pharmacological inhibitors against several epigenetic marks including writers (DOT1L, H3K79 methylase), erasers (LSD1, H3K4 demethylase) and readers (BET family of histone acetylation readers) represent promising potential anti-cancer therapeutics, especially in blood cancers [3, 5-10]. Although they have been shown to be effective against certain cancers, further investigation into their anti-cancer mechanisms is needed to improve efficacy and overcome drug resistance.

H3K4 Methylation in Tumorigenesis

Histone H3K4 methylation is associated with active gene expression [74, 75]. The Set1-MLL complex is the major H3K4 methyltransferase complex in mammals and is

comprised of either SET1A, SET1B, MLL1, MLL2, MLL3, or MLL4 as catalytic subunits, each with specific and overlapping functions [27-29, 76, 77]. For full methylation activity, each catalytic subunit requires a complement of non-catalytic core subunits consisting of WDR5, RBBP5, ASH2L, and DPY30 [27-29, 76, 77]. Mutations and altered expression of these catalytic and non-catalytic core subunits have been identified in many cancers including blood cancers [78-88]. For example, *MLL1* (*MLL*) is a common target of chromosomal translocations in human acute myeloid leukemias, which may require the function of an intact allele for pathogenesis [88-90]. Thus, the SET1-MLL complexes represent druggable targets that can be exploited at multiple points within each complex.

DPY30, a non-catalytic core subunit, plays a direct role in facilitating genome-wide H3K4 methylation [27]. DPY30 has been shown to regulate cell growth, differentiation, and senescence [27, 91, 92]. Depletion of DPY30 in human primary hematopoietic progenitor cells (HPCs) and MLL-rearranged leukemia cells inhibits proliferation due to, at least in part, a reduction in the expression of the transcription factor c-Myc [93]. These studies suggest that Dpy30 may promote tumorigenesis through its role in H3K4 methylation. DPY30 associates with SET1-MLL complexes by binding directly to ASH2L in the core module [31, 94-98]. ASH2L is upregulated in patient tumor biopsies which is supported by experiments showing that overexpression of ASH2L promotes tumorigenic transformation of primary fibroblasts [82]. While it appears that DPY30 and ASH2L have functional roles in tumor pathogenesis, it is important to determine if the interaction between these two core subunits is a key

mechanism that can be exploited as an epigenetic target in anti-cancer therapeutic approaches [4].

ASH2L Plays a Complex Role in Oncogenesis

Ash2l (Absent, small or homeotic discs-like 2) is a core subunit of the Set1-Mll complex that has been well characterized. Ash2l is about 630 amino acids in length and about 69kDa in size and contains an N-terminal PHD motif (which binds methylated histones) followed by a winged helix motif (DNA binding motif) which has been shown to be important for binding directly to the beta-hemoglobin promoter [96, 99]. This indicates that Ash2l and the other core subunits can promote gene specific regulation of the SET1-MLL complex. In the C-terminus portion of the protein, Ashl2 contains a SPRY domain, through which it binds directly to the ABM domain of RbBP5, followed by a 30 amino acid alpha-helix characterized as the Dpy30 binding motif (DBM) which serves as a docking site for Dpy30 [96, 99]. The DBM is also referred to as the SDI domain for the Sdc1 (yeast Dpy30) interacting domain [97]. Mutating Ash2l residue Arginine 343 to an Alanine (R343A), within the SPRY domain, disrupts RbBP5 specific interaction and dramatically reduces in vitro H3K4 methylation by the SET1-MLL complex [95, 96]. In addition, mutating hydrophobic Leucine residues 513 and 517 and Valine 520 (L513E, L517E, V520E) within the SDI domain disrupted the interaction between Ash2l and Dpy30 [95, 96]. Although many studies have characterized the core module as non-catalytic, others indicate that the core subunits themselves may have intrinsic methyltransferase activity independent of the catalytic subunits [27-29, 76, 77, 100, 101]. Research has shown that Ash2l and RbBP5 form a heterodimer independent of

complex association and may have catalytic ability, as Ash2l is capable of binding S-andenosyl-L-methionine (SAM), the substrate for methyltransferases [15, 76, 95]. Furthermore, depletion of Ash2l in HeLa cells leads to a dramatic reduction in global H3K4me3 [15, 76, 95]. These studies suggest that Ash2l may promote H3K4 methylation through intrinsic methyltransferase activity, in addition to its role in core module assembly of the SET1-MLL complex.

Ash2l is not considered to be an oncogene. However, growing studies show that oncogenic drivers corrupt the normal function of chromatin modifying complexes to promote tumorigenic gene expression [15]. An established method for studying the oncogenic potential of certain genes is the ex vivo transformation of primary fibroblast cells. It has been shown that Ash2l overexpression in combination with constitutively active H-Ras and c-Myc promotes transformation of rat embryonic fibroblasts [82]. However, depletion of Ash2l with the addition of oncogenes like E1a and myc or the dominant negative construct of the tumor suppressor p53, did not suppress REF transformation [82]. Furthermore, this study showed that Ash2l levels were increased across a panel of tumor patient samples. While, Ash2l depletion in rat fibroblasts did not impair transformation, depletion of Ash2l impaired proliferation in human cancer cell lines (HeLa and U2OS). Ash2l oncogenic potential is likely due to the interaction between the N-terminal region of Ash2l and the C-terminal HLH motif of c-Myc [82, 102]. Although c-Myc does not appear to directly affect the methyltransferase activity of the SET1-MLL complex , it does appear to recruit SET1-MLL complexes to certain Myc dependent promoters through its interaction with Ash2l [82, 102].

Ash2l also promotes the activity of the tumor suppressor p53 [103]. P53 expression leads to a shift in chromatin landscape from repressive H3K9me to active H3K4me at pro-apoptotic genes, which is dependent on the recruitment of Ash2l [103]. Although Ash2l was not required for p53 binding to its targets, it is import for activation of these pro-apoptotic genes, in part through regulation of the transcription initiation machinery around these p53 dependent promoters [103]. This leaves the question of whether Ash2l functions as a tumor suppressor or if it has oncogenic activity. This suggests a potential context specific regulation of tumorigenesis by Ash2l. The increased expression levels of Ash2l driven by other oncogenic drivers like Myc may induce the expression and activity of p53 to promote apoptosis. Furthermore, the loss of p53 as a secondary oncogenic insult may be a driving force for Ash2l to abandon its anti-tumor role [103]. Interestingly the hyperactivation of c-Myc in MEFs leads to the overexpression of Ash2l [93, 104]. These studies suggest that the mechanism of the SET1-MLL complex can be swayed in a cancer specific manner mediated by Ash2l activity. While there have been many studies performed to understand the molecular function of Ash2l, both in cancer and development, targeting the structure function of Ash2l in a cancer specific way has yet to be demonstrated.

DPY30 Structure Function Within the SET1-MLL Complex

Dpy30 is one of the lesser studied core subunits of the SET1-MLL complex. The ability of Dpy30 to bind to Ash2l is evolutionarily conserved from yeast to mammals. Leucine 65 and 66 of SDC1, the yeast homolog of Dpy30, are important for interacting with Bre2, the yeast homolog of Ash2l [97]. Previous studies have determined that Dpy30 binds to the C-terminal domain of Ash2l as a dimer [31, 97]. The C-terminal half

of Dpy30 contains three consecutive alpha-helices (alpha 0, alpha 1, and alpha 2) which facilitate dimerization and binding to Ash2l [31]. The binding pocket is formed by dimerization of DPY30 C-terminus alpha helices 1 and 2 [31]. Deletion of the region between alpha1 and alpha2 inhibits the interaction between Dpy30 and Ash2l [97]. This intervening region is Proline rich, which we hypothesize gives rigidity to DPY30 to be able to form this dimer pocket for Ash2l binding [31]. While these studies indicate that DPY30 forms a dimer to bind to Ash2l, other studies have begun to investigate the higher order stoichiometry of Dpy30 binding [31, 97, 98, 105]. Mass spectrometry studies have shown that DPY30 may form trimers and larger oligomer confirmations in order to bind to Ash2l. Furthermore, the level of oligomerization may vary with association of specific SET1-MLL subunit assemblies [98, 105]. While this structural analysis of Dpy30 is intriguing, there is more to be discovered about this small elusive subunit of the complex.

FUNCTIONAL ROLE OF DPY30 IN MYC-DRIVEN TUMORIGENESIS

by

THEODORE BUSBY, ZHENHUA YANG, KUSHANI SHAH, ROBERT WHITAKER, , KEITH GILES, ALIREZA KHODADADI-JAMAYRAN, WEI LI, JING HU, BI SHI, ZHENJIA WANG, CHONGZHI ZANG, WILLIAM PLACZEK, AND HAO JIANG

Journal of Clinical Investigation. Zhenhua Yang, Kushani Shah, **Theodore Busby**, Keith Giles, Alireza Khodadadi-Jamayran, Wei Li, and Hao Jiang. Hijacking a key chromatin modulator creates epigenetic vulnerability for Myc-driven cancer. *Journal of Clinical Investigation.* 8:3605-3618, 2018

Experimental Cell Research. Kushani Shah, Robert Whitaker, **Theodore Busby**, Jing Hu, Bi Shi, Zhenjia Wang, Chongzhi Zang, William Placzek, and Hao Jiang, Specific inhibition of DPY30 activity by ASH2L-derived peptides suppresses blood cancer cell growth. *Experimental Cell Research*. (19)30326, 2019.

CHAPTER 6

FUNCTIONAL ROLE OF DPY30 IN MYC-DRIVEN TUMORIGENESIS

Abstract

Multiple levels of Myc regulation occur in Myc-dependent tumorigenesis, as it relates to the Set1-Mll complex. First, the Set1/Mll complex promotes expression of the Myc endogenous gene locus. The second level of regulation comes from the interactions between the methyltransferase complex and Myc at its target genes to promote tumorigenesis. This dissertation chapter shows that Dpy30, a non-catalytic subunit of the Set1-Mll complex, is amplified in Burkitt lymphoma, a B-cell cancer driven by Myc hyperactivation. Upregulation of Dpy30 in these cells promotes Myc chromatin binding and subsequent gene expression. Furthermore, Dpy30 heterozygosity suppresses Myc-dependent tumorigenesis in both in vivo and ex vivo models. Targeting Dpy30 activity by peptide inhibition impairs grow in leukemia cells that express high levels of Myc. This study provides a proof of principal that Dpy30 is a suitable target for anti-cancer therapeutic strategies in Myc-dependent tumors.

Introduction

Cancer cells acquire adaptations at multiple points throughout disease progression [1]. Regulation of the chromatin landscape in cancer cells is important for the activation

and maintenance of key oncogenes (Figure 1A) [1, 2]. Epigenetic modulators regulate gene expression in many cell and context specific processes, including tumorigenesis [1, 3-6]. Thus, epigenetic modulators have emerged as promising therapeutic targets in certain cancers, including blood cancers.

MYC is a common oncogenic driver in many human cancers, yet available therapeutics to directly target MYC are inefficient [7]. BET inhibitors, which block BRD4, are effective against a range of blood cancers in part by down regulating MYC gene expression [3, 4, 8, 9]. However, some cancers can become resistant to BET inhibitors [10, 11]. As H3K4 methylation and histone acetylation co-occupy active genomic elements, targeting modulators of H3K4 methylation may be a feasible approach to inhibiting MYC-driven cancers, especially blood cancers, either alone or in combination with BET inhibitors.

The Set1-Mll complex is the major Histone 3 Lysine 4 (H3K4) methyltransferase complex in mammals [5, 6, 12, 13]. H3K4 methylation is associated with active promoters and enhancers [6, 14]. Each catalytic subunit of the Set1/MLL complex depends on a non-catalytic core module containing WDR5, RBBP5, ASH2L and DPY30 (WRAD) to facilitate efficient H3K4 methylation (Figure 1B) [6]. Mutations and altered expression of Set1-MLL subunits have been identified across different cancers. Translocations that lead to fusion proteins with the catalytic subunits Mll1, Mll2, or Mll3 have been associated with initiating cancers of the hematopoietic system known as MLL-rearranged leukemias [15].

Dpy30 is an understudied subunit of the Set1-Mll complex. Previous studies have shown that DPY30 directly facilitates genome-wide H3K4 methylation, differentiation,

and hematopoiesis in human hematopoietic stem cells (HPCs) [16, 17]. Dpy30 is also important for promoting endogenous Myc gene expression in normal hematopoietic cells as well as in MLL-rearranged leukemia cells [18, 19]. Depletion of Dpy30 inhibits growth and proliferation in MLL-rearranged leukemia cells [16]. Furthermore, Myc overexpression leads to the upregulation of Dpy30 as well as the other core subunits WDR5, RBBP5, AND ASH2L in mouse embryonic fibroblasts (MEFs) [17]. In this chapter, the role of DPY30 is dissected in Myc-dependent tumors.

Little is known about the oncogenic or tumor suppressive roles of SET1-MLL non-catalytic subunits [15-19]. In this study, we show that DPY30 regulates mechanisms that promote tumorigenesis in an *in vivo* MYC-driven lymphoma mouse model. We also demonstrate that amplified Dpy30 expression is required for transformation of MEFs into tumor-like cells. Inhibiting Dpy30 association with the Set1-Mll complex by peptide dissociation selectively suppresses growth and proliferation of Myc-dependent cancer cells of the hematopoietic system. Our results led us to begin screening small molecule inhibitors for stable delivery and inhibition of Dpy30 mediated gene activation and proliferation. These studies establish DPY30 as a druggable target in cancer cells that express elevated levels of the MYC oncogene.

Results

Connection Between Set1-MLL Complex Alterations and Cancer Occurrences.

To dissect the relationship between genetic alteration in SET1-MLL subunits and how they correlate with the occurrence of different cancers, we assessed information deposited in the cBio Cancer Genomics Portal (http://www.cbioportal.org/). Our search found that the catalytic subunits Mll1, Mll2, Mll3, Mll4, Set1a, and Set1b frequently harbored mutations associated with different cancers, as in the case with Mll-rearranged leukemias (Figure 2B) [19, 20]. However, we observed that WDR5, RBBP5, ASH2L, and DPY30 (WRAD) were expressed at elevated levels across many of their associated cancers (Figure 2A) [19]. This suggests that expression of the WRAD core module may be fine-tuned to promote tumorigenesis [19]. Previous studies in mouse embryonic fibroblasts (MEFs) show that WRD5 and DPY30 are both amplified due to overexpression of c-Myc [16, 17]. This is supported by findings demonstrating that Ash2l RNA expression is also elevated by c-Myc and can cooperatively work with c-Myc to promote the expression of an oncogenic gene program [21, 22]. Upon re-addressing the cBioportal data we saw that just under half of all reported tumor studies that showed elevated levels of c-Myc also showed elevated levels of the core subunit Dpy30 in both solid and non-solid tumors [19]. However, elevated levels of these two factors do not always overlap. Thus, it is important to understand the mechanism that bring them together.

DPY30 Promotes Myc Chromatin binding in Myc-Driven Tumors Cell

Mll-AF9 derived, acute myeloid leukemia cells depleted of Dpy30 displayed a reduced growth rate, in part due to a reduction of Myc expression [18]. Thus, we probed Dpy30 activity in Burkitt lymphoma which is caused by a chromosomal translocation between the Myc gene on chromosome 8 and the IgH enhancer on chromosome 14 [23]. Data was mined from patient tumor samples of Burkitt lymphoma compared to non-Burkitt lymphoma samples [24]. Mll1, Mll2, Set1a, and Set1b were either downregulated or had no expression change in non-BL patient samples (Figure 3A) [19, 24]. Mll4, another catalytic subunit, displayed a significant increase in expression in BL samples (Figure 3A) [19, 24]. We hypothesize that Mll4 may be increased to promote Myc-specific enhancer activity [5, 25, 26].

Upon examining expression data in primary B-cells taken from the Eμ-Myc transgenic mouse model of Burkitt lymphoma, we saw that core subunits Dpy30, Wdr5, Ash2l, and Rbbp5 were up-regulated, as opposed to the catalytic subunits (Figure 3B) [19, 24]. This data recapitulates our observations from the patient samples. Furthermore, the corresponding ChIP data probing for Myc binding demonstrates that Myc has enhanced chromatin binding to the genomic loci of the subunits of the core module and only the Set1a catalytic subunit when comparing B-lymphocytes from Eμ-Myc mice to wild type mice (Figure 3C) [19, 27]. These data suggest a role for Myc in promoting oncogenesis via augmenting the expression levels of the WRAD core module of the SET1-MLL complex.

To begin to understand the role of Dpy30 in Myc dependent cancers, we depleted Dpy30 by shRNA in two blood cancer cell lines, Raji (Burkitt lymphoma) and Jurkat

(acute lymphoblastic leukemia cells), each of which depends on Myc expression [16] . Depletion of Dpy30 caused a reduction of growth rate and Myc gene expression, which confirmed findings that Dpy30 was important for Myc function in leukemias [16, 19]. We also dissected the overlap between Dpy30 overexpression and Myc overexpression in the context Burkitt lymphoma by using a human cell line model, P493-6 cells, with an inducible Myc expression [19]. Depletion of Wdr5 and Dpy30 both led to a reduction in the growth rate of P493-6 cells [19]. Moreover, global gene expression changes due to Dpy30 depletion overlapped significantly with the absence of Myc expression in these BL cells [19]. Specifically, genes that were upregulated by the induction of Myc expression were downregulated by Dpy30 depletion (Figure 3D) [19]. Consequently, many genes that were suppressed by the absence of Myc expression were upregulated by the depletion of Dpy30 (Figure 3D) [19]. These data all suggest that there may be a cooperative regulation of gene expression in Myc driven lymphomagenesis.

Dpy30 promotes endogenous Myc gene expression in leukemia cells driven by Mll-chromosomal translocations [16, 19]. In the case of Burkitt lymphoma, driven by the IgH-Myc translocation, and in the P493-6 cells, driven by tetracycline-induced Myc expression, depletion of Dpy30 does not affect oncogenic Myc expression [19]. This indicates that Dpy30 regulates c-Myc protein activity in addition to promoting endogenous Myc expression [19]. When P493-6 cells were depleted of Dpy30, Myc binding to promoters was significantly reduced at a subset of Myc target genes, and a moderate reduction of DNA binding globally (Figure 3E) [19]. Myc promoter binding was increased at another subset of genes not considered to be Myc specific targets (Figure 3E) [19]. However, there was an overlap between a decrease in Myc chromatin

binding and a reduction in H3K4me3 association (Figure 3E) [19]. This was confirmed by ChIP-QPCR detecting changes in Myc promoter binding [19]. Pro-survival and proliferation genes displayed reduced Myc binding and H3K4me3 levels in Dpy30 depleted P493-6 cells compared with control cells [19]. This further suggests that elevated Dpy30 expression promotes Myc mediated gene expression in blood cancers [18].

Myc-Dependent B-Cell Lymphoma Requires Elevated Dpy30 Expression

To examine the role of Dpy30 in promoting Myc-dependent lymphoma, we took a genetic approach to reducing Dpy30 expression levels. Dpy30 is an essential gene and ubiquitous deletion leads to embryonic lethality in mice [16-18]. Conditional deletion of Dpy30 in the hematopoietic lineage leads to pancytopenia, or the loss of all cells derived from hematopoietic stem cells (HSCs), and is visible by the loss of coloration of the bone marrow [16-18]. Therefore, we used a ubiquitous, heterozygous deletion of Dpy30 (Dpy30+/-) to understand how Dpy30 expression levels factor into Myc-driven tumorigenesis. Dpy30 heterozygosity in embryos at developmental stages E14.5 and E15.5 leads to an approximate 50% reduction in both Dpy30 RNA and protein expression levels [19]. This was accompanied with a moderate reduction in H3K4me3 but no apparent physiological differences in these embryos [19]. In adult mice, there were no differences in the life span or peripheral blood profiles of Dpy30+/- mice compared to WT littermates (Figure 3F) [19]. While modest, Dpy30 heterozygous mice had significantly reduced body weights compared to WT littermates (Figure 3F) [19]. These results suggest that the Dpy30 heterozygous mice maintain overall normal physiology.

We next examined the relationship between Dpy30 expression levels and Myc-driven tumorigenesis in the Eμ-Myc Burkitt lymphoma mouse model [28, 29]. Dpy30 heterozygous mice appeared normal compared to WT littermates (Figure 3F) [19]. However, on an Eμ-Myc background Dpy30 heterozygosity improved the median survival time by approximately 50% (Figure 3E) [19]. One hallmark of this tumorigenesis is splenomegaly, or the enlargement of the spleen [28-30]. Eμ-Myc mice that were heterozygous for Dpy30 had a reduced average spleen size compared to Eμ-Myc mice that had two functional Dpy30 alleles (Figure 3G) [19]. We also observed a significant decrease in proliferation with a dramatic increase in apoptotic splenic B cell populations [19]. Interestingly, the increase in apoptosis was not due to reactive oxygen species or DNA damage as apparent by the lack of change in gamma-H2Ax phosphorylation [19].

Observing expression levels of Dpy30 in B-cells from WT mice, Dpy30+/- mice, Eμ-Myc mice, and Eμ-Myc ; Dpy30+/-, RNA levels of Dpy30 were reduced by 50% in Dpy30 heterozygous mice compared to WT mice [19]. Dpy30 expression levels are increased by 2-fold in Eμ-Myc mice compared to WT mice [19]. This is consistent with the difference in Dpy30 expression levels in Burkitt lymphoma compared to non-Burkitt lymphoma patient samples (Figure 3A) [19]. Furthermore, Dpy30 levels were reduced by over half in Eμ-Myc ; Dpy30+/- mice compared to Eμ-Myc mice [19]. Dpy30 expression levels in Eμ-Myc ; Dpy30+/- cells were similar to those observed in WT mice, which indicated that normal levels of Dpy30 are insufficient for the full effects of Myc-driven lymphomagenesis [19]. Similar to P493-6 cells, there were no changes in Myc expression levels in this model as a result of Dpy30 depletion [19].

DPY30 Haploinsufficiency Impairs Myc-Dependent Transformation of Primary Fibroblasts

Hyperactivation of Myc drives the upregulation of Dpy30 in Burkitt lymphoma [19, 23, 24, 27]. Dpy30 heterozygosity does not cause an observable defect in the normal physiology of mice [19]. However, the absence of one Dpy30 allele has a suppressive effect on tumorigenesis in the Eμ-Myc Burkitt lymphoma mice [19]. Thus, we wanted to know if the level of Dpy30 expression affects the transformation of normal cells into tumor cells driven by oncogenic Myc expression. To do so, we took an ex vivo approach of inducing a tumor like phenotype in normal primary MEFs.

We isolated primary Dpy30+/+ (WT) and Dpy30+/- (Het) MEFs. As with mice, there is no difference in the growth rate of WT MEFS compared to Dpy30+/- MEFs (Figure 4A) [19]. We hypothesized that Dpy30 heterozygosity would negatively influence tumorigenic MEF transformation [28-30]. WT and Het MEFs were transduced with retrovirus to express either only HRasG12V, a constitutively active Ras oncogene, or in combination with c-Myc [21, 22, 28-30]. As with previous studies, Ras expression alone is not sufficient for promoting MEF transformation (Figure 4B) [19]. MEF cells expressing only Ras undergo senescence when plated sparsely in colony formation assays (Figure 4B) [19]. WT MEFs transduced with the combination of Ras and Myc form colonies 4 days and 7 days after plating while Dpy30+/- MEFs inefficiently form colonies (Figure 4B) [19].

Anchorage independent growth is a feature of solid tumor cells when the cell-cell contacts are altered between tumor cells and the surrounding tissue. We tested the tumorigenicity of these cells in an in vitro anchorage independent colony formation assay

where these cells were grown in soft agar suspension. WT MEFs transduced with Ras alone do not form colonies in the soft agar while the WT MEFs transduced with both Ras and Myc efficiently form colonies (Figure 4C) [19]. However, anchorage-independent growth is dramatically decreased in the heterozygous MEFs when compared to WT MEFs, which indicates inefficient transformation of heterozygous MEFs (Figure 4C) [19]. Furthermore, heterozygous Ras+Myc MEFs form 80% fewer colonies than those formed by WT Ras+Myc MEFs (Figure 4D) [19]. However, these results are not due to an unequal expression level of oncogenes. Expression of Ras and Myc are comparable between WT and Het MEFs while Dpy30 expression is reduced by approximately 50% when comparing Dpy30+/- MEFs to WT MEFs (Figure 4E) [19]. In both WT and Dpy30+/- MEFs, Dpy30 expression is significantly increased compared to non-transduced MEFs (Figure 4E) [19]. This indicates that Dpy30 hyperactivation is required for Myc-dependent tumorigenesis. Taken together, these results suggest Dpy30 haplo-insufficiency suppresses Myc-dependent transformation of primary fibroblasts.

Although proliferation in these cells remains comparable, apoptosis is increased in Ras+Myc Dpy30 het MEFs compared to Ras+Myc WT MEFs (Figure 5A-C) [19]. Next, we wanted to test the ability of the Ras+Myc transduced MEF cells to form tumors in animals. To do so we performed subcutaneous injections of WT Ras+Myc transduced MEFs into the left flank and Dpy30+/- MEFs transduced with Ras+Myc into the right flank of NSG immune deficient mice. After two weeks of tumor growth in these mice, Dpy30+/- MEFS form significantly smaller tumors than WT Ras+Myc MEFs (Figure 5D). Moreover, the average weight of a Dpy30+/- tumor is approximately 75% lower

than the average weight of a WT Ras+Myc tumor (Figure 5D). This data further suggests that excess Dpy30 expression is needed to form Myc-dependent tumors.

DPY30 Overexpression Induces Transformation of Primary Fibroblasts Independent of Myc Expression.

Myc-dependent transformation of primary fibroblasts requires elevated levels of Dpy30. However, Dpy30 has not been reported to have oncogenic potential. Since reducing the expression levels of Dpy30 by half suppresses tumor formation, we wanted to determine if high levels of Dpy30 could promote tumorigenesis in the absence of Myc. Previous studies show that overexpression of Ash2l, the Dpy30 binding partner, in combination with oncogenic Ras, promotes transformation of primary rat embryonic fibroblasts independent of Myc expression [21]. We transduced WT MEF cells with lentiviral overexpression constructs of Ras and Flag-HA-tagged Dpy30 (Figure 5E) [19]. Ash2l is also upregulated in Myc-dependent lymphoma cell lines (Figure 2) [19]. Thus, we also transduced WT MEFs with Ras and Flag-HA-tagged Ash2l constructs (Figure 5E) [19]. We then subjected these cells to the soft agar assay to test for anchorage-independent growth. Transduction of Ras+Dpy30 induces the transform MEFs as observed by their ability form colonies in soft agar (Figure 5E) [19]. Furthermore, Ras+Ash2l transduction also induces tumorigenic transformation in MEFs (Figure 5E) [19]. While this suggests that elevated levels of Dpy30 or Ash2l promotes tumorigenic growth, these combinations are not as efficient as Ras+Myc transduction for promoting a tumor phenotype in MEFs (Figure 5E) [19]. Thus, decreasing Dpy30 is suppressive

against tumor cell phenotypes while overexpression enhances tumorigenesis (Figure 5F) [19].

Dpy30 Association With the Set1-Mll Complex Is Disrupted By Ash2l SDI Domain Peptides

Dpy30 binds directly to Ash2l in the core module of the SET1-MLL complex (Figure 1B) [19]. Depletion of Ash2l by shRNA reduces growth rate, Myc promoter binding, and H3K4me3 levels in P493-6 cells as observed with Dpy30 depletion [19]. Furthermore, Myc binds directly to Ash2l but not to Dpy30 [19, 22].

Dpy30 and Ash2l promote a tumor phenotype through their function in the Set1-Mll complex. However, targeting the Dpy30-Ash2l interface for a potential anti-cancer therapeutic strategy had not been investigated. To begin dissecting the interaction between Dpy30 and Ash2l, we used an inhibitory protein peptide sequence that could sequester Dpy30 away from the SET1-MLL complex [31]. This peptide includes the Sdc1 interacting (SDI) domain of Ash2l, corresponding to amino acids 510-529 in the c-terminus of Ash2l (Figure 6A) [32-34]. An HIV derived TAT protein transduction motif is included to the N-terminus to ensure the ability of the peptide to enter the cell (Figure 6A) [31, 32]. In addition, an HA epitope tag is included for downstream experiments (Figure 6A) [31, 32]. This peptide is referred to hereafter as the wild type (WT) peptide in these experiments (Figure 6A) [32]. For comparison, we use two additional Ash2l peptides based on previous structure function studies. The first, a negative control peptide with three mutated residues corresponding to Leucine 513, Leucine 514, and Valine 520,

important for hydrophobic interactions between Dpy30 and Ash2l [33, 34]. These three residues were each changed to a positively charged Arginine, hereafter referred to as the 3R or loss of function peptide (Figure 6A) [32]. Protein binding assays demonstrate that the WT peptide, but not the 3R peptide, is capable of binding to HA-tagged Dpy30 immobilized onto resin (Figure 6A) [32]. Mutating the tyrosine residue at amino acid 518 of Ash2l leads to enhanced binding between Dpy30 and Ash2l [33, 34]. Thus, we also use a Y518R peptide with increased binding potential to Dpy30 (Figure 6A) [32]. Furthermore, the Y518R gain of function peptide binds to Dpy30 with the highest affinity compared to both the WT and 3R peptides [32].

We next wanted to determine if these peptides could disrupt Dpy30 activity. Protein binding assays show that flag-tagged full length Ash2l binds to Dpy30 (Figure 6B) [32]. Addition of the WT peptide leads to a modest reduction in the amount of Dpy30 pulled down with Ash2l bound beads (Figure 6B) [32]. However, the 3R loss of function peptide does no effect Ash2l-Dpy30 binding (Figure 6B) [32]. In vitro histone methyltransferase (HMT) assays also show that Histone H3K4me3 is reduced with the addition of either WT or Y518R peptides [32]. However, addition of the 3R peptide has no effect on Dpy30 induced levels of H3K4me3 [32]. This data indicates that disrupting Dpy30 association with the complex affects its activity.

Blocking the Interaction Between Dpy30 and Ash2l Inhibits Growth in Myc-Dependent Leukemia Cells

Depletion of Dpy30 inhibits growth and proliferation in MLL-rearranged leukemia cells (MLL-AF9) but not in erythroleukemia cells (BCR-ABL) [16]. In this study we use a panel of leukemia cell lines to determine if targeting the Dpy30-Ash2l interface would inhibit cancer cells with specificity. Blocking Dpy30 activity with WT or Y518R peptides reduces the growth rate of MLL-rearranged leukemia cells including THP-1 and MOLM-13 (MLL-AF9), KOPN-8 (MLL-ENL), and RS4;11 (MLL-AF4) (Figure 7A) [32]. In contrast, the 3R peptide does not cause a significant change in the growth rates of these cells (Figure 7A) [32]. We also observe reduced growth rate in the Myc-dependent B-lymphoma cell lines P493-6, Raji, and Jurkat treated with WT and Y518R peptides compared to 3R treatment (Figure 7B-C) [32]. However, when we treat the BRC-ABL erythroleukemia cell line K562 and normal human CD34+ hematopoietic stem cells with these peptides, the WT and Y518R peptides have no effect on the growth rate of cells compared with 3R peptide (Figure 7B-C) [32]. Furthermore, disrupting the interaction between Dpy30 and Ash2l with the WT or Y518R peptides inhibits the self-renewal ability of MOLM13 (MLL-AF9) cells (Figure 7D-E) [32]. This data supports a mechanism mediated by Dpy30 to promote the growth of cancer cells derived from the hematopoietic system with specificity.

Dpy30 heterozygosity leads to increased apoptosis in B-cells from Eμ-Myc (BL) mice and Ras+Myc MEFs [19]. We hypothesized that peptide inhibition on growth and self-renewal may be caused by changes in proliferation or cell death [19]. MOLM-13 cells treated with the Y518R gain of function peptide have a moderate but significant

decrease in the percentage of proliferating cells as indicated by BrdU+ staining (Figure 8A-B) [32]. AnnexinV staining reveals a moderate but significant increase in apoptotic MOLM13 cells with Y518R peptide treatment compared with the 3R peptide (Figure 8C-E) [32]. However, treatment with the WT peptide causes a slight but insignificant decrease in proliferation and increase in apoptosis (Figure 8C-E) [32]. We also tested the effect of peptide inhibition on Myc-driven P493-6 cells. Similar to MOLM-13 cells, treatment with the Y518R peptide results in a decrease in proliferation and an increase in apoptosis (Figure 8A-B) [32]. This data indicates that disrupting the interaction between Dpy30 and Ash2l results in slowed growth and an increased apoptotic cell population, as observed with depletion of Dpy30 (Figure 8C-E) [32].

Chromatin regulation is a complex process that involves multiple modulators working with a myriad of spatiotemporal relationships [35]. The Set1-Mll complex associates with chromatin around active promoters and enhancers in cooperation with many other positive and negative chromatin regulators [36]. Among these are the bromodomain family of chromatin readers that bind to acetylated histones to promote gene expression [3, 4, 8, 10, 11, 37]. Specifically, the bromodomain protein Brd4 has been the target of new epigenetic therapeutic strategies [9]. We wanted to determine if treating MOLM-13 cells with a combination of the Y518R peptide and the Brd4 inhibitor JQ1 would cause a synergistic effect on the growth rate of MLL-AF9 leukemia cells [38-40]. Combinatorial treatment of JQ1 and Y518R peptide causes a synergistic inhibition of growth rate in MOLM-13 cells (Figure 9A-C) [32]. EZH2 is the enzymatic subunit of the PRC2 H3K27me3 methyltransferase complex, which associates with promoters similar to the Set1-Mll complex and is reported to be required for MLL-AF9 leukemia [41, 42].

However, unlike the Set1-Mll complex, the PRC2 complex represses gene expression[41, 43]. We also test two EZH2 inhibitors GSK126 and EPZ6438 in combination with the Y518R peptide on MOLM-13 growth [44, 45]. Similar to Brd4 inhibition, the combined inhibition of Ezh2 with the Y518R peptide causes a significant additive decrease in the growth rate of MOLM-13 cells, although modest (Figure 9D-E) [32]. This data supports a proof of principal that Dpy30 is a viable target for therapeutic inhibition in Myc-dependent cancers, including those of the hematopoietic system. Furthermore, Dpy30 can be targeted in combination with other therapeutic strategies directed at inhibiting chromatin modulators.

Small Molecule Compound Inhibition of the Dpy30-Ash2l Interface

Disrupting the Dpy30-Ash2l interface via peptide inhibition prompted us to begin exploring pharmacological means to target this interaction. We thus performed a high-throughput screen of small molecule compounds targeting Dpy30 in a collaboration with Southern Research Institute. A library of 202, 268 molecules were assessed in a primary screen for their ability to induce dissociation of Dpy30 from a FITC-conjugated, WT Ash2l peptide via high-throughput Fluorescence Polarization Assay (FPA) (Figure 10A). In our secondary screen we tested 117 compounds using side-by-side high-throughput assays. In brief, we used the colorimetric MTT assay to assess the effects of compound inhibition on MOLM-13 (MLL-AF9 leukemia) cell proliferation (Figure 10B). We simultaneously examined the ability of these compounds to disrupt Dpy30 regulated gene expression in a 293T cell based, dual luciferase reporter assay (Figure 10C and D) [12]. To do so we utilized a stably integrated chromatin construct which includes a Gal4

promoter upstream of a luciferase reporter. The activation of this luciferase reporter is promoted in part by recruitment of a Gal4-VP16 transcriptional activator by the Set1-Mll complex (Figure 10D). Depletion of Dpy30 by shRNA knockdown has been previously reported to decrease luciferase activity in this assay by about 40% [13]. Thus, these two assays were suitable for our high throughput screening strategy.

Each compound was administered at 1uM and 10uM concentrations, all in duplicate simultaneously to 293T-luc cells and MOLM-13 cells. Although knockdown of Dpy30 leads to a luciferase signal of about 60% of that of control cells, we wanted to be able to capture a wider range of inhibition. Thus, we set our threshold of inhibition to 80% signal compared to vehicle treated cells. From the dual luciferase assay we identified 78 compounds that caused a reduction of luciferase activity to 80% signal or lower (Figure 10F). We selected to be more stringent when analyzing our MTT results. We identified 31 compounds the led to a 50% decrease in MOLM-13 cell proliferation (Figure 10E and F). Furthermore, we identified 24 compounds that reproducibly led to a 50% percent or greater decrease in proliferation and a 20% or greater decrease in luciferase signal (Figure 10F). This data indicates that chemical compounds capable of disrupting the Dpy30-Ash2l interface lead to an inhibition in molecular and cellular functions that mirror depletion of Dpy30.

Disrupting Dpy30 preferentially impacts MLL-AF9 leukemia cells compared to BCR-ABL erythroleukemia cells (Figure 7A-B) [16, 19]. We treated MOLM-13 and K562 cells with our top nine compound hits. We identified four compounds that elicited a greater inhibition in MOLM-13 cells compared to K562 cells (Data not shown). These data suggest that pharmacologically targeting Dpy30 inhibits Set1-Mll complex driven

gene activation. Furthermore, Dpy30 inhibition by small molecules impaired MOLM-13 cell growth as we observed with peptide treatment and genetically reducing the expression levels of Dpy30 in heterozygous mice.

Discussion

Our results show that in Burkitt Lymphoma (BL) driven by a Myc chromosome translocation, Dpy30 gene expression is hyperactivated. Eμ-Myc driven lymphoma cells also upregulate DPY30 and deletion of one Dpy30 allele in mice delays lymphomagenesis without affecting normal physiology. This is in part due to Dpy30 recruitment of Myc to its chromatin targets and subsequent induction of gene expression. We also found that Dpy30 heterozygosity suppresses tumorigenic transformation of primary fibroblasts suggesting that Dpy30 may play a role in tumorigenesis across tissue types. Dpy30 associates with Set1-MLL complexes through the core module by binding directly to the Ash2l non-catalytic core subunit. Both Dpy30 and Ash2l play a role in all levels of H3K4 methylation, including mono-methylation, a prominent chromatin mark at enhancers. Interestingly, blocking the interaction between Dpy30 and Ash2l impaired MLL-rearranged leukemia and BL cells. This was further illustrated by our high-throughput screening of small molecules to target Dpy30 binding to Ash2l. Together, these results suggest DPY30 is a critical regulator for MYC-driven tumorigenesis and may be an effective pharmacological target to exploit an epigenetic vulnerability in different cancers, especially blood cancers. This chapter highlights the importance of the Set1-MLL non-catalytic core module in Myc-driven lymphoma and the need to further

investigate the functional role of the interaction between Dpy30 and Ash2l in promoting tumorigenesis.

MYC drives the expression of core subunits in SET1-MLL complexes to promote lymphomagenesis. Previous studies have shown that the non-catalytic subunits ASH2L and WDR5 are overexpressed in certain cancers [21, 46]. The data represented in this chapter focus on targeting Dpy30. We also began to dissect the effects of Ash2l heterozygosity on Eu-Myc tumorigenesis and MEF transformation due to its direct interaction with Dpy30 and Myc. As Dpy30 has been shown to interact with other complexes, including the Golgi trafficking protein BIG1, the RNA binding family of AKAP proteins, and the ATPase-dependent NURF chromatin remodeling complex, it is important to further investigate the full spectrum of Dpy30 function in Myc-dependent malignancies [34, 47].

MYC regulates activation and suppression of key genes to facilitate tumorigenesis [7]. Another common oncogenic insult that may accompany Myc is the inactivation of the tumor suppressor p53 [7, 48]. Ash2l has been shown to regulate p53 activity to promote apoptosis in cancer cells [48]. Furthermore, in mice, a combined genetic background of Eu-Myc with a complete knock out of p53 expediates tumor formation and death [28, 29]. Future research directions should seek to determine if Ash2l or Dpy30 heterozygosity would suppress p53 knock out induced tumorigenesis.

Previously, the only subunits of the Set1-Mll complex to be targeted for therapeutic treatment development in cancer have been Mll1, Wdr5, and Menin [47, 49-51]. The specificity of inhibition from the Ash2l WT and Y518R peptides have allowed us to target and block the interaction between Dpy30 and the Set1-Mll complex. This

study is a proof-of-principal that targeting the DPY30-ASH2L interface is a feasible therapeutic strategy for certain malignancies of the hematopoietic system. Our results led us to further develop a more effective strategy to target Dpy30 for cancer treatment using small molecule inhibitors with better pharmacological efficacy.

We found that treatment of cancer cells from the hematopoietic system with peptide sequences corresponding to the C-terminal SDI domain of Ash2l led to a significant reduction in overall growth rate. However, with overnight peptide treatment there was only a modest reduction of proliferation and apoptosis in these cells. When we treat MOLM-13 and P493-6 cells with peptides over the course of the growth assay, we did not see a change in proliferation or apoptosis. This is potentially due to the efficiency of cell entry as well as stability of the peptides in the media and in the cells. In addition, the peptides may also elicit cell death through necrosis instead of apoptosis [17].

As the major Histone H3K4 methylation enzymes in mammals, the SET1-MLL complexes represent potential drug targets in epigenetic therapeutics due to the intimate connection of H3K4 methylation with gene expression, and their extensive association with multiple cancers. However, the complex interactions between subunits of these complexes in cancer is not fully understood. Our small molecule screen generated a narrow number of potential compounds to be further tested for in vivo efficacy. Subsequent steps to interrogate these compounds include inhibition of Ash2L-Dpy30 binding through fluorescence polarization assays (FPA) and co-IP assays as well as their effects on leukemia cell colony formation. Further testing will also determine if the compounds inhibit Dpy30 in enhancing H3K4 methylation in vitro and in cells or if they inhibit recruitment of Dpy30 to genomic targets by ChIP-sequence. Therapeutic

strategies targeting Dpy30 in combination with other inhibitors of chromatin regulators like Ezh2 and Brd4 may lead to significant strides in cancer treatment against Myc dependent malignancies.

Methods adopted from Yang et al. 2018 [19]

Cell Culture, Gene Depletion, Growth Assays, And MEF Transformation Assays.

P493-6 cells lymphoma cells (gifted from Alanna Ruddell at the Fred Hutchinson Cancer Research Center, WA), Raji, and Jurkat cells (gifted from Tim Townes, UAB, AL) were all cultured in RPMI 1640 medium supplemented with 10% FBS. Primary MEF cells were isolated from E13.5 embryos and cultured in MEF medium consisting of DMEM supplemented with L-glutamine, 10% FBS, 0.1 mM nonessential amino acids, and 55 μM β-mercaptoethanol (Invitrogen, Thermo Fisher Scientific). The passage number before transformation was kept to a minimum of less than four passages. Retroviral particles were produced by transfecting 293T cells in combination with pWZL–c-MYC–bsd (Addgene, 10674) or pBabe-HRas-V12-puro (Addgene, 1768) and an ecotropic packaging vector using Polyethylenimine (PEI) (Polysciences Inc.). Viral supernatants were filtered through a 0.45μM syringe filter. MEF cells were infected with HRAS-V12 and C-MYC viral particles and were subsequently selected in puromycin at 2μg/ml and blasticidin at 2μg/ml. Soft agar, anchorage independent growth, colony formation assays were performed by plating transformed MEF cells in a 24 well plate at 2x10^3 cells/well. To set up the assay, a base layer was plated consisting of MEF culture media in 0.6% agar that was then covered by a MEF cell containing layer consisting of

MEF culture media, cells, and 0.3% agar. The cells were fed with a fresh layer of normal growth media every four days over the course of 21 days. Dpy30 was stably depleted in P493-6 cells or MEF cells after they were infected with lentiviruses expressing control shRNA or shRNAs targeting Dpy30 then were subsequently selected by puromycin at 2μg/ml for 72 hours after infection. P493-6 cell and MEF cell growth was measured by hemocytometer and CellTiter 96 AQueous One Solution Cell Proliferation Assay (Promega) respectively.

Mice and Tumor Analyses

Dpy30+/– mice (generated by our laboratory [18]) and Eμ-Myc mice (purchased from Jackson Laboratory stock no. 002728) were crossed to generate WT, Dpy30+/–, Eμ-Myc, and Eμ-Myc Dpy30+/– mice. Hemavet 950 system (Drew Scientific) was used to measure peripheral blood profiles. GraphPad Prism software was used to analyze mouse survival rates. Transduced MEFs (2 × 106 cells in 100 μl) were subcutaneously injected for xenografts into the flanks of 8-week-old male NSG (NOD.Cg-Prkdcscid Il2rgtm1Wjl/SzJ) mice from Jackson Laboratory at 2x10^6 cells per 100μl. After two weeks, tumors were measured for size and weight.

Methods Adopted From Shah et al 2019 [32]

Peptides

The peptides were generated using a solid-phase peptide synthesis strategy on the Prelude system (Gyros Protein Technologies). Once cleaved from resin, the peptides were purified by HPLC (Agilent), and the purity was confirmed by mass spectrometry.

Following purification, the peptides were lyophilized and stored at −20°C. At the time of assays, lyophilized peptides were reconstituted with sterile and deionized water.

Assays for Cell Growth, Colony Formation, Proliferation, and Apoptosis

Growth assays were performed staring with 200,000 cells per well plated and were grown in 750 µl Advanced RPMI (Gibco) supplemented with 2.5% FBS (Gibco) in triplicate wells for 5 days with addition of the indicated peptides at 10µM every 12 hours. Live cells were counted using a hemocytometer on indicated days. To determine the synergistic effect of combining JQ1 and the Y518R peptide, JQ1 at 40nM was added to cells once at the start of the growth assay and the peptide was added to the cells every 12 hours. For EZH2 synergy with the peptide, GSK126 at 5nM or EPZ6438 at 20nM were added to cells once at the start of the growth assay. Methylcellulose colony formation assays were performed by plating 10,000 MOLM-13 cells in human methylcellulose base media (R&D Systems) with no supplements, containing the indicated peptides at 100µM. Proliferation and apoptosis were determined by BrdU incorporation and Annexin V staining kit assays (BD Scientific), followed by flow cytometry.

Reference

1. Dawson, M.A. and T. Kouzarides, *Cancer epigenetics: from mechanism to therapy.* Cell, 2012. **150**(1): p. 12-27.
2. Kouzarides, T., *Chromatin modifications and their function.* Cell, 2007. **128**(4): p. 693-705.
3. Dawson, M.A., et al., *Inhibition of BET recruitment to chromatin as an effective treatment for MLL-fusion leukaemia.* Nature, 2011. **478**(7370): p. 529-33.
4. Delmore, J.E., et al., *BET bromodomain inhibition as a therapeutic strategy to target c-Myc.* Cell, 2011. **146**(6): p. 904-17.
5. Shilatifard, A., *The COMPASS family of histone H3K4 methylases: mechanisms of regulation in development and disease pathogenesis.* Annu Rev Biochem, 2012. **81**: p. 65-95.
6. Shilatifard, A., *Molecular implementation and physiological roles for histone H3 lysine 4 (H3K4) methylation.* Curr Opin Cell Biol, 2008. **20**(3): p. 341-8.
7. Dang, C.V., *MYC on the path to cancer.* Cell, 2012. **149**(1): p. 22-35.
8. Mertz, J.A., et al., *Targeting MYC dependence in cancer by inhibiting BET bromodomains.* Proc Natl Acad Sci U S A, 2011. **108**(40): p. 16669-74.
9. Zuber, J., et al., *RNAi screen identifies Brd4 as a therapeutic target in acute myeloid leukaemia.* Nature, 2011. **478**(7370): p. 524-8.
10. Fong, C.Y., et al., *BET inhibitor resistance emerges from leukaemia stem cells.* Nature, 2015. **525**(7570): p. 538-42.
11. Rathert, P., et al., *Transcriptional plasticity promotes primary and acquired resistance to BET inhibition.* Nature, 2015. **525**(7570): p. 543-547.
12. Jiang, H., et al., *Regulation of transcription by the MLL2 complex and MLL complex-associated AKAP95.* Nat Struct Mol Biol, 2013. **20**(10): p. 1156-63.
13. Jiang, H., et al., *Role for Dpy-30 in ES cell-fate specification by regulation of H3K4 methylation within bivalent domains.* Cell, 2011. **144**(4): p. 513-25.
14. Rickels, R., et al., *An Evolutionary Conserved Epigenetic Mark of Polycomb Response Elements Implemented by Trx/MLL/COMPASS.* Mol Cell, 2016. **63**(2): p. 318-328.
15. Thiel, A.T., et al., *MLL-AF9-induced leukemogenesis requires coexpression of the wild-type Mll allele.* Cancer Cell, 2010. **17**(2): p. 148-59.
16. Yang, Z., et al., *The DPY30 subunit in SET1/MLL complexes regulates the proliferation and differentiation of hematopoietic progenitor cells.* Blood, 2014. **124**(13): p. 2025-33.
17. Yang, Z., et al., *Physical Interactions and Functional Coordination between the Core Subunits of Set1/Mll Complexes and the Reprogramming Factors.* PLoS One, 2015. **10**(12): p. e0145336.
18. Yang, Z. and K. Shah, *Dpy30 is critical for maintaining the identity and function of adult hematopoietic stem cells.* 2016. **213**(11): p. 2349-2364.
19. Yang, Z., et al., *Hijacking a key chromatin modulator creates epigenetic vulnerability for MYC-driven cancer.* J Clin Invest, 2018. **128**(8): p. 3605-3618.
20. Mohan, M., et al., *Licensed to elongate: a molecular mechanism for MLL-based leukaemogenesis.* Nat Rev Cancer, 2010. **10**(10): p. 721-8.
21. Lüscher-Firzlaff, J., et al., *The human trithorax protein hASH2 functions as an oncoprotein.* Cancer Res, 2008. **68**(3): p. 749-58.

22. Ullius, A., et al., *The interaction of MYC with the trithorax protein ASH2L promotes gene transcription by regulating H3K27 modification.* Nucleic Acids Res, 2014. **42**(11): p. 6901-20.
23. Maifrede, S., et al., *IGH/MYC Translocation Associates with BRCA2 Deficiency and Synthetic Lethality to PARP1 Inhibitors.* Mol Cancer Res, 2017. **15**(8): p. 967-972.
24. Hummel, M., et al., *A biologic definition of Burkitt's lymphoma from transcriptional and genomic profiling.* N Engl J Med, 2006. **354**(23): p. 2419-30.
25. Ernst, P. and C.R. Vakoc, *WRAD: enabler of the SET1-family of H3K4 methyltransferases.* Brief Funct Genomics, 2012. **11**(3): p. 217-26.
26. Yang, W. and P. Ernst, *Distinct functions of histone H3, lysine 4 methyltransferases in normal and malignant hematopoiesis.* Curr Opin Hematol, 2017. **24**(4): p. 322-328.
27. Sabò, A., et al., *Selective transcriptional regulation by Myc in cellular growth control and lymphomagenesis.* Nature, 2014. **511**(7510): p. 488-492.
28. Barna, M., et al., *Suppression of Myc oncogenic activity by ribosomal protein haploinsufficiency.* Nature, 2008. **456**(7224): p. 971-5.
29. Truitt, M.L., et al., *Differential Requirements for eIF4E Dose in Normal Development and Cancer.* Cell, 2015. **162**(1): p. 59-71.
30. Hsieh, A.C., et al., *Genetic dissection of the oncogenic mTOR pathway reveals druggable addiction to translational control via 4EBP-eIF4E.* Cancer Cell, 2010. **17**(3): p. 249-61.
31. Polo, J.M., et al., *Specific peptide interference reveals BCL6 transcriptional and oncogenic mechanisms in B-cell lymphoma cells.* Nat Med, 2004. **10**(12): p. 1329-35.
32. Shah, K.K., et al., *Specific inhibition of DPY30 activity by ASH2L-derived peptides suppresses blood cancer cell growth.* Exp Cell Res, 2019. **382**(2): p. 111485.
33. South, P.F., et al., *A conserved interaction between the SDI domain of Bre2 and the Dpy-30 domain of Sdc1 is required for histone methylation and gene expression.* J Biol Chem, 2010. **285**(1): p. 595-607.
34. Tremblay, V., et al., *Molecular basis for DPY-30 association to COMPASS-like and NURF complexes.* Structure, 2014. **22**(12): p. 1821-1830.
35. Yadav, T. and J.P. Quivy, *Chromatin plasticity: A versatile landscape that underlies cell fate and identity.* 2018. **361**(6409): p. 1332-1336.
36. Pekowska, A., et al., *H3K4 tri-methylation provides an epigenetic signature of active enhancers.* Embo j, 2011. **30**(20): p. 4198-210.
37. Filippakopoulos, P., et al., *Selective inhibition of BET bromodomains.* Nature, 2010. **468**(7327): p. 1067-73.
38. Chapuy, B., et al., *Discovery and characterization of super-enhancer-associated dependencies in diffuse large B cell lymphoma.* Cancer Cell, 2013. **24**(6): p. 777-90.
39. Fulciniti, M., et al., *Non-overlapping Control of Transcriptome by Promoter- and Super-Enhancer-Associated Dependencies in Multiple Myeloma.* Cell Rep, 2018. **25**(13): p. 3693-3705.e6.

40. Lovén, J., et al., *Selective inhibition of tumor oncogenes by disruption of super-enhancers.* Cell, 2013. **153**(2): p. 320-34.
41. Mills, A.A., *Throwing the cancer switch: reciprocal roles of polycomb and trithorax proteins.* Nat Rev Cancer, 2010. **10**(10): p. 669-82.
42. Xu, B., et al., *Selective inhibition of EZH2 and EZH1 enzymatic activity by a small molecule suppresses MLL-rearranged leukemia.* 2015. **125**(2): p. 346-57.
43. Latham, J.A. and S.Y. Dent, *Cross-regulation of histone modifications.* Nat Struct Mol Biol, 2007. **14**(11): p. 1017-24.
44. Knutson, S.K., et al., *Durable tumor regression in genetically altered malignant rhabdoid tumors by inhibition of methyltransferase EZH2.* Proc Natl Acad Sci U S A, 2013. **110**(19): p. 7922-7.
45. McCabe, M.T., et al., *EZH2 inhibition as a therapeutic strategy for lymphoma with EZH2-activating mutations.* Nature, 2012. **492**(7427): p. 108-12.
46. Kim, J.Y., et al., *A role for WDR5 in integrating threonine 11 phosphorylation to lysine 4 methylation on histone H3 during androgen signaling and in prostate cancer.* Mol Cell, 2014. **54**(4): p. 613-25.
47. van Nuland, R., et al., *Quantitative dissection and stoichiometry determination of the human SET1/MLL histone methyltransferase complexes.* Mol Cell Biol, 2013. **33**(10): p. 2067-77.
48. Mungamuri, S.K., S. Wang, and J.J. Manfredi, *Ash2L enables P53-dependent apoptosis by favoring stable transcription pre-initiation complex formation on its pro-apoptotic target promoters.* 2015. **34**(19): p. 2461-70.
49. Andersson, R., et al., *An atlas of active enhancers across human cell types and tissues.* Nature, 2014. **507**(7493): p. 455-461.
50. Christensen, C.L., et al., *Targeting transcriptional addictions in small cell lung cancer with a covalent CDK7 inhibitor.* Cancer Cell, 2014. **26**(6): p. 909-922.
51. Rao, R.C. and Y. Dou, *Hijacked in cancer: the KMT2 (MLL) family of methyltransferases.* Nat Rev Cancer, 2015. **15**(6): p. 334-46.

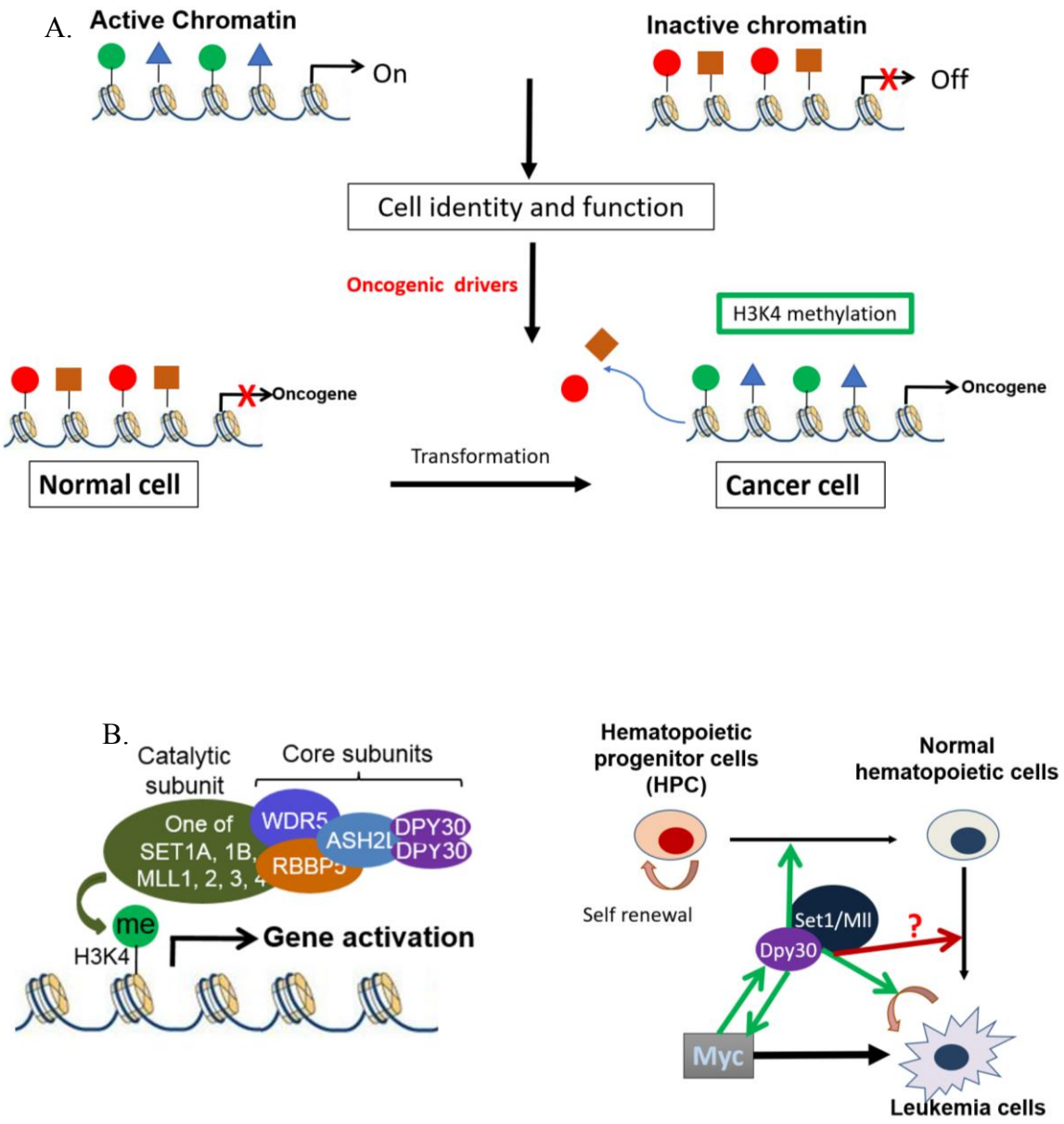

Figure 1. (A) Epigenetic changes occur over the course of tumorigenesis. (B) The SET1-MLL complex deposits the active chromatin mark H3K4me and is important for normal homeostasis as well as disease development.

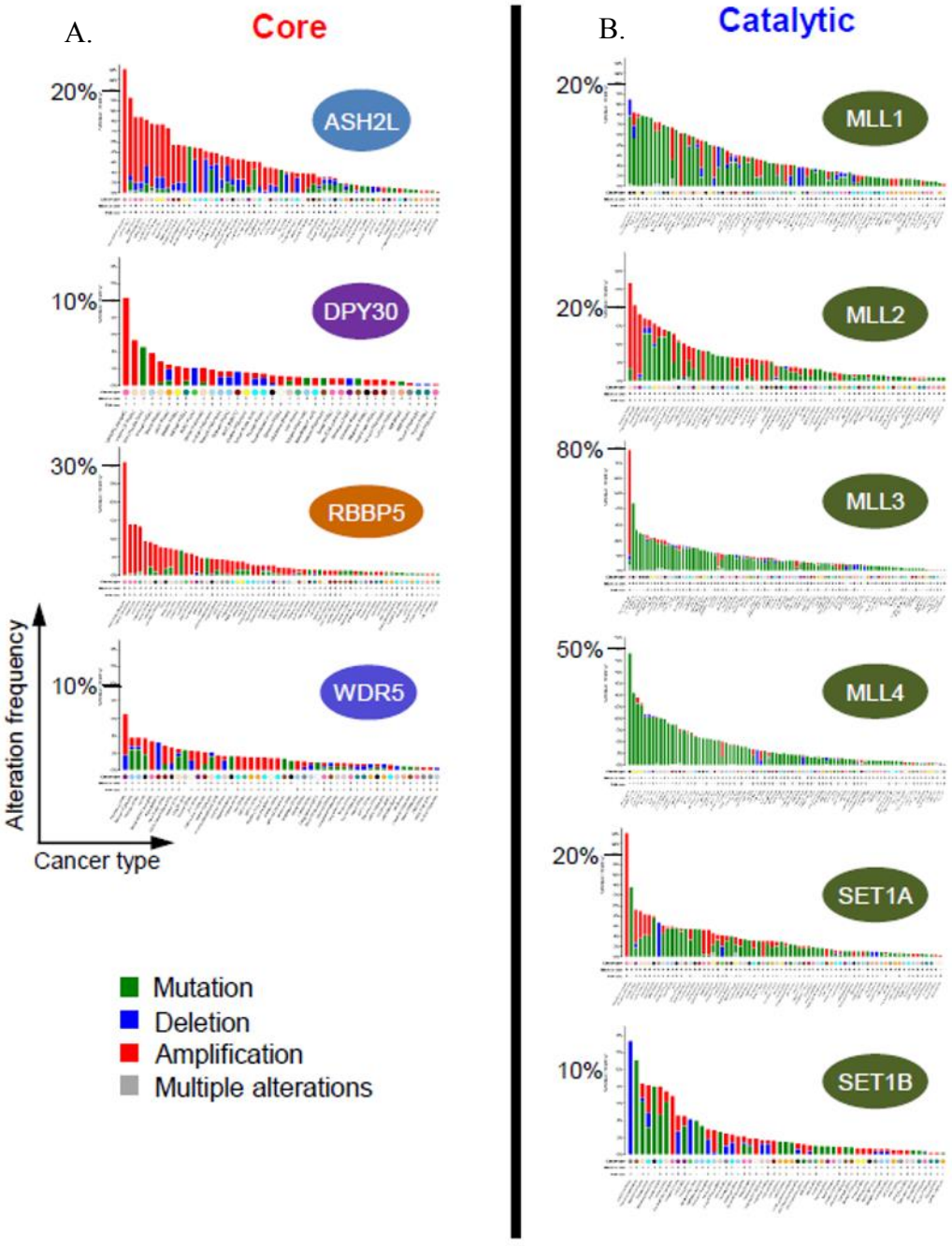

Figure 2. Alterations of the core versus catalytic subunits of the SET1-MLL complexes in human cancer samples. Data were generated from cBioPortal http ://www cbioportal org/ [72]. (A) The non-catalytic core subunits. (B) The catalytic methyltransferase subunits.

A.

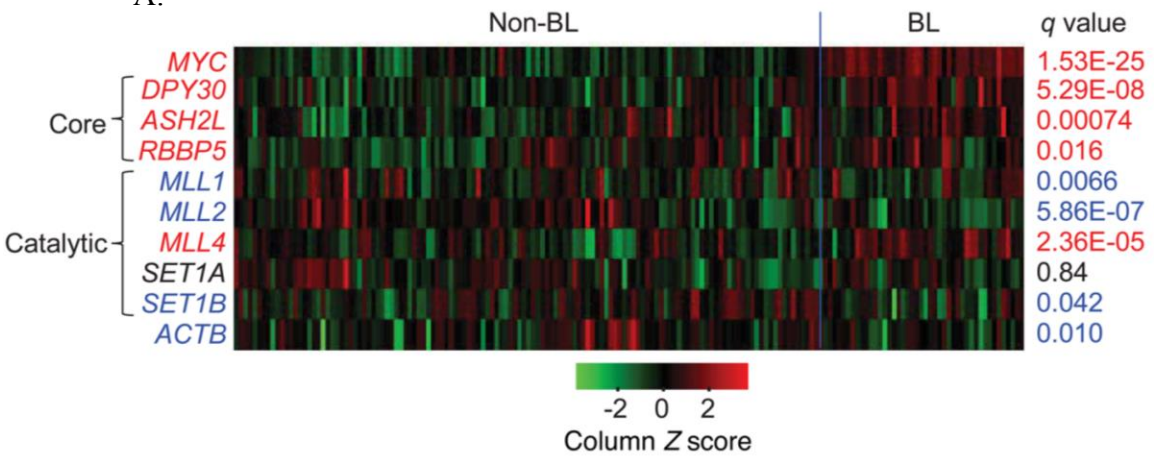
Non-BL
BL
q value
MYC
DPY30
ASH2L
RBBP5
MLL1
MLL2
MLL4
SET1A
SET1B
ACTB
Core
Catalytic
1.53E-25
5.29E-08
0.00074
0.016
0.0066
5.86E-07
2.36E-05
0.84
0.042
0.010
-2 0 2
Column Z score

B.

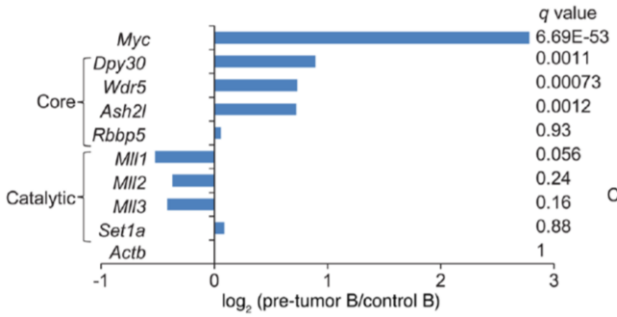
q value
Myc
Dpy30
Wdr5
Ash2l
Rbbp5
Mll1
Mll2
Mll3
Set1a
Actb
Core
Catalytic
6.69E-53
0.0011
0.00073
0.0012
0.93
0.056
0.24
0.16
0.88
1
log2 (pre-tumor B/control B)

C.

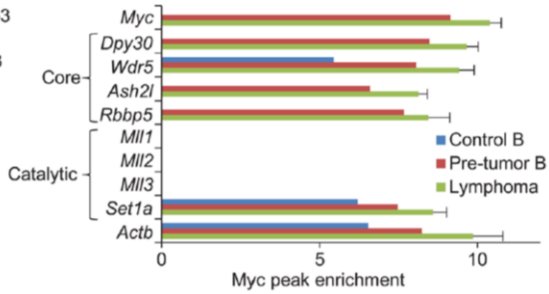
Myc
Dpy30
Wdr5
Ash2l
Rbbp5
Mll1
Mll2
Mll3
Set1a
Actb
Core
Catalytic
Control B
Pre-tumor B
Lymphoma
Myc peak enrichment

D.

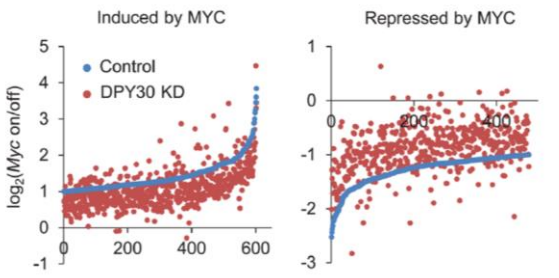
Global gene expression changes (Myc induced genes)
Induced by MYC
Repressed by MYC
Control
DPY30 KD
log2(Myc on/off)

E.

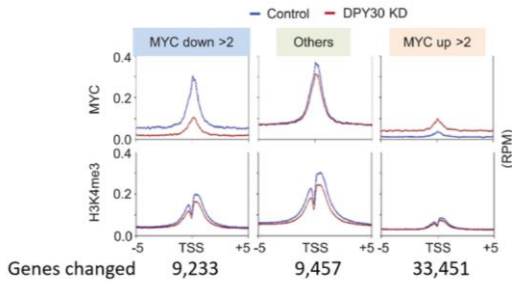
Myc chromatin binding
Control
DPY30 KD
MYC down >2
Others
MYC up >2
MYC
H3K4me3
TSS
(RPM)
Genes changed
9,233
9,457
33,451

F.

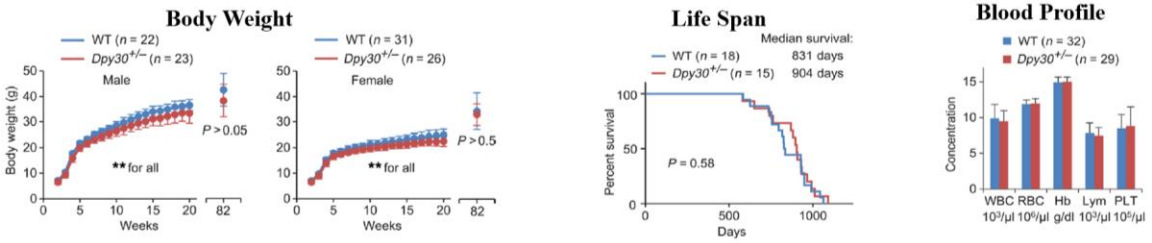

Eμ-Myc Mice

G.

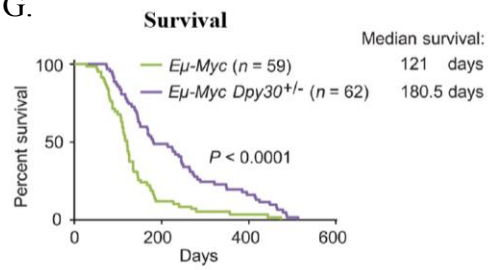

H.

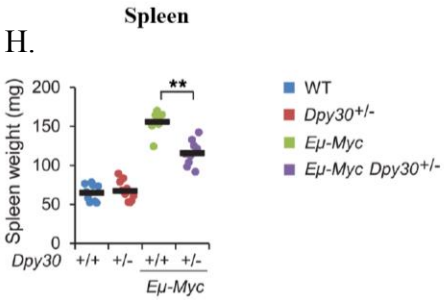

Figure 3. (A) Expression of SET1-MLL complex subunits in primary samples from Burkitt lymphoma patients versus samples from non-Burkitt lymphoma patients (GEO accession no. GSE4475). Columns represent individual samples, and rows represent indicated genes (red= increased expression in BL, blue= decreased expression in BL). (B and C) Data obtained from Eμ-Myc mice (GEO accession no. GSE51011). (B) Expression changes of SET1-MLL complex subunits between B cells from control mice and pre-tumor B cells from Eμ-Myc transgenic mice. (C) ChIP assays showing Myc chromatin binding to the promoters of SET1-MLL complex subunits (mean ± SD). (D) P493-6 cells stably expressing shRNA control or shRNA targeting Dpy30 were treated with tetracycline to activate Myc expression followed by harvest 0 and 4 hours after withdrawal of tetracycline to be used for microarray analyses. Logarithmic fold changes from the presence and absence of Myc were plotted for the genes upregulated or down regulated by more than 2-fold compared to control cells. Genes are represented by individual dots. (**E**) Myc ChIP and H3K4me3 ChIP signals at TSSs in P493-6 cells. (**F**) Differences in mouse body weight. (F) Peripheral blood profiles for 8-week-old littermate mice (mean + SD). (**G**) Survival rates of littermates shown on a Kaplan-Meier curves. (H) Spleen weights 4-week-old mice. Each animal is represented by an individual dot. [72]

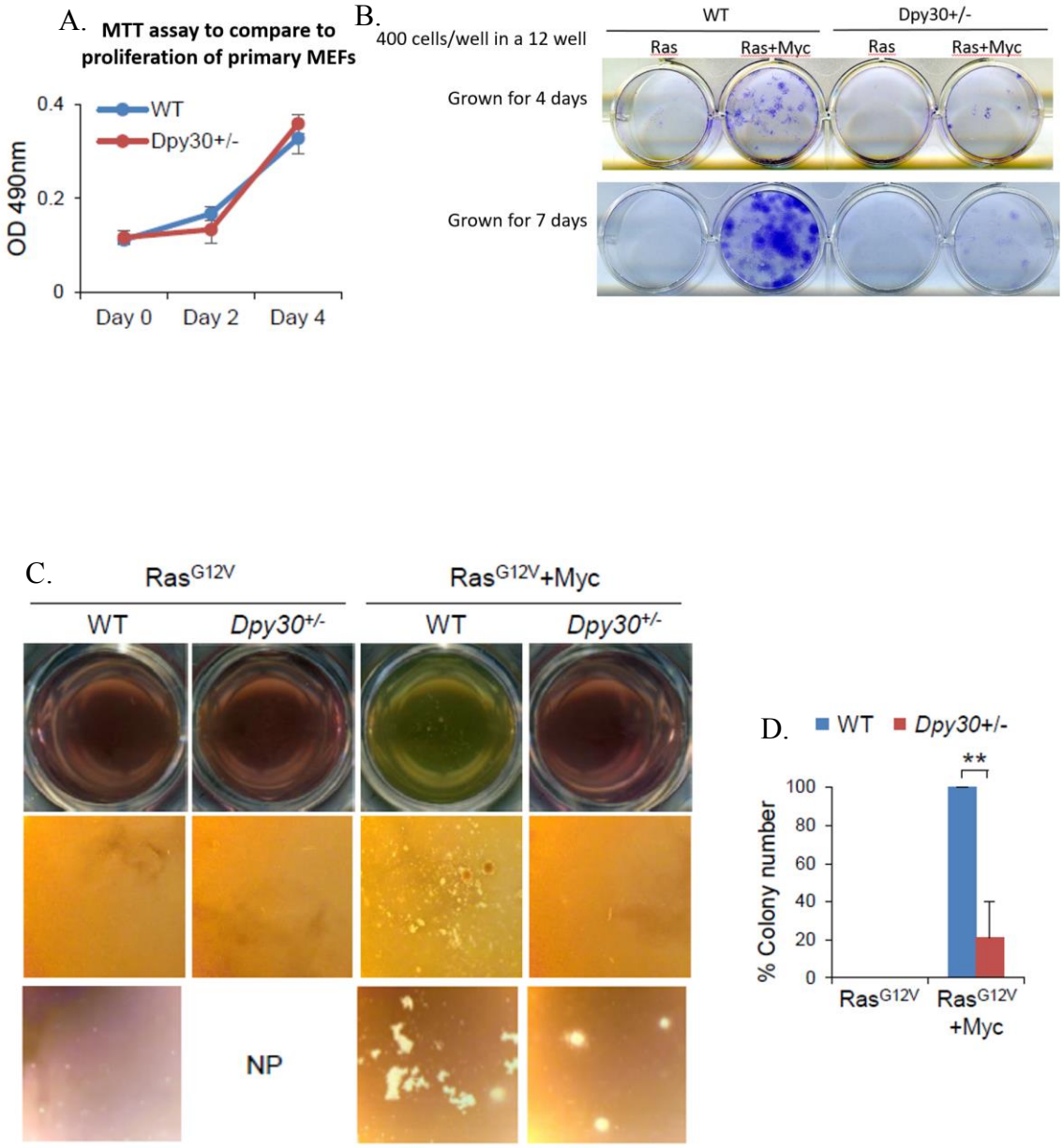
A.
MTT assay to compare to proliferation of primary MEFs
OD 490nm
0.4
0.2
0
WT
Dpy30+/-
Day 0
Day 2
Day 4
B.
400 cells/well in a 12 well
Grown for 4 days
Grown for 7 days
WT
Dpy30+/-
Ras
Ras+Myc
Ras
Ras+Myc
C.
RasG12V
RasG12V+Myc
WT
Dpy30+/-
WT
Dpy30+/-
NP
D.
WT
Dpy30+/-
**
% Colony number
100
80
60
40
20
0
RasG12V
RasG12V +Myc

E.

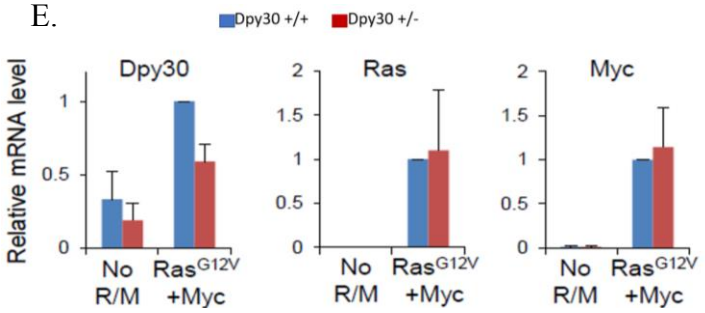

Figure 4. (**A**) Growth assay for WT and *Dpy30*+/– MEF assessed by MTT assay performed in 3 biological replicates. (B) Crystal violet staining to visualize colony formation in WT and *Dpy30*+/– MEFs transduced with H-RasV12 or H-RasV12 + cMyc. (C) Soft agar colony formation assay images for HRAS-G12V+MYC transduced oncogenic transformation of WT and Dpy30+/- MEF. (**D**) The percentage of colonies formed by Dpy30+/- MEFs to WT MEFs. (**E**) Relative mRNA expression Dpy30, Ras, and Myc primary MEFs compared to Ras+Myc transduced MEFs as determined by Q-RT-PCR (expression was normalized to beta-Actin mRNA levels). mRNA expression in WT Ras+Myc transduced MEFs was set to 1. [72]

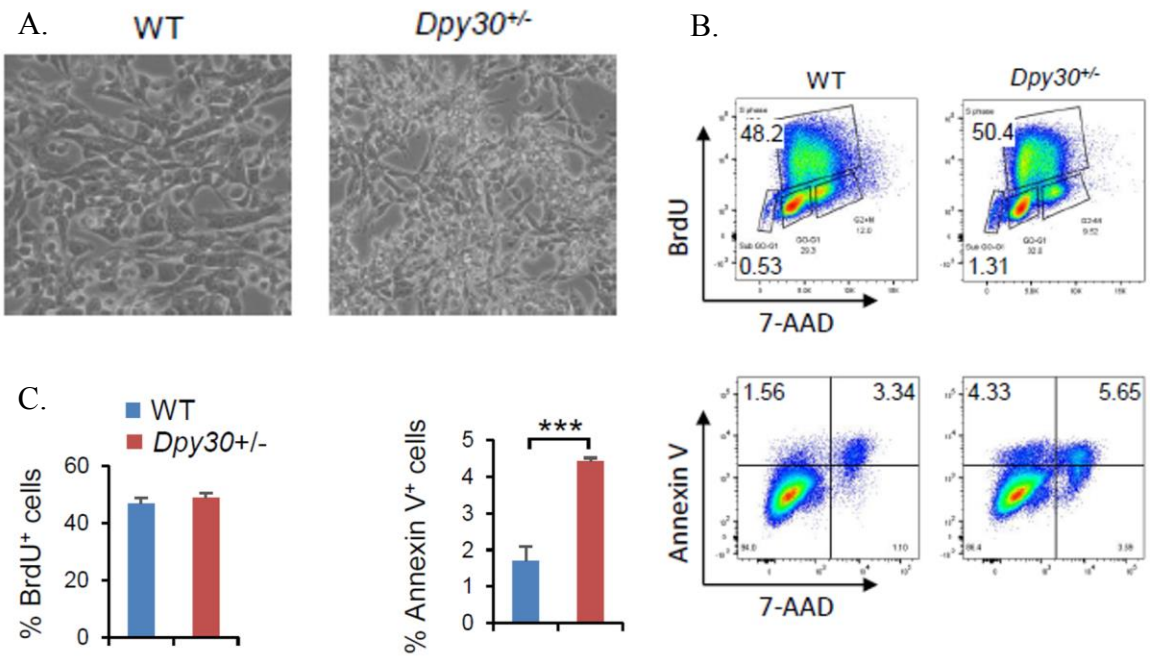
A.
WT
Dpy30+/-
B.
WT
Dpy30+/-
48.2
0.53
50.4
1.31
BrdU
7-AAD
C.
WT
Dpy30+/-
% BrdU+ cells
60
40
20
0
% Annexin V+ cells
***
5
4
3
2
1
0
1.56
3.34
4.33
5.65
Annexin V
7-AAD

D.


WESTCOTT
WT
(Left flank)
Het
(Right flank)
Mouse: 1 2 3 4 5 6 7

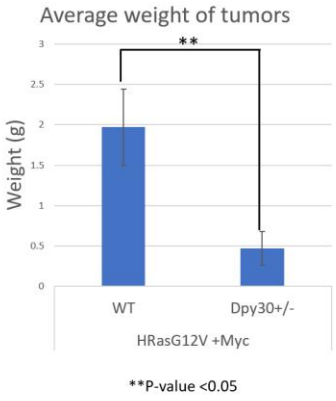
Average weight of tumors
**
Weight (g)
3
2.5
2
1.5
1
0.5
0
WT
Dpy30+/-
HRasG12V +Myc
**P-value <0.05

E.

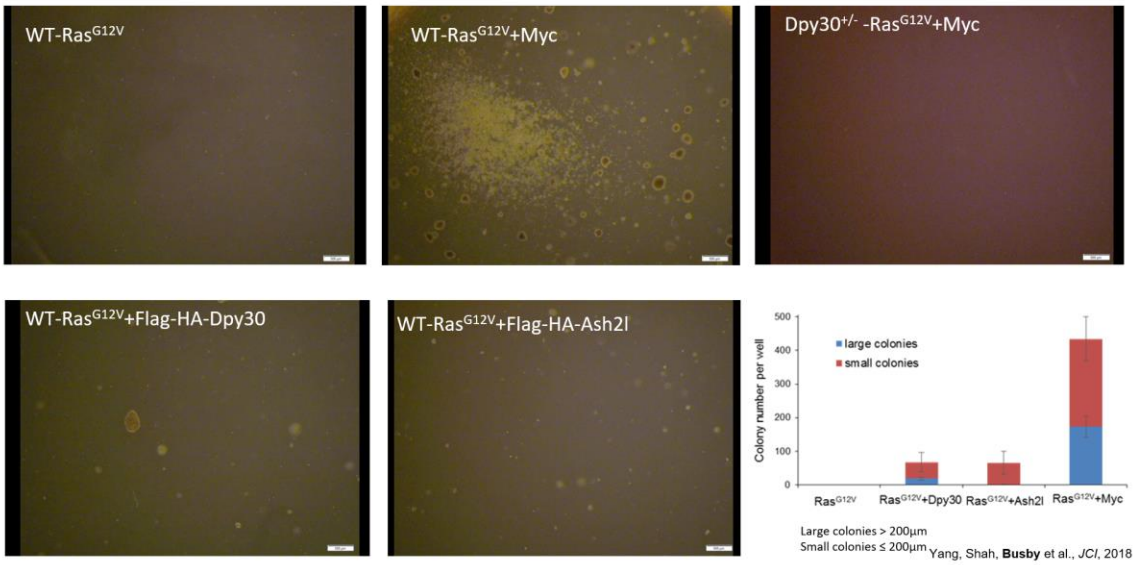
WT-Ras^{G12V}
WT-Ras^{G12V}+Myc
Dpy30$^{+/-}$ -Ras^{G12V}+Myc
WT-Ras^{G12V}+Flag-HA-Dpy30
WT-Ras^{G12V}+Flag-HA-Ash2l
Colony number per well
large colonies
small colonies
Ras^{G12V}
Ras^{G12V}+Dpy30
Ras^{G12V}+Ash2l
Ras^{G12V}+Myc
Large colonies > 200μm
Small colonies ≤ 200μm
Yang, Shah, **Busby** et al., *JCI*, 2018

F.

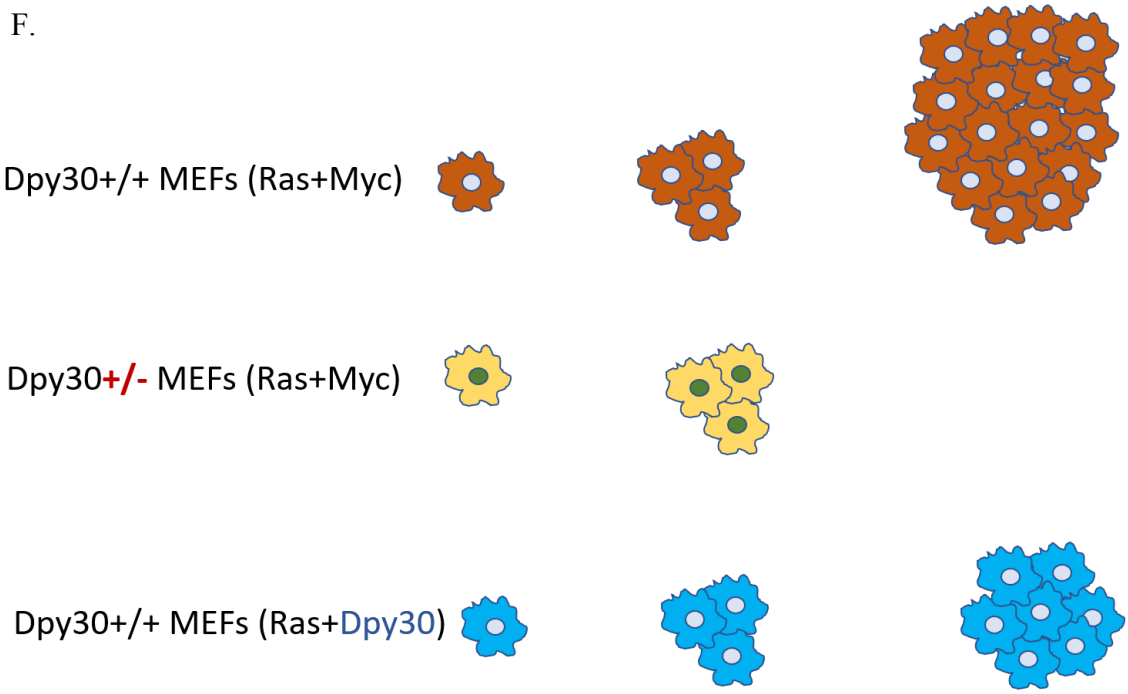
Dpy30+/+ MEFs (Ras+Myc)
Dpy30+/- MEFs (Ras+Myc)
Dpy30+/+ MEFs (Ras+Dpy30)

Figure 5. (**A)** Representative images of Ras+Myc transduced MEFs in culture. (B-C) BrdU and Annexin V staining in MEFs to determine percent proliferation and apoptosis, respectively, followed by flow cytometry analysis. (D) WT and Dpy30+/– MEFs transduced with Ras+Myc viruses were injected into the left and right flanks, respectively, of NSG mice. After weeks, tumors were measured and weighed. (E) Primary WT MEF cells were transduced with a combination ofHRas-G12V with either Flag-HA-tagged Dpy30 or Flag-HA-tagged Ash2l. These cells were subsequently subjected to the soft agar assay. Colonies sized 0.2mm or larger in diameter were to be determined to be large colonies relative to the normal size of WT MEFs transduced with Raas+Myc. (F) Myc promote tumorigenic growth in primary MEFs after transduction. The absence of one Dpy30 allele has a suppressive effect on this transformation. However, overexpression of Dpy30 promotes tumorigenic transformation independent of Myc expression. [72]

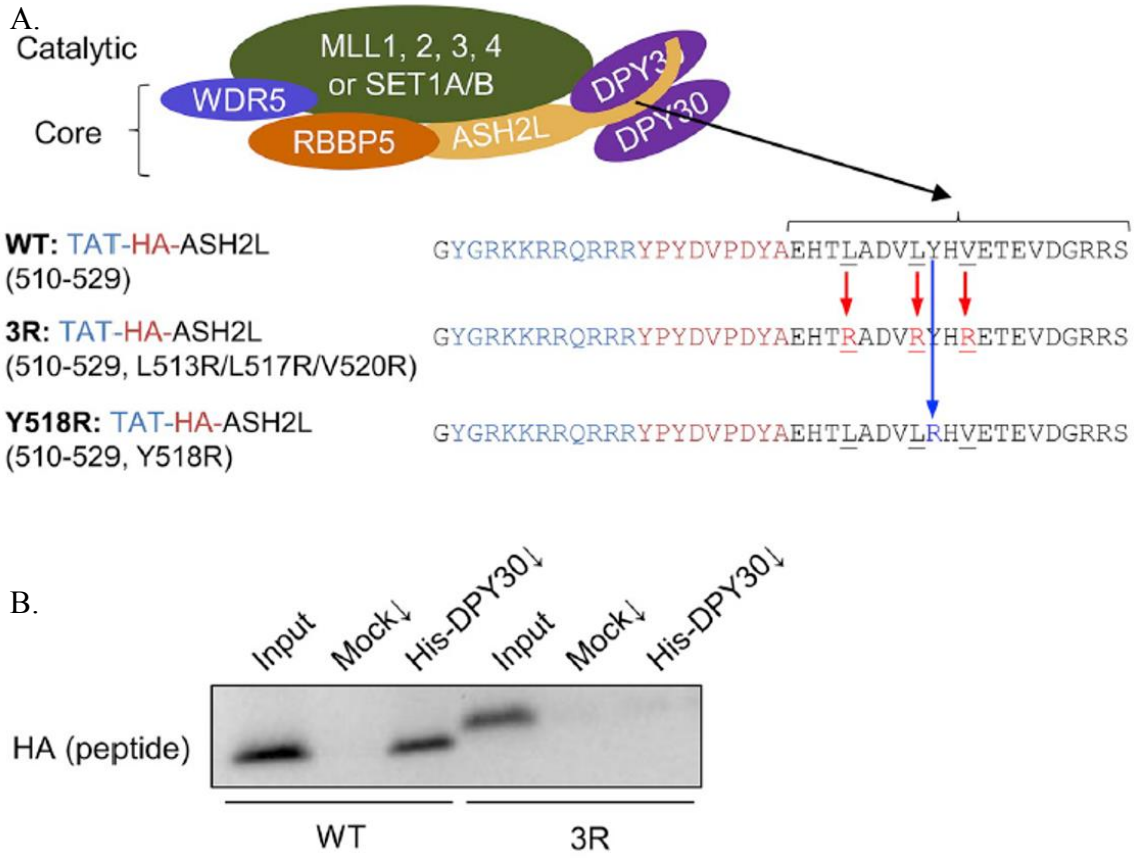

Figure 6. Peptide design and binding to Dpy30 protein. (A) Peptide amino acid sequence representing the WT peptide, 3R negative control peptide, and Y518R increased affinity peptide. (B) Protein-protein interactions between the WT and 3R peptides and His-tagged Dpy30 via nickel affinity purification. [73]

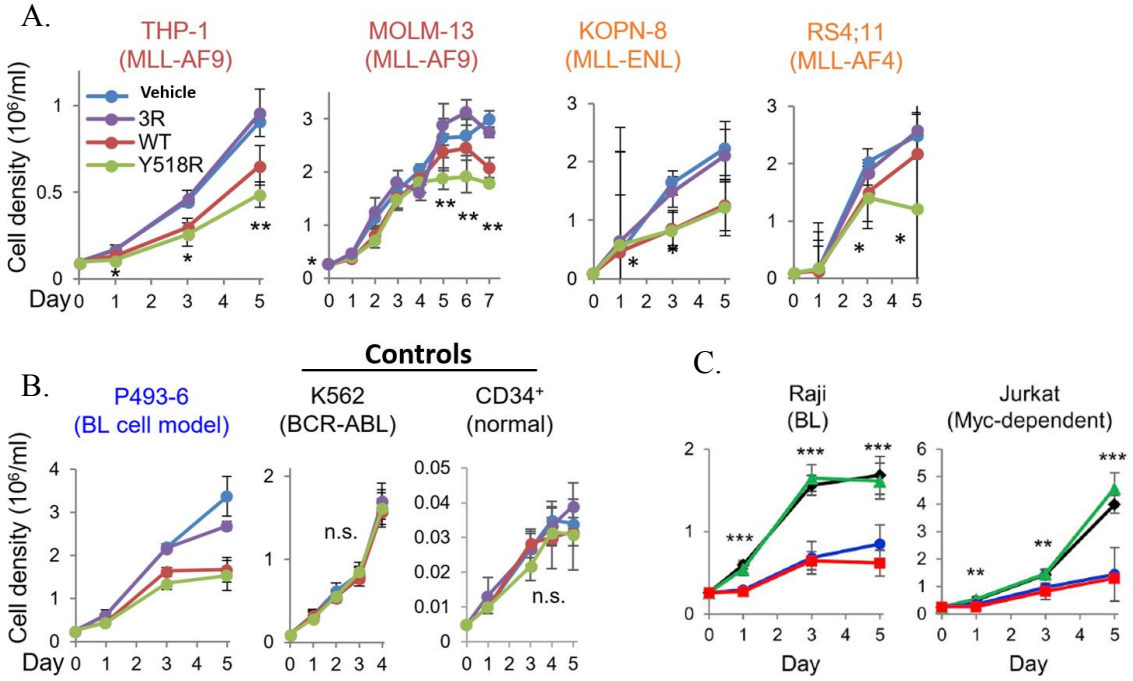
A.
THP-1
(MLL-AF9)
MOLM-13
(MLL-AF9)
KOPN-8
(MLL-ENL)
RS4;11
(MLL-AF4)
Vehicle
3R
WT
Y518R
Cell density (10⁶/ml)
Day
B.
Controls
P493-6
(BL cell model)
K562
(BCR-ABL)
CD34⁺
(normal)
n.s.
n.s.
C.
Raji
(BL)
Jurkat
(Myc-dependent)
Day
Day

D.

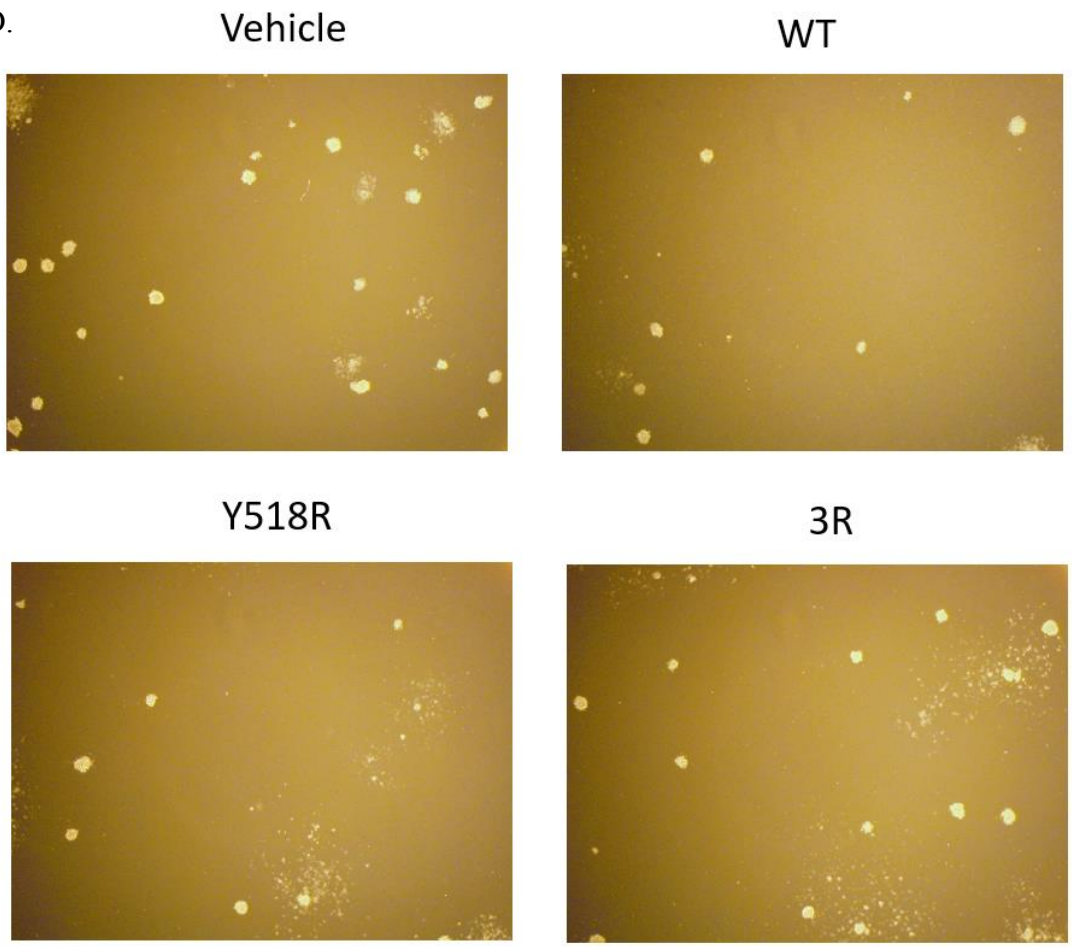

E.

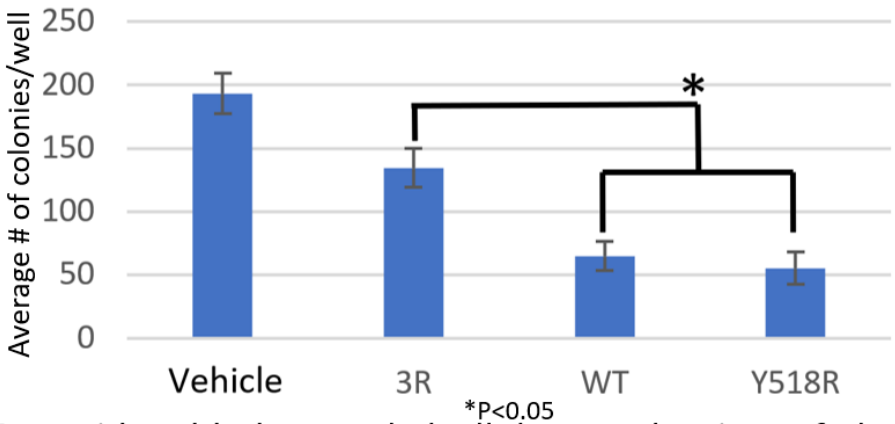

*P<0.05

100uM peptide added to methylcellulose at the time of plating.

Figure 7. (A) Growth assay was performed on a panel of MLL-rearranged leukemia cell lines treated with vehicle, WT, 3R, and Y518R peptides (SD, *$P < 0.05$, **$P < 0.01$, ***$P < 0.001$). (B-C) Growth assays were also performed onMyc dependent hematologic cancer cells line P493-6 cells, K562 leukemia cells and normal CD34+ human cells treated with the panel of peptides. Additional Myc dependent hematologic cancer cell lines Raji and Jurkat were also subjected to peptide treatment and grow assay. (D-E) Methylcellulose colony formation assay was performed on MOLM-13 cells treated with the panel of peptides. [73]

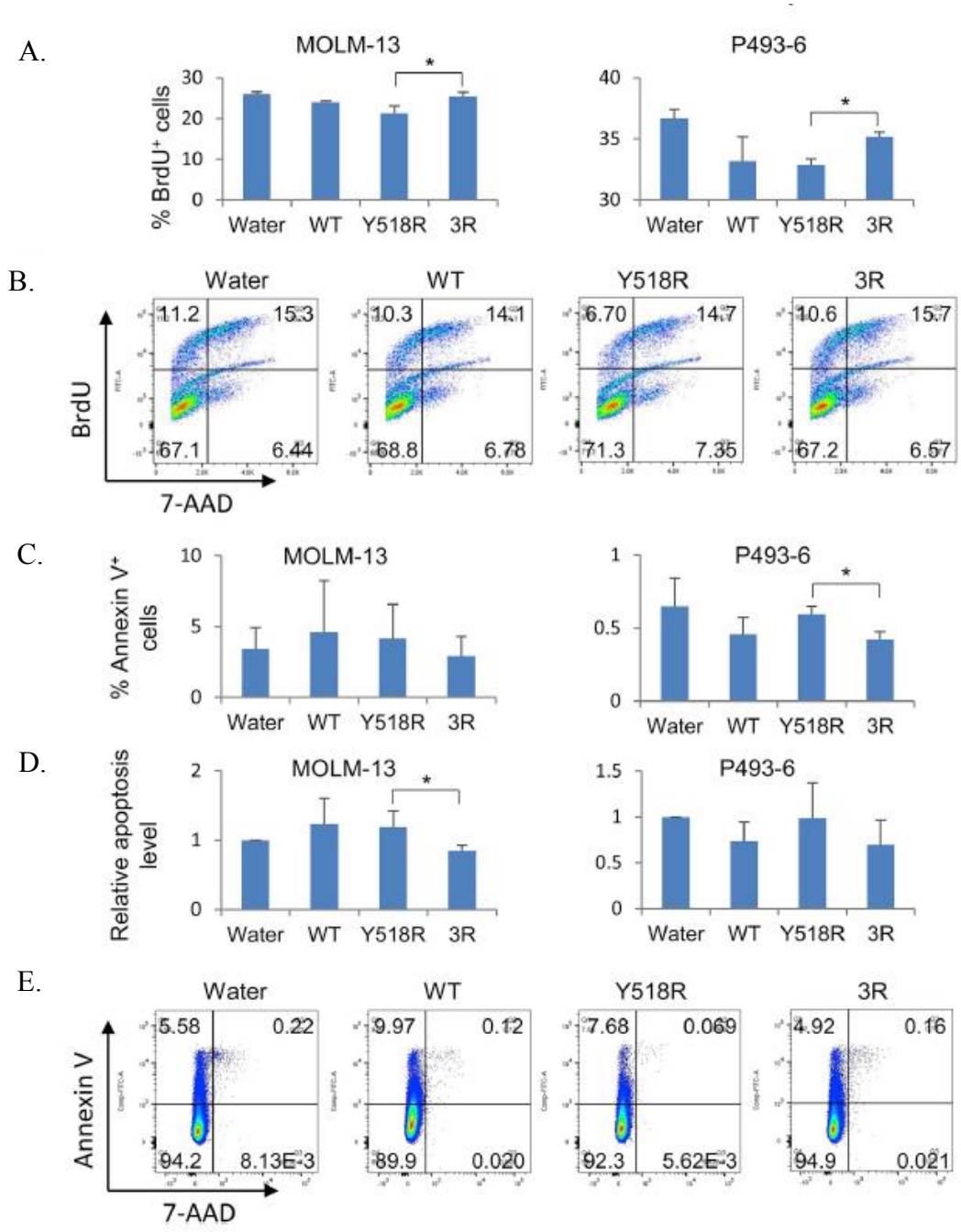

Figure 8. (A) BrdU staining to determine percent of proliferating MOLM13 and P493-6 cells treated with a panel of inhibitory peptides. (B) Flow cytometry analysis representing proliferation in MOLM-13 cells from the BrdU assays. (C-D) Annexin V staining shows percentage in apoptotic MOLM-13 and P493-6 cells treated with the panel of peptides. (E) Flow cytometry analysis demonstrates apoptotic MOLM-13 cells. [73]

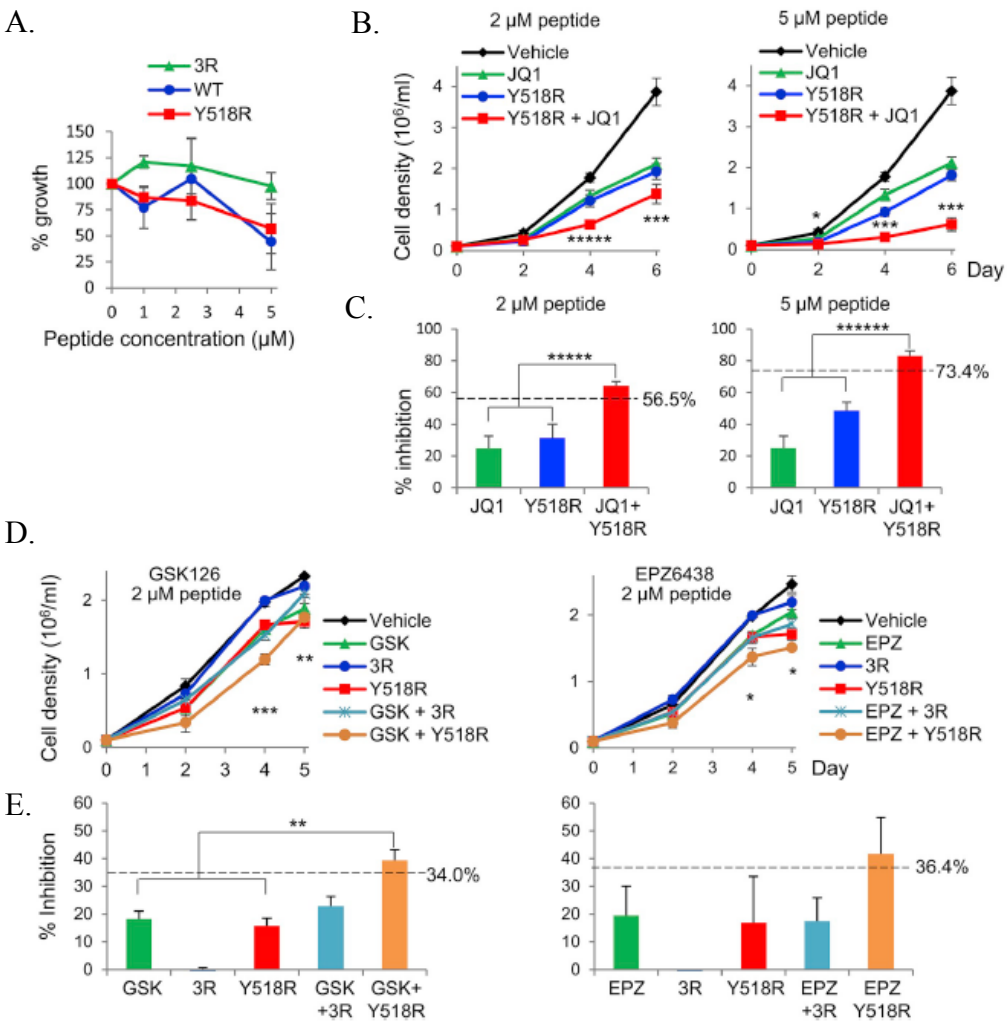

Figure 9. (A) Peptide concentrations were titrated to the MOLM-13 cells over the course of 7 days to determine the effects on the growth curve. (B-E) Effects of Y518R peptide and the BET inhibitor JQ1 (B, C) or Y518R peptide and EZH2 inhibitors GSK126 (GSK) or 20 nM of EPZ6438 (EPZ) (D, E) on growth in MOLM-13 cells growth. MOLM-13 cells were treated with 40nM JQ1 (B, C) , 5nM GSK126, or 20nM EPZ6438 (D, E). (B, D) Representative growth curves for BET inhibitors and EZH2 inhibitors, respectively. (C, E) Bar graphs demonstrate the percent inhibition in inhibitor treated cells relative to the vehicle (DMSO) treated cells (SD= **P* < 0.05, ***P* < 0.01, ****P* < 0.001, ******P* < 10^-5, *******P* < 10^-6. [73]

A.

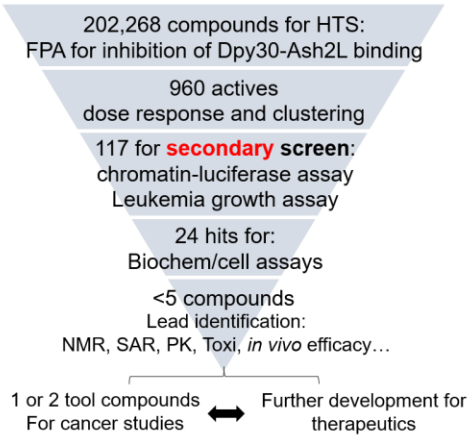
202,268 compounds for HTS:
FPA for inhibition of Dpy30-Ash2L binding
960 actives
dose response and clustering
117 for secondary screen:
chromatin-luciferase assay
Leukemia growth assay
24 hits for:
Biochem/cell assays
<5 compounds
Lead identification:
NMR, SAR, PK, Toxi, in vivo efficacy…
1 or 2 tool compounds
For cancer studies
Further development for
therapeutics

B.

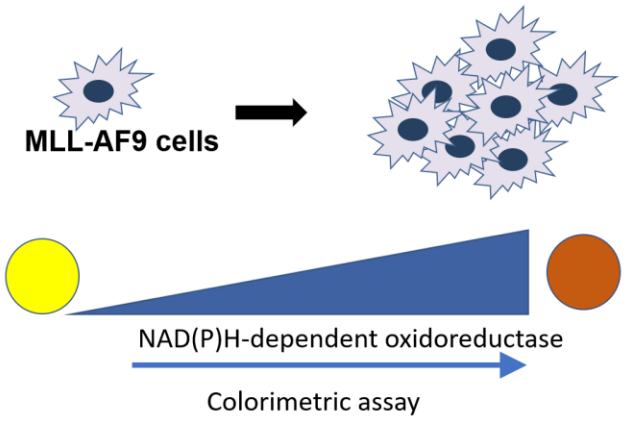
MLL-AF9 cells
NAD(P)H-dependent oxidoreductase
Colorimetric assay

C.

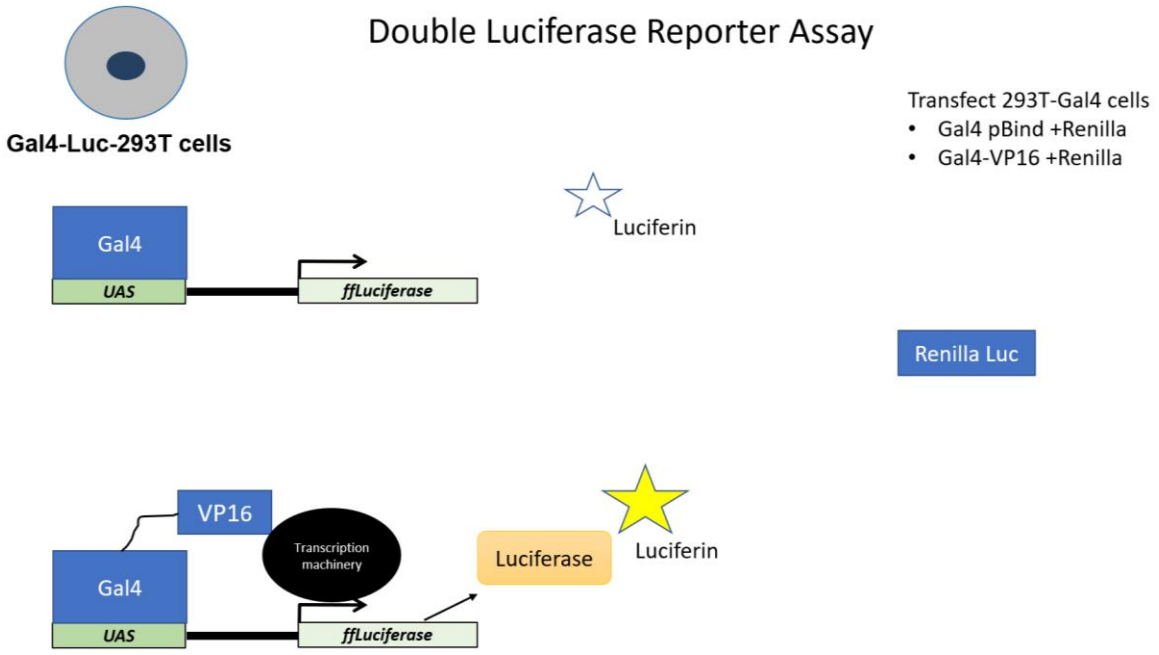
Double Luciferase Reporter Assay
Gal4-Luc-293T cells
Transfect 293T-Gal4 cells
• Gal4 pBind +Renilla
• Gal4-VP16 +Renilla
Luciferin
Gal4
UAS
ffLuciferase
Renilla Luc
VP16
Transcription machinery
Luciferase
Luciferin

D.

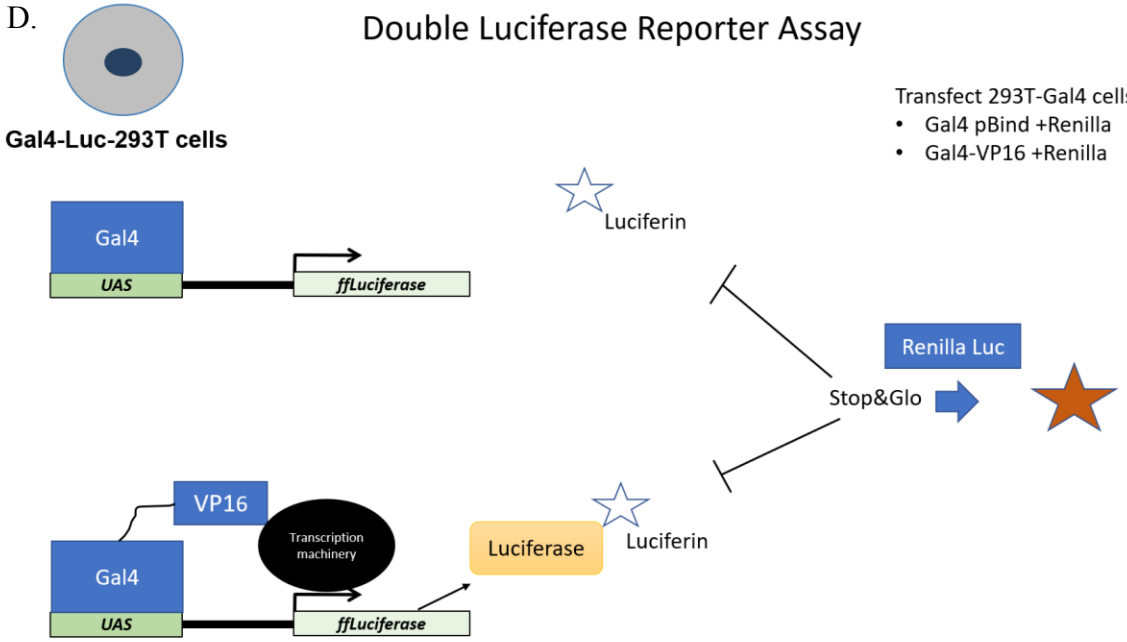
Double Luciferase Reporter Assay
Gal4-Luc-293T cells
Transfect 293T-Gal4 cells
• Gal4 pBind +Renilla
• Gal4-VP16 +Renilla
Luciferin
Gal4
UAS
ffLuciferase
Renilla Luc
Stop&Glo
VP16
Transcription machinery
Luciferase
Luciferin

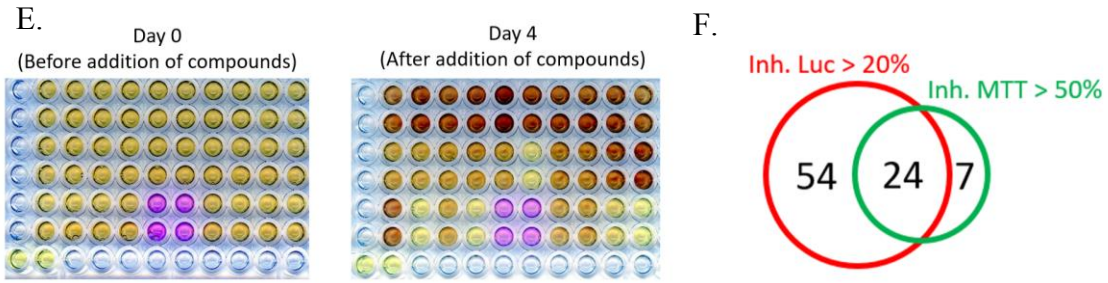

Figure 10. Small molecule inhibition of Dpy30. (A) Flow chart describing the high-throughput primary and secondary screening assays. (B) Model of the MTT secondary screen assay. (C-D) Model of the Dual Luciferase Activity (DLA) secondary screen assay. (E) MTT colorimetric results for the first round of compounds screened. All compounds were tested in duplicate at 1μM and 10μM each. (F) 24 compounds were identified to meet the threshold of inhibition for both MTT and DLA assays.

CHAPTER 7

DISSECTING THE MECHANISMS THAT UNDERLY DPY30 FUNCTION IN THE SET1-MLL COMPLEX

Myc-driven lymphoma cells express high levels of the Set1-MLL non-catalytic core subunits, including DPY30 and ASH2L [106]. DPY30 heterozygosity impairs lymphomagenesis in Eμ-Myc mice as well as tumorigenic transformation of MEFs by Ras+Myc expression [106]. We hypothesize that both Dpy30 and Ash2l are required at elevated levels in a stoichiometric relationship to promote pathogenesis of Myc-dependent cancers. One future direction of this project is to determine if Dpy30 overexpression is important for increased ASH2L interaction or if high levels Dpy30 promote tumorigenesis via other mechanisms. To determine if Dpy30 promotes tumorigenic transformation by regulating H3K4 methylation, we would transduce *Dpy30*+/+ and *Dpy30*+/- MEFs expressing Ras+Myc with constructs to express wild type Dpy30 or a Dpy30 mutant, P77A, P78A, P80A (3PA), that fails to bind to Ash2l [31, 96, 97]. These three proline residues are located within the C-terminal region of Dpy30 that connects the last two alpha helices of the protein sequence and allow for dimerization and binding to Ash2l [31, 96, 97]. These cells would then be subjected to both anchorage-independent colony formation assays as well as subcutaneous injection into NSG immune deficient mice. This data would further support our findings from the peptide inhibition of the Dpy30-Ash2l interface. We also hypothesize that overexpression

of wild type Dpy30 would rescue tumorigenic growth of Dpy30 +/- Ras+Myc MEFs while expression of the Dpy30-3PA mutant, unable to bind to Ash2l, would fail to rescue tumorigenicity of Ras+Myc MEFs.

We also consider the role of Ash2l hyperactivation in Myc-driven tumorigenesis. To determine if Ash2l levels influence normal hematopoiesis and lymphomagenesis similar to Dpy30 levels, we would compare life span, body weight, spleen weight, and blood profiles between *Ash2l+/+, Ash2l+/-, Eμ-Myc* and *Eμ-Myc; Ash2l+/-* littermates. We hypothesize that Ash2l heterozygosity would impair proliferation and induce apoptosis in B-cells on an *Eμ-Myc* background [103]. Previous studies show that Ash2l binds directly to oncogenic Myc and associates with the tumor suppressor p53 [82, 102, 103]. Thus, Ash2l may play an integral role in promoting Myc dependent function in cancer cells in the absence of p53.

Dpy30 haplo-insufficiency impairs tumor formation of MEFs transformed by co-transduction of oncogenic Ras and c-Myc. Another future direction along this path would be to determine if Ash2l heterozygosity also impairs tumor formation in transformed MEFs. Due to the relationship between Ash2l and p53, this could be extended to ex vivo transformation of Ash2l MEFs with a dominant negative p53 construct in combination with oncogenic Ras. The SPRY domain of Ash2l binds to both Dpy30 as well as RBBP5, which binds directly to the catalytic subunit in each SET1-MLL complex [96, 107]. It is possible that Ash2l promotes tumorigenic transformation by providing a docking site for Dpy30 activity in the Set1-MLL complex. Overexpression assays using *Ash2l+/+* and *Ash2l+/-* Ras+Myc MEFs transduced with constructs for conditional expression of either wild type Ash2l, RBBP5-binding defective Ash2l mutant (R343A), or a C-terminal Ash2l

truncation mutant (ΔC30) lacking the Dpy30 binding motif would further dissect the mechanism through which Ash2l functions to promote tumorigenesis [31, 83, 96]. We hypothesize that Ash2l heterozygosity would inhibit transformation in MEFs as we have observed in Dpy30+/- MEFs and that expression of either Ash2l mutant would fail to restore tumorigenic potential in these cells. Furthermore, examining the interaction between the subunits of the Set1-Mll non-catalytic core module would provide a better understanding of the mechanisms disrupted by small molecule inhibition.

SET1-MLL complexes regulate multiple levels of H3K4 methylation, including mono-methylation (H3K4me1), a prominent chromatin mark found at enhancers along with H3K27 acetylation, BRD4, and MED1 [108-110]. Enhancers are distal genomic elements that drive and maintain the expression of many of their associated genes by bringing developmental, tissue-, and context-specific transcription factors into close-proximity with promoters [16, 111-115]. It has been reported that cancer cells acquire oncogenic enhancers and super enhancers, which are large clusters of enhancers occupied by high levels of chromatin marks, to promote pathogenesis [16, 111-115]. Super enhancers (SEs) are highly sensitive, relative to typical enhancers (TEs), to perturbation of enhancer marks due to a dependence on cooperative binding of chromatin regulators at these sites [16, 111-115]. This is evident by the pharmacological inhibition of BRD4 binding to acetylated histones, which was identified as an epigenetic vulnerability in multiple myeloma cells [16]. DPY30 facilitates H3K4me1, thus we hypothesize that the elevated interaction between DPY30 and ASH2L may be critical for regulating TE and SE associated genes in tumorigenesis [92, 109]. Using our Dpy30 and Ash2l heterozygous models in mice and MEFs, we could determine if elevated levels of the

core module function to direct Set1-Mll complex in H3K4me1 at these Myc-specific enhancers and super-enhancers. Furthermore, Dpy30 depletion in human, zebrafish and mouse cells all results in reduction of global H3K4 methylation including H3K4me1 [92]. As super enhancers have been shown to regulate cell and context specific gene expression, including oncogenic drivers, it is important to understand the function of DPY30 at these genomic elements, especially in cancer cells.

CHAPTER 8

BAF45A ACTIVITY IN THE BAF CHROMATIN REMODELING COMPLEX

The mammalian SWI/SNF (BAF) chromatin remodeling complex slides nucleosomes into an open conformation. Cells need to compact over 2 meters of DNA into a ~5μm diameter nucleus [116]. This compaction takes the effort of histone modifications, structural RNA, and DNA methylation [2, 116]. However, after compaction, coding genes need to become accessible for transcriptional activation. The process of relaxing the DNA around histones in these regions is made possible in part by the ATPase-dependent mechanisms of the BAF complex [116]. The BAF complex relaxes the DNA around the histone octamers by two mechanism referred to as twist-diffusion and loop-recapture [116-118]. The twist-diffusion mechanism suggests that the DNA must untwist and separate almost completely from the histones before re-twisting back into place [116-118]. However, the DNA may instead loosen around the histone octamers [116-118]. A recent study generated a model to show that both mechanisms are possible, and this depends on multiple factors including metabolism, sequence specificity, and histone modifications [119]. However, the mechanism of chromatin remodeling is not fully understood. Chromatin remodeling assays using purified histones and BAF complex subunits do not require a full complement of non-catalytic subunits for remodeling [116]. Like the SET1-MLL complex, the BAF complex promotes active gene expression and crosstalk with other chromatin factors. BAF chromatin remodeling

complexes are recruited to promoters where activating histone acetylation occurs [118, 119]. However, methylation of histone H1 by the repressive PRC methyltransferase complex stabilizes chromatin in an in active confirmation, blocking the activity of BAF chromatin remodelers [118]. Furthermore, the BAF complex regulates tissue specific gene expression through multiple subunit assemblies [120]. These studies further highlight a need to better understand the mechanism that govern complex interactions between chromatin modulators.

BAF45A Homology and PBAF Assembly

The 2MDa BAF complex is comprised of 15 different subunits derived from 29 homologs [120]. Phf10 (PHD Finger Protein 10), also known as Baf45a, is one of four Baf45 homologs in addition to Baf45B (Dpf1), Baf45C (Dpf3), and Baf45D (Dpf2) [121]. One distinguishing difference between Baf45A and the other Baf45 homologs is that Baf45A associates with the poly-bromo BAF (PBAF) sub-complex, whereas Baf45B, Baf45C and Baf45D associate with canonical BAF complex assemblies [121, 122]. Like other BAF subunits, BAF45 homologs exhibit tissue specific expression patterns [123]. During nervous system development, for example, the neuro progenitor specific BAF complexes (npBAFs) contain BAF45A, BAF45D, and BAF53A, which are replaced by BAF45B, BAF45C and Baf53B respectively in mature neural-BAF complexes (nBAF) [123]. Depletion of BAF45A and BAF53A in neuro progenitor cells leads to reduced proliferation in neurons [123-125]. Although these studies suggest a class switch dependent exchange of BAF subunits at different phases of development, we do not fully understand the contributions of the individual subunits to the overall complex

function. Depletion of BAF45A in bone marrow cells does not lead to a change in the expression levels of other Baf45 homologs [121]. In addition, there appears to be a correlation between the expression levels BAF45A and BAF45D in opposition with Baf45B and Baf45C [121, 124, 125]. These studies suggest that in specific cells types, replacement of one BAF45 homolog with another is not a sufficient compensation for the function of another BAF45 subunit.

BAF45 Homolog Structure

Structural similarities and significant differences hold the information to potential tissue, cell, and context-specific function of BAF45A compared to BAF45B, BAF45C, and BAF45D. BAF45A motifs include an amino-terminal Supporter of Activation of Yellow Protein (SAY) domain and two carboxyl-terminus Plant Homology Domains (PHD) [121, 122, 126]. Like BAF45A, both BAF45B and BAF45D consist of two C-terminal PHD motifs whereas Baf45c (Dpf3) has only one PHD motif [121, 122]. However, instead of the N-terminal SAY domain of Baf45A, homologs Baf45B, Baf45c, and BAF45d contain an N-terminal Kruppel-like zinc finger (KLF) motif [121, 122, 126]. Furthermore, the SAY domain of Baf45a shares homology with the sequence and structure of the N-terminal winged helix DNA binding domain of the core BAF subunit Ini1 (Baf47) [122]. It has also been reported that Baf45a has four major isoforms. Two of which contain the consensus PHD motifs and 2 with a truncated version which removes the PHD motifs while generating a Phosphorylation-Dependent SUMOylation Motif (PDSM) [127, 128]. These features likely hold a key piece of information as to why Baf45a functions within the PBAF complex but not in the canonical Baf complex.

BAF45A Promotes Transcription

BAF45A exhibits specific activity independent of the other BAF45 homologs evident by the inclusion of a SAY domain. The SAY domain is evolutionarily conserved between *Drosophila melanogaster* SAYP (Baf45A) and mammalian Phf10 [129, 130]. In support of a role for transcriptional activation by BAF45A, SAYP recruits the Swi/Snf ATPase subunit Brahma with TFIID to couple chromatin remodeling and transcriptional initiation [129]. The resulting complex, otherwise known as BTFly is then recruited by STAT to gene promoters downstream of Jak signaling [129]. This function is facilitated through the SAY domain, which shares homology with the Baf47 WH domain, also shown to activate transcription [122, 129]. Studies also show that SAYP is able to pause transcription and the initiation of transcription by RNA PolII [130]. Future research will need to be conducted to understand the role of DNA recognition by BAF45A and how it contributes to PBAF mediated chromatin remodeling.

Gene expression during development is regulated by BAF45A. In neural progenitors and bone marrow cells, Baf45A regulates gene programs to promote cell cycle progression including activation of p27, while repressing Ccnd1 and Ccne2 expression [121, 124, 125]. Furthermore, depletion of Baf45A in gastric tumors promotes Caspase3 induced apoptosis, leading to reduced tumor size [131]. Recent studies have shown that microRNAs like mIR-23a regulates BAF45A in osteoblasts [22, 132]. In addition, Baf45A is repressed by mIR-409-3p in gastric cancer to promote apoptosis [133]. These studies suggest that Baf45a activity regulates tissue and context specific

gene activation. This provides a basis to further investigate PBAF specific activity at the biochemical and spatiotemporal level.

Chromatin Instability Around the BAF45A Gene Locus Leads to Disease

Chromosomal deletions and frameshifts in the Baf45A genomic region has been associated with uveal melanoma and leads to poor prognosis [134]. This comes in the form of a deletion in the Chr 6q27 region where the Baf45A genomic DNA sequence resides [134]. The loss of this region leads to lowered survival rate and increased metastasis [134]. In addition to melanoma, deletion of the 6q27 chromosomal region in patients leads to morphological changes in the brain and many other development related diseases [134-138]. Although these developmental abnormalities are largely associated with other genes within the region, except for in uveal melanoma, it is important to consider the consequences of losing Baf45A on development and disease.

BAF45A MEDIATED CHROMATIN REMODELING PROMOTES TRANSCRIPTIONAL ACTIVATION FOR OSTEOGENESIS AND ODONTOGENESIS

by

THEODORE BUSBY, TANNER GODFREY, MOHAMMAD REHAN, BENJAMIN WILDMAN, ASHLEE WILLIAMS, DELORES STACKS, YUECHUAN CHEN, QUAMARUL HASSAN

Theodore Busby, Tanner Godfrey, Mohammad Rehan, Benjamin Wildman, Ashlee Williams, Delores Stacks, Yuechuan Chen, Quamarul Hassan. Baf45a mediated chromatin remodeling promotes transcriptional activation for osteogenesis and odontogenesis (Manuscript in preparation)

CHAPTER 9

BAF45A MEDIATED CHROMATIN REMODELING PROMOTES TRANSCRIPTIONAL ACTIVATION FOR OSTEOGENESIS AND ODONTOGENESIS.

Abstract

Chromatin remodeling is vital for lineage commitment through activation of tissue specific transcription programs. A key step in this remodeling and gene activation process is through SWI/SNF (BAF) chromatin remodeling, which functions to slide or eject nucleosomes allowing for physical accessibility of lineage specific transcriptional machinery involved in gene expression. Chromatin regulation specific to mineralized tissues is an understudied avenue of gene regulation. This study shows that Baf45a and Baf45d, two Baf45 homologs belonging to the ATPase-dependent SWI/SNF chromatin remodeling complex, are preferentially expressed in osteoblasts and odontoblasts compared to Baf45b and Baf45c. Recently, numerous biochemical studies have revealed that Baf45a associates with Polybromo-associated BAF (PBAF) complex, however the Baf45d subunit belongs to polymorphic BRG1-associated factor (BAF) complex. Protein profiles of primary osteoblast differentiation uncovered significant increase of PBAF subunits during in vitro osteogenesis. Chromatin immunoprecipitation (ChIP) in bone marrow stromal cells showed that histone H3K9 and H3K27 acetylation modifications support that Baf45a and Baf45d are important and allows BMSCs commitment to

osteoblast lineage differentiation. Evidence indicates that tissue specific transcription factors regulate or interact with discreet BAF subunits to orchestrate distinct transcription programs. Bone and tooth specific RUNX2 binding to the Baf45a and Baf45d transcriptional start site indicate Runx2 regulation is critical for BAF mediated chromatin remodeling. Furthermore, depletion of Baf45a in osteoblasts and odontoblasts leads to markedly altered chromatin accessibility and gene regulation. These data indicate that Baf45a promotes PBAF mediated mechanisms in mineralized tissues.

Introduction

Cellular differentiation is an essential part of tissue development. From stemness to terminally differentiated cell states, many pathways and cellular processes must be orchestrated in concert to ensure that the correct patterning and tissue specificity occur. These events are regulated in part by tissue specific epigenetic regulation and the resulting gene expression patterns [1, 2]. Chromatin regulation occurs through a series of cross talk events between active and repressive cell type specific regulators [2, 3]. The Brahma-associated factors (BAF) chromatin remodeling complex is an ATPase-dependent epigenetic machine with affinity to bind nucleosome, that promotes gene expression around active promoters and enhancers [4-6]. Tissue specific regulation by the BAF complex arises from the 29 homologs that make up this 2 MDa complex [4, 5, 7]. Each BAF complex consists of 15 out of 29 homologs including either Brg1 or Brm as the ATPase subunits [4-6, 8]. Many studies have aimed to characterize tissue specific BAF complex assemblies during neurogenesis, hematopoiesis, immune responses, and embryonic stem cell function [4, 5, 9-12]. However, very little is known about the BAF complex in differentiation or maintenance of mineralized tissue [13-17].

Osteogenesis is the process of bone formation [18, 19]. An important step in this process is the differentiation of mesenchymal stem cells into osteoblasts [19, 20]. During maintenance of the bone, there is a constant balance between mineralization by osteoblasts and resorption by chondrocytes, which becomes unbalanced in osteoporosis patients [14]. Much of what we know about the regulation of this gene program comes from our understanding of bone lineage specifying transcription factors such as Runx2 and Osterix/Sp7 [21]. Furthermore, growing studies about the epigenetic regulation involved in osteogenesis primarily focus on histone post-translational modification and non-coding RNAs [22]. However, the tissue specific mechanisms involved in the openness of the histones around active genes is understudied in osteogenesis and craniofacial development.

Odontogenesis is a process in which cells derived from the neural crest cell lineage differentiate into a mesenchymal cell like phenotype and develop into dental pulp cells, including odontoblasts [23, 24]. Odontoblasts produce dentin, the major mineral portion of the tooth [23, 24]. During differentiation, pre-odontoblasts deposit pre-dentin, which promotes terminal differentiation of the pre-odontoblasts into mature odontoblasts [25, 26]. Mature odontoblasts then convert the pre-dentin into mature dentin [25, 26]. Like osteoblasts, little is known about the epigenetic regulation in odontoblasts, and less is known about chromatin remodeling in either tissue type [25-28].

Previous studies demonstrate that the BAF complex subunit BAF45A promotes osteogenesis [13]. There are four BAF45 homologs including Phf10 (BAF45A), Dpf1 (BAF45B), Dpf3 (BAF45C), and Dpf2 (BAF45D) [29]. Some reports indicate that BAF45D may be expressed ubiquitously and is part of the canonical BAF complex [30,

31]. However, other studies have shown that a homolog switch occurs from BAF45A and BAF45D in neuro-progenitors to BAF45B and BAF45C in terminally differentiated neurons [12, 32, 33]. Interestingly, BAF45A has been identified as an integral subunit of the Polybromo-BAF (PBRM1/BAF180) containing PBAF sub-complex [8, 29]. BAF45a is unique from other BAF45 subunits in its N-terminal DNA binding SAY domain, as opposed to the Krupple like DNA binding domains of the other BAF45 homologs (Figure 1) [29]. In this chapter, we show that BAF45A is important for promoting tissue specific gene expression during differentiation in cells of mineralized tissues. Deletion of BAF45A in osteoblasts affects chromatin landscape around gene promoters and enhancers important for mineral deposition. Furthermore, we begin to dissect the global gene expression profiles regulated by the expression of BAF45A in osteoblasts and odontoblasts.

Results

BAF45A is a Preferred Subunit of the Swi/Snf Chromatin Remodeling Complex During Osteoblast Differentiation

Baf45a associated chromatin remodeling complexes have been identified as important regulators during osteogenic differentiation [13]. Changes in the chromatin landscape of a gene are indicative of shifts in gene expression and the propensity for a gene to be expressed [2]. To dig deeper into this relationship, we examined ChIP-seq data from primary osteoblasts over the course osteogenic differentiation (Figure 2) [34]. The

genomic region around the Baf45a gene locus is active during osteogenic differentiation. High levels of the active histone modifications H3K27ac and H3K9ac marked to the promoter regions of the Baf45a and Baf45d gene loci (Figure 2A and D) [34]. This was also evident by the expression levels of Baf45a and Baf45d (Godfrey et al. in preparation, Figure 2F). Absences of the repressive histone modifications H3K27me3 and H3K9me3 around the Baf45a and Baf45d gene loci further demonstrated an active state of these genes during osteoblast differentiation (Figure 2A and D) [34]. In contrast, the chromatin landscape around Baf45c was repressed (Figure 2C) [34]. The Baf45c locus displayed the highest and most pronounced peaks among the repressive marks H3K9me3 and H3K27me3 but lacked any activating chromatin marks (Figure 2C) [34]. Interestingly the Baf45b locus displayed moderate levels of both active and repressive chromatin marks (Figure 2B) [34]. RNA levels for Baf45b are close to negligible at the start of differentiation and are reduced to undetectable levels over the course of osteogenic differentiation (Figure 2E) [34]. These results indicate that Baf45a as well as Baf45d are the selected subunits of the osteogenic BAF complexes.

Osteogenic Differentiation Promotes the Expression of PBAF Complex Subunits

Polybromo1 (Pbrm1) containing subcomplexes (PBAF) are similar in function to the canonical BAF (cBAF) complexes with a few exceptions [8, 35]. One of which is the incorporation of BAF45A as a subunit [8, 36]. Since Baf45a was an expressed factor in osteoblasts, we hypothesized that additional PBAF sub-complex subunits would also be active during osteogenic differentiation [13]. Protein expression of subunits specific to the PBAF complex were increased as a result of osteogenic differentiation (Figure 3A)

[34]. This was further illustrated by the active chromatin landscape around PBAF subunits Pbrm1 (Baf180), Arid2 (Baf200), and Brd7 (Figure 3B-C) [34]. Smarca4 (Brg1) and Smarcc1 (Baf155), subunits that comprise both the cBAF and PBAF complexes, also displayed active chromatin landscapes with increased protein expression levels (Figure 3A, E-F) [34]. This data suggests that osteogenic differentiation induces the expression of PBAF complex subunits. In addition, Runx2 protein levels were elevated and the chromatin around the Runx2 genomic locus displayed active chromatin marks, confirming that the PBAF complex is needed at the same time during differentiation as osteogenic lineage markers (Figure 3A, E-F) [34].

BAF45A Expression is Important for Regulating Chromatin and Gene Expression in Osteoblasts

The PBAF complex, like the cBAF complex, promotes gene activation. We hypothesized that changes in Baf45a expression levels would affect RNA expression in osteoblasts. Overexpression of Baf45a in MC3T3-E1 osteoblast cells (MC3T3) induced the upregulation of osteogenic marker genes Alkaline phosphatase (Alp), Runx2, and Sp7 (Figure 4A). This was corroborated by the upregulation of Col1a1, Osteocalcin, and Osteopontin, bone related extracellular matrix genes (Figure 4A). We also saw an upregulation of developmental patterning genes in the Hox cluster (Figure 4A). Additionally, overexpression of Baf45a also promoted a gene program to inhibit cell cycle progression (Figure 4B). This shift in gene expression profile indicates that Baf45a overexpression promotes cells to no longer go through proliferation and to begin the differentiation process.

We next wanted to determine if the loss of Baf45a would affect gene expression during osteogenesis. We deleted loxP flanked alleles of Baf45a (Baf45aflox/flox) in primary calvaria osteoblasts using a 4-hydroxytamoxifen inducible Cag-cre genetic background followed by induction of osteogenic differentiation [37]. RNA sequencing revealed global gene expression changes at day 10 of differentiation (Godfrey et al. in preparation). These data indicate that Baf45a regulates genes involved in mineralized tissue development and maintenance.

The function of the PBAF complex is to promote an active and open chromatin landscape. We hypothesized that loss of Baf45a would alter chromatin accessibility. Loss of Baf45a leads to a decrease in accessibility at the Runx2 and Sp7 gene loci (Figure 4C). Dramatic reduction of accessibility at Klf4 and Atf4 gene loci was observed as well (Figure 4D). The change in these transcription factors represent a change in the ability for these cells to differentiate. We also found that gene loci involved in osteogenesis and odontogenesis also underwent reductions in chromatin accessibility (Figure 4E). Chromatin accessibility at the gene body of Spp1/Osteopontin became inaccessible as a result of Baf45a loss (Figure 4E). An enhancer region between the Dmp1 and Dspp gene loci was modestly reduced (Figure 4E). In addition, enhancer regions associated with the enamelin (Enam) genomic region had reduced chromatin accessibility (Figure 4F). We performed ChIP-QPCR in Baf45a knock out osteoblasts at the Enam downstream enhancer region. We probed for H3K27ac at this region and found that the histone acetylation was dramatically decreased at both day 3 and day 10 of osteogenic differentiation (Figure 4G). This data demonstrates that Baf45a is important for

regulating the chromatin landscape in osteoblasts. Furthermore, this indicates that Baf45a may also regulate genes involved in tooth development.

Mineralization of the Tooth is Modestly Reduced by the Loss of BAF45A

We hypothesized that Baf45a would promote tooth mineral density. Thus, we deleted Baf45a by breeding Prrx1-Cre into a Baf45aflox/flox background to target early bone development [37]. Molars from two-month-old male mice had a moderate reduction of tooth mineralization in the enamel and dentin layers (Figure 5A-B). However, we did not see a difference in the mandible bone density of these same mice (Figure 5A-B). In 2-month old female mice, we did not observe a difference in the mineral density in either the mandible or the molars (Figure 5C-D). We postulated that we were targeting Baf45a in the early mesenchyme and potentially not in the tooth.

Although Baf45a knock out caused dramatic gene expression changes but did not reflect the results observed as it related to craniofacial bone development, we still suspected that Baf45a was an important driver of differentiation. One potential reason for this discrepancy may be due to compensatory regulation from another Baf45a homolog. Evidence of homolog switching comes from previous studies showing that the expression of Baf45a and Baf45d switch to Baf45b and Baf45c during development in early neurogenesis [12, 32]. Considering the moderate levels of both active and inactive chromatin markers deposited at the Baf45b gene locus, we hypothesized that Baf45b may be a poised gene (Figure2C). Thus, further examination of Baf45b gene expression from

the mandibles and dental pulp cells of Prrx1-Cre ; Baf45aflox/flox mice would determine if this a compensatory mechanism.

BAF45A Regulates Gene Expression in Odontoblast Cells

Our results suggest a relationship between Baf45a as a subunit of the PBAF complex and osteoblast differentiation. To identify Baf45a homologs important for odontoblast function, we subjected OD21 odontoblast cells to odontogenic differentiation for twenty days. Baf45a RNA was expressed at high levels early during differentiation before lowering by about 50% at around day 12 of differentiation, corresponding to the mineral maturation period (Figure 2A and Figure 6A). Relative to Baf45a expression, Baf45b and Baf45c were negligible, similar to what was observed in osteoblasts (Figure 6B). Baf45d was also expressed in odontoblast, though to a lower relative level compared to Baf45a (Figure 6C). This suggests that like osteoblasts, Baf45a and Baf45d are preferred subunits of the BAF complex in odontoblast cells. Indeed, Bmp2 treatment of OD21 cells promoted Baf45a expression similar to that of Col1a1 (Figure 6D and F). Although genes that are promoted by BMP2 signaling tend to be repressed by TGF-beta signaling, treatment of OD21 cells with TGF-beta did not inhibit Baf45a expression (Figure 6D). In contrast, for Baf45d, Bmp2 induction did not affect RNA expression while TGF-beta significantly inhibited Baf45d (Figure 6E). This data suggests Baf45a is an important subunit of the odontogenic BAF complex.

Tissue specific BAF complex assemblies promote gene programs to define cell type identity [4-6, 9-12]. To understand how Baf45a expression regulates odontoblast

gene expression, we depleted Baf45a in OD21 cells by stable shRNA depletion [26]. Baf45a depletion caused a reduction in gene expression of transcription factor genes Klf4, Atf4, and Runx2 (Figure 6F). In addition, we saw that Baf45a knock down cells had reduced RNA expression of Dmp1 and Dspp, genes important for dentin matrix formation (Figure 6G). We also saw that the expression levels of Baf45d was decreased (Figure 6H). While these changes suggest that, like osteoblasts, Baf45a is important for odontoblast cells, we wanted to take a global look at the effect of Baf45a depletion on RNA expression.

We next performed RNA-seq analysis on control and Baf45a shRNA depleted OD21 odontoblast cells. Knockdown of Baf45a led to a global shift in the gene program (Figure 7A). While there remained overlap in expression between control and Baf45a knockdown cells, 1049 gene were no longer expressed in Baf45a depleted cells and there was a gain of expression in 457 genes compared to control cells (Figure 7B). Amongst these genes, the gene program to promote cell cycle progression was reduced in Baf45a depleted OD21 cells (Figure 7C). Interestingly, all Baf45 homologs were decreased in Baf45a knock down cells compared to control (Figure 7D). RNA transcript levels of tooth matrix genes Enam and Dmp1 as well as transcription factor genes Atf4, Runx2, and Myc were also decreased (Figure 7D). However, bone specific genes Spp1, Sp7, and Bglap were increased resulting from Baf45a depletion (Figure 7D). We also found that Baf45a reduction led to an increase in cell cycle progression genes Ccnd1 and Cdkn1a (Figure 7D). These results support a mechanism for Baf45a to regulate transcriptional activation in odontoblasts during differentiation, as we observed in osteoblasts.

Discussion

This study demonstrates that BAF45A is an important Baf45 homolog for BAF chromatin remodeling in both tooth and bone. Baf45a expression regulates gene programs to promote mineralized tissue development and maintenance. This regulation is in part due to BAF45A function in PBAF mediated chromatin accessibility in osteoblasts (Figure 8). The loss and depletion of Baf45a in osteoblasts and odontoblasts, respectively, led to global gene expression changes. Taken together, Baf45a and Baf45d contribute to the assembly of BAF complexes specific to mineralized tissues.

RNA-seq analysis showed that Baf45a expression levels effect global gene expression changes. However, this data requires a deep analysis to fully understand what these changes mean. To this point, our initial QPCR analysis in OD21 cells depleted of Baf45a indicated a decrease in the expression levels of Sp7, a lineage specifying transcription factor in osteogenesis, whereas our RNA-seq data showed the opposite. In addition, RNA expression data suggests a relationship between Baf45a and cell cycle progression. Overexpression of Baf45a led to a down-regulation of Ccnd1 (Cycin-D1) in osteoblasts while depleting Baf45a in odontoblasts led to an upregulation of Ccnd1[38]. Although this relationship indicates that Baf45a may inhibit proliferation, we saw Cdkn1a, an inhibitor of cell cycle progression, was also increased in odontoblasts depleted of Baf45a [38]. Thus, unraveling the information from our combined RNA-seq analysis will provide a wider breadth of understanding of Baf45a tissue specific regulation as well as its role in the PBAF complex.

A current avenue of research focuses on the assembly of the BAF complex. As each complex is assembled from 15 subunits that derive from about 29 different

homologs, it is important to understand tissue specific assemblies and how each contributes to chromatin accessibility in a spatiotemporal manner. Baf45a belongs to the PBAF complex [8, 35, 36]. However, Baf45a is not ubiquitously expressed [32]. Biochemical analysis of the complex has demonstrated integral connection points between three major modules within the complex, an ATPase module, a core module, and an intervening module. Baf45a was identified to associate with the ARID2 containing intervening module of the PBAF complex [8]. Our data indicates that Baf45a and Baf45d are both expressed in odontoblasts and osteoblasts. We also found that the genomic locus of Baf45b appeared poised based on the combination of chromatin marks but there was no detectable RNA expression. Thus, there may be a compensatory mechanism for Baf45b in these cell types in the absence of Baf45a and Baf45d [32]. Understanding these mechanisms would provide further information on the biochemical properties of the Baf45 homologs and how each subunit contributes to chromatin remodeling.

Chromatin landscape changes occur as a result of combinatorial regulation from multiple epigenetic modulators [1, 2]. A decrease in H3K27ac was associated with a loss of accessibility at the Enam gene. Furthermore, previous reports have documented the co-regulation between the BAF complex and other chromatin activators like the Set1-Mll complex [2, 3, 39]. This dissertation chapter highlights the importance to understand the complex regulation of the genome through a myriad of epigenetic modulators.

Methods

Cell Culture

MC-3T3-E1 mouse calvaria osteoblast cells and primary calvaria osteoblasts were cultured in Alpha Minimum Essential Medium (alpha-MEM) (Cellgro, VA) supplemented with 10% fetal bovine serum (Atlanta Biologicals, GA) and 100U/ml Penicillin-Streptomycin (Gibco, NY). HEK-293T and OD-21 rat odontoblast cells were cultured in Dulbecco's Modified Eagle's Medium (DMEM) (Cellgro, VA) supplemented with 5% FBS and 100U/ml Penicillin-Streptomycin. All cells were maintained in 5% CO2 at 32^{O}C. Osteogenic differentiation was induced by the addition of ascorbic acid at 50g/ml and beta-glycerophsphate at 10mM (Sigma-Aldrich, MO). Odontogenic differentiation was induced by the addition of ascorbic acid at 50g/ml and beta-glycerophsphate at 10mM, and 100nM dexamethasone. Cag-Cre deletion of Baf45a exons 3 and 4 flanked by LoxP sites in primary calvaria osteoblasts was induced by the addition of 4-hydroxy-tamoxifen at 1μM for 48 hours (Sigma-Aldrich, MO).

Stable Expression of shRNA Targeting Baf45a

pLKO.1-puro lentiviral backbone (Addgene, MA) was used to clone shRNA targeting exons 1 and 3 of Baf45a mRNA or an empty vector to generate control shRNA. Viral particles were generated in HEK-293T cells by co-transfection of pLKO.1 shRNA plasmids with packaging vectors pCMVΔR-8.91 and pMD2.G using polyethylenimine (PEI) (Polysciences). 48 hours after transfection, viral supernatants were collected, filtered through a 0.45 μm syringe filter, and added to OD-21 cells for spin infection followed by 24 hours in incubation before adding fresh medium. Selection was

performed on infected cells by supplementing the media with puromycin at 2µg/ml for 72 hours. Baf45a RNA expression changes were confirmed by Q-RT-PCR analysis.

RNA Isolation, Q-RT-PCR, and RNA-Sequencing

RNA was isolated from osteoblast and odontoblast cells by TRIzol reagent extraction (Invitrogen, NY) followed by DNAse1-treatment for differentiation time courses. RNA was extracted from shControl and shRNA-Baf45a odontoblasts by Direct-zol RNA kits (Zymo Research, CA). cDNA was reverse transcribed from mRNA extractions using a One-step RT-qPCR kit (Takara, CA). cDNA levels were determined by Q-RT-PCR using a Luna® Universal qPCR Master Mix (NEB, MA). Gene expression levels were normalized to beta-Actin or Gapdh expression. Total RNA from OD-21 cells stably expressing controls or Baf45a targeted shRNA was submitted for cDNA library generation followed by next-generation RNA sequencing (Novogene, CA).

ChIP-Sequencing and ATAC-Sequencing

Chromatin immunoprecipitation followed by sequencing (ChIP-seq) was analyzed from previously published data (Wu et al., 2017) using antibodies against H3K27ac (Millipore, 07-360), H3K27me3 (Millipore, 07-449), H3K9ac (Active Motif, 39137), and H3K9me3 (Abcam, Ab8898) (Accession Number: GSE76074). Assay for Transposase-Accessible Chromatin using sequencing (ATAC-seq) was performed as previously published (Buenrostro et al., 2015) and analyzed using MACS2 for peak calling by Dr. David Crossman of the UAB Genomics Science Core.

MicroCT Analysis

Baf45a$^{flox/flox}$ (Phf10tm1.1Grc/J) mice and Prrx1-Cre (B6.Cg-Tg(Prrx1-cre)1Cjt/J) mice were obtained from Jackson Laboratory and crossed to delete Baf45a at embryonic day 9 in mineralized tissue. Mandibles were isolated from WT and Baf45a knockout mice at 2 months of age then were fixed in 70% ethanol. MicroCT was performed on whole mandibles by Dr. Maria Johnson in the UAB Small Animal Phenotyping Core.

References

1. Wang, G.G., C.D. Allis, and P. Chi, *Chromatin remodeling and cancer, Part II: ATP-dependent chromatin remodeling.* Trends Mol Med, 2007. **13**(9): p. 373-80.
2. Yadav, T. and J.P. Quivy, *Chromatin plasticity: A versatile landscape that underlies cell fate and identity.* 2018. **361**(6409): p. 1332-1336.
3. Dawson, M.A. and T. Kouzarides, *Cancer epigenetics: from mechanism to therapy.* Cell, 2012. **150**(1): p. 12-27.
4. Ho, L. and G.R. Crabtree, *Chromatin remodelling during development.* Nature, 2010. **463**(7280): p. 474-84.
5. Kadoch, C. and G.R. Crabtree, *Mammalian SWI/SNF chromatin remodeling complexes and cancer: Mechanistic insights gained from human genomics.* Sci Adv, 2015. **1**(5): p. e1500447.
6. Kadoch, C., et al., *Dynamics of BAF-Polycomb complex opposition on heterochromatin in normal and oncogenic states.* Nat Genet, 2017. **49**(2): p. 213-222.
7. Clapier, C.R., et al., *Mechanisms of action and regulation of ATP-dependent chromatin-remodelling complexes.* Nat Rev Mol Cell Biol, 2017. **18**(7): p. 407-422.
8. Mashtalir, N., et al., *Modular Organization and Assembly of SWI/SNF Family Chromatin Remodeling Complexes.* Cell, 2018. **175**(5): p. 1272-1288.e20.
9. Bauer, D.E., et al., *An erythroid enhancer of BCL11A subject to genetic variation determines fetal hemoglobin level.* Science, 2013. **342**(6155): p. 253-7.

10. Choi, J., et al., *The SWI/SNF chromatin remodeling complex regulates germinal center formation by repressing Blimp-1 expression.* Proc Natl Acad Sci U S A, 2015. **112**(7): p. E718-27.

11. Narayanan, R. and T.C. Tuoc, *Roles of chromatin remodeling BAF complex in neural differentiation and reprogramming.* Cell Tissue Res, 2014. **356**(3): p. 575-84.

12. Sokpor, G., et al., *Chromatin Remodeling BAF (SWI/SNF) Complexes in Neural Development and Disorders.* Front Mol Neurosci, 2017. **10**: p. 243.

13. Godfrey, T.C., et al., *Epigenetic remodeling and modification to preserve skeletogenesis in vivo.* Connect Tissue Res, 2018. **59**(sup1): p. 52-54.

14. Nguyen, K.H., et al., *SWI/SNF-Mediated Lineage Determination in Mesenchymal Stem Cells Confers Resistance to Osteoporosis.* Stem Cells, 2015. **33**(10): p. 3028-38.

15. Pico, M.J., et al., *Glucocorticoid receptor-mediated cis-repression of osteogenic genes requires BRM-SWI/SNF.* Bone Rep, 2016. **5**: p. 222-227.

16. Sepulveda, H., A. Villagra, and M. Montecino, *Tet-Mediated DNA Demethylation Is Required for SWI/SNF-Dependent Chromatin Remodeling and Histone-Modifying Activities That Trigger Expression of the Sp7 Osteoblast Master Gene during Mesenchymal Lineage Commitment.* Mol Cell Biol, 2017. **37**(20).

17. Seth-Vollenweider, T., et al., *Novel mechanism of negative regulation of 1,25-dihydroxyvitamin D3-induced 25-hydroxyvitamin D3 24-hydroxylase (Cyp24a1) Transcription: epigenetic modification involving cross-talk between protein-*

arginine methyltransferase 5 and the SWI/SNF complex. J Biol Chem, 2014. **289**(49): p. 33958-70.

18. Hassan, M.Q., et al., *BMP2 commitment to the osteogenic lineage involves activation of Runx2 by DLX3 and a homeodomain transcriptional network.* J Biol Chem, 2006. **281**(52): p. 40515-26.
19. Miron, R.J. and Y.F. Zhang, *Osteoinduction: a review of old concepts with new standards.* J Dent Res, 2012. **91**(8): p. 736-44.
20. Wu, M., G. Chen, and Y.P. Li, *TGF-β and BMP signaling in osteoblast, skeletal development, and bone formation, homeostasis and disease.* Bone Res, 2016. **4**: p. 16009.
21. Rashid, H., et al., *Sp7 and Runx2 molecular complex synergistically regulate expression of target genes.* Connect Tissue Res, 2014. **55 Suppl 1**(0 1): p. 83-7.
22. Husain, A. and M.A. Jeffries, *Epigenetics and Bone Remodeling.* Curr Osteoporos Rep, 2017. **15**(5): p. 450-458.
23. Chai, Y., et al., *Fate of the mammalian cranial neural crest during tooth and mandibular morphogenesis.* Development, 2000. **127**(8): p. 1671-9.
24. Vaahtokari, A., et al., *The enamel knot as a signaling center in the developing mouse tooth.* Mech Dev, 1996. **54**(1): p. 39-43.
25. Bae, C.H., et al., *New population of odontoblasts responsible for tooth root formation.* Gene Expr Patterns, 2013. **13**(5-6): p. 197-202.
26. Heair, H.M., et al., *MicroRNA 665 Regulates Dentinogenesis through MicroRNA-Mediated Silencing and Epigenetic Mechanisms.* Mol Cell Biol, 2015. **35**(18): p. 3116-30.

27. Ari, G., S. Cherukuri, and A. Namasivayam, *Epigenetics and Periodontitis: A Contemporary Review.* J Clin Diagn Res, 2016. **10**(11): p. Ze07-ze09.

28. Li, B., et al., *EZH2 Impairs Human Dental Pulp Cell Mineralization via the Wnt/β-Catenin Pathway.* 2018. **97**(5): p. 571-579.

29. Krasteva, V., G.R. Crabtree, and J.A. Lessard, *The BAF45a/PHF10 subunit of SWI/SNF-like chromatin remodeling complexes is essential for hematopoietic stem cell maintenance.* Exp Hematol, 2017. **48**: p. 58-71.e15.

30. Huber, F.M., et al., *Histone-binding of DPF2 mediates its repressive role in myeloid differentiation.* Proc Natl Acad Sci U S A, 2017. **114**(23): p. 6016-6021.

31. Zhang, W., et al., *The BAF and PRC2 Complex Subunits Dpf2 and Eed Antagonistically Converge on Tbx3 to Control ESC Differentiation.* Cell Stem Cell, 2019. **24**(1): p. 138-152.e8.

32. Lessard, J., et al., *An essential switch in subunit composition of a chromatin remodeling complex during neural development.* Neuron, 2007. **55**(2): p. 201-15.

33. Tang, J., A.S. Yoo, and G.R. Crabtree, *Reprogramming human fibroblasts to neurons by recapitulating an essential microRNA-chromatin switch.* Curr Opin Genet Dev, 2013. **23**(5): p. 591-8.

34. Wu, H., et al., *Chromatin dynamics regulate mesenchymal stem cell lineage specification and differentiation to osteogenesis.* Biochim Biophys Acta Gene Regul Mech, 2017. **1860**(4): p. 438-449.

35. Hodges, C., J.G. Kirkland, and G.R. Crabtree, *The Many Roles of BAF (mSWI/SNF) and PBAF Complexes in Cancer.* Cold Spring Harb Perspect Med, 2016. **6**(8).

36. Brechalov, A.V., S.G. Georgieva, and N.V. Soshnikova, *Mammalian cells contain two functionally distinct PBAF complexes incorporating different isoforms of PHF10 signature subunit.* Cell Cycle, 2014. **13**(12): p. 1970-9.

37. Elefteriou, F. and X. Yang, *Genetic mouse models for bone studies--strengths and limitations.* Bone, 2011. **49**(6): p. 1242-54.

38. Fenerich, B.A., et al., *NT157 has antineoplastic effects and inhibits IRS1/2 and STAT3/5 in JAK2(V617F)-positive myeloproliferative neoplasm cells.* 2020. **5**: p. 5.

39. Brès, V., S.M. Yoh, and K.A. Jones, *The multi-tasking P-TEFb complex.* Curr Opin Cell Biol, 2008. **20**(3): p. 334-40.

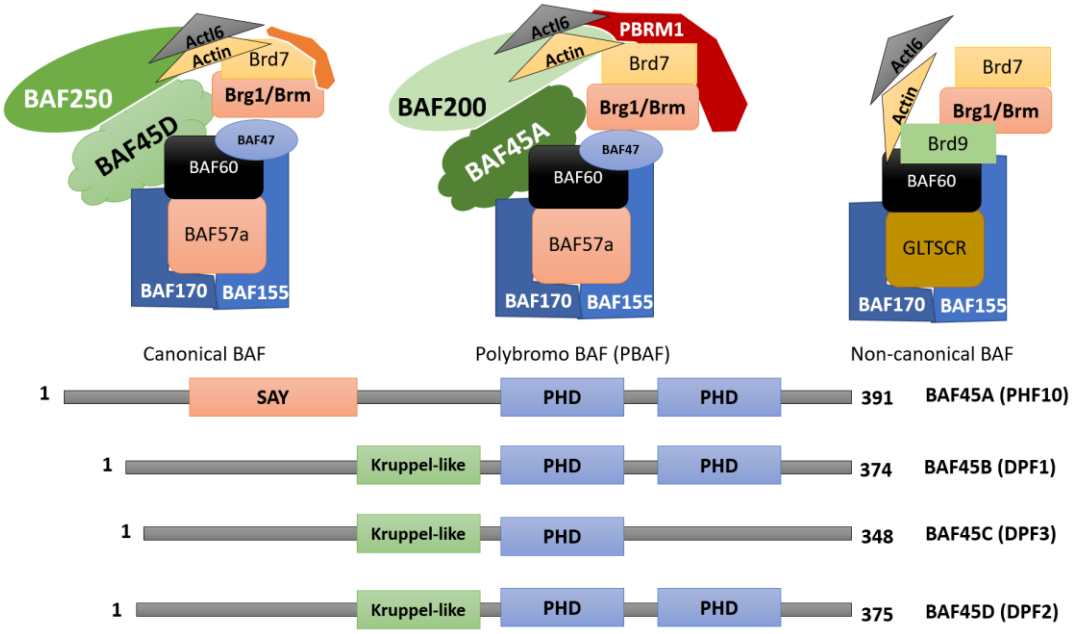

Figure 1. BAF45A homologs regulate chromatin accessibility through the mammalian Swi/Snf complex. The mammalian Swi/Snf, or Brahma-associated factor (BAF), ATPase-dependent chromatin remodeling complexes open nucleosomes of active gene loci for transcriptional machinery. BAF complexes can be divided into three major sub-complexes: canonical BAF, polybromo-BAF (PBAF), and the non-canonical (ncBAF). Permutations of complex assemblies give rise to tissue specific gene regulation. Four homologs occupy the BAF45 position. BAF45A differs from the other three homologs in the DNA binding SAY domain and the association with the PBAF complex. These assemblies have become a major focus of studies into the BAF complex function.

A.

Baf45a

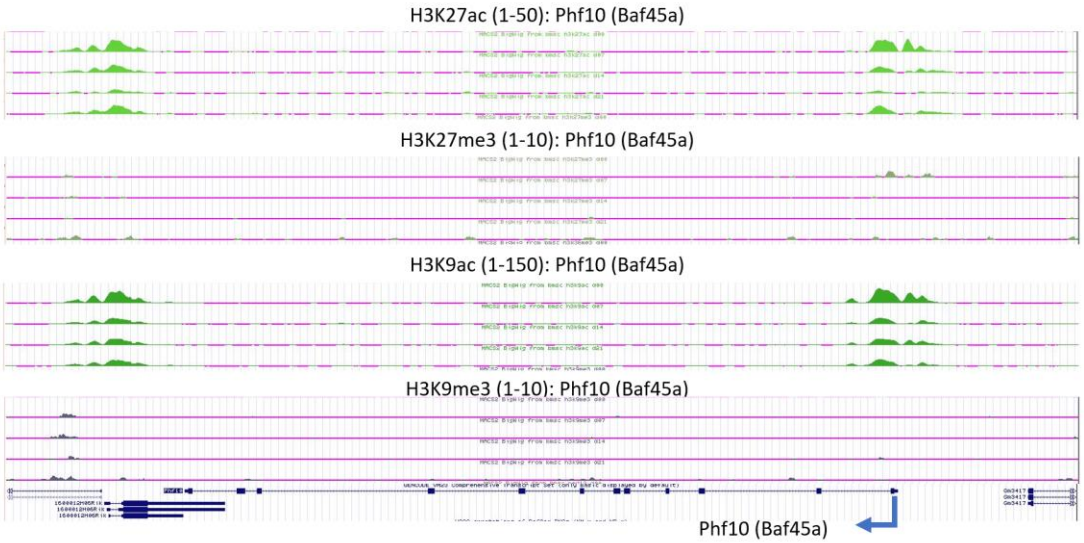

B.

Baf45b

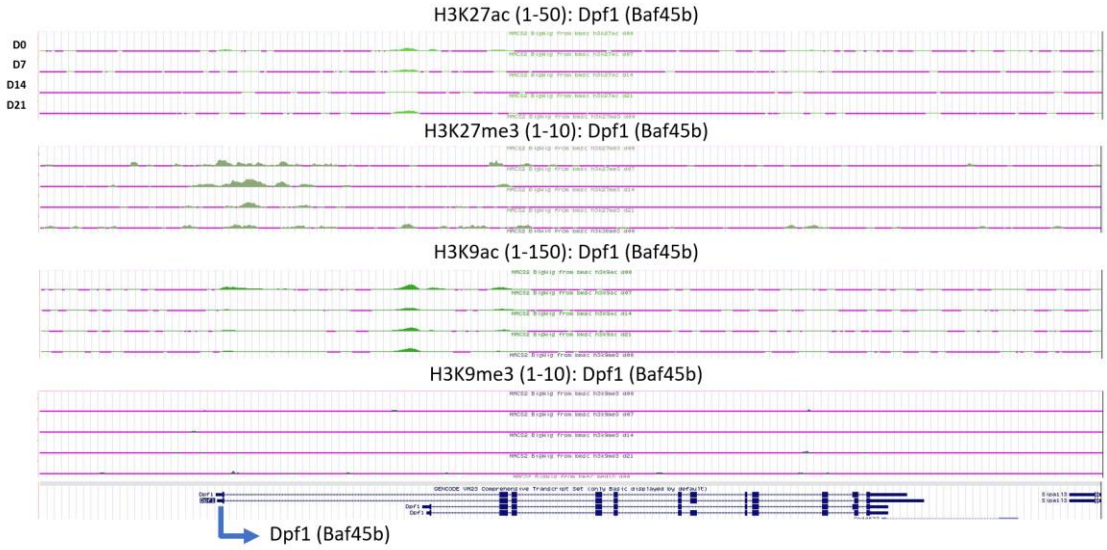

C.

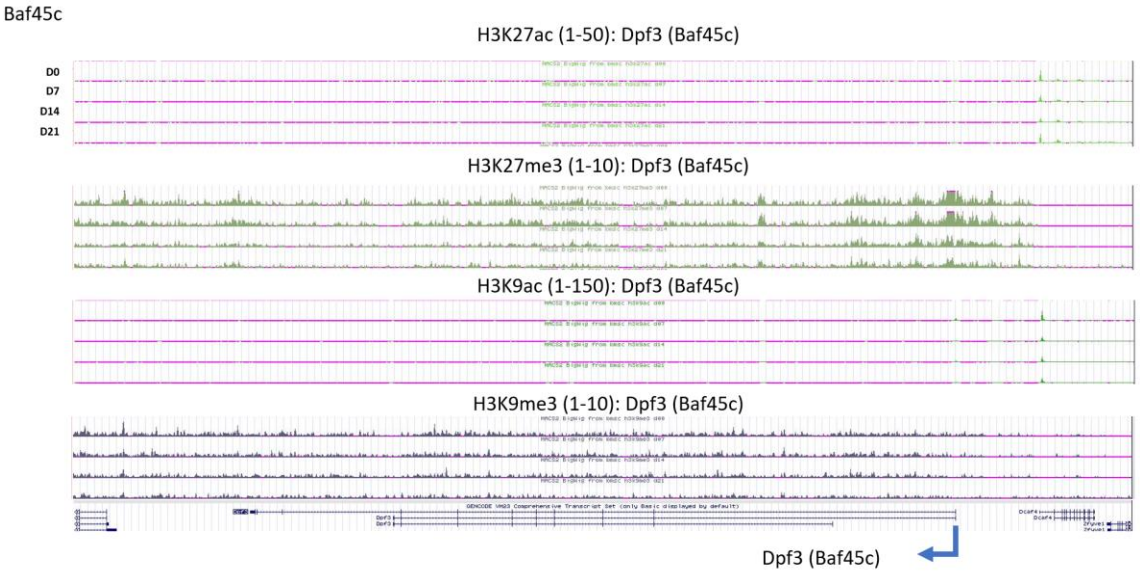
Baf45c
H3K27ac (1-50): Dpf3 (Baf45c)
D0
D7
D14
D21
H3K27me3 (1-10): Dpf3 (Baf45c)
H3K9ac (1-150): Dpf3 (Baf45c)
H3K9me3 (1-10): Dpf3 (Baf45c)
Dpf3 (Baf45c)

D.

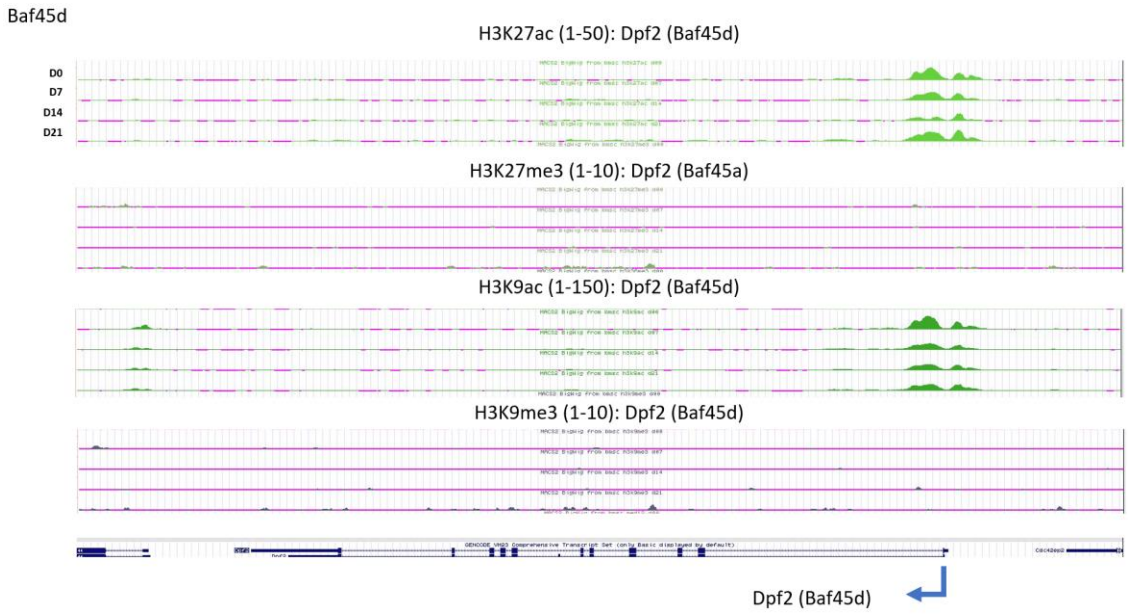
Baf45d
H3K27ac (1-50): Dpf2 (Baf45d)
D0
D7
D14
D21
H3K27me3 (1-10): Dpf2 (Baf45a)
H3K9ac (1-150): Dpf2 (Baf45d)
H3K9me3 (1-10): Dpf2 (Baf45d)
Dpf2 (Baf45d)

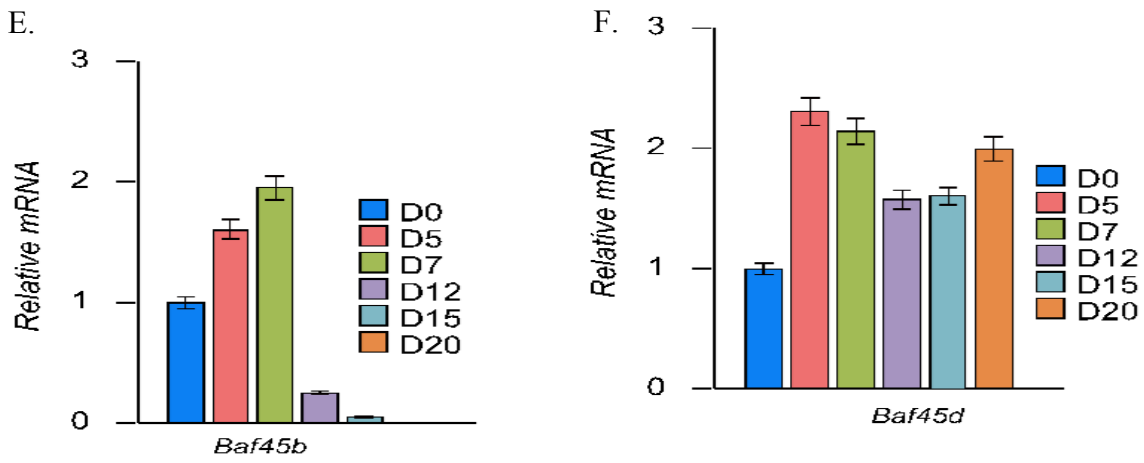

Figure 2. Baf45a and Baf45d genomic loci harbor an active chromatin landscape. Primary osteoblast progenitors were isolated from the bone marrow of mice were grown under osteogenic differentiation conditions and harvested at days 0, 7, 14, and 21. (A-D.) ChIP-seq analysis of histone modifications at the gene loci of Baf45 homologs. Peaks representing active chromatin marks H3K9ac and H3K27ac as well as peaks representing repressive chromatin marks H3K9me3 and H3K27me3 at (A.) Baf45a, (B.) Baf45b, (C.) Baf45c, and (D.) Baf45d gene bodies. (E-F.) RNA expression levels were analyzed during osteogenic differentiation for (E.) Baf45b and (F.) Baf45d. Relative expression levels were normalized to (Gapdh).

A.

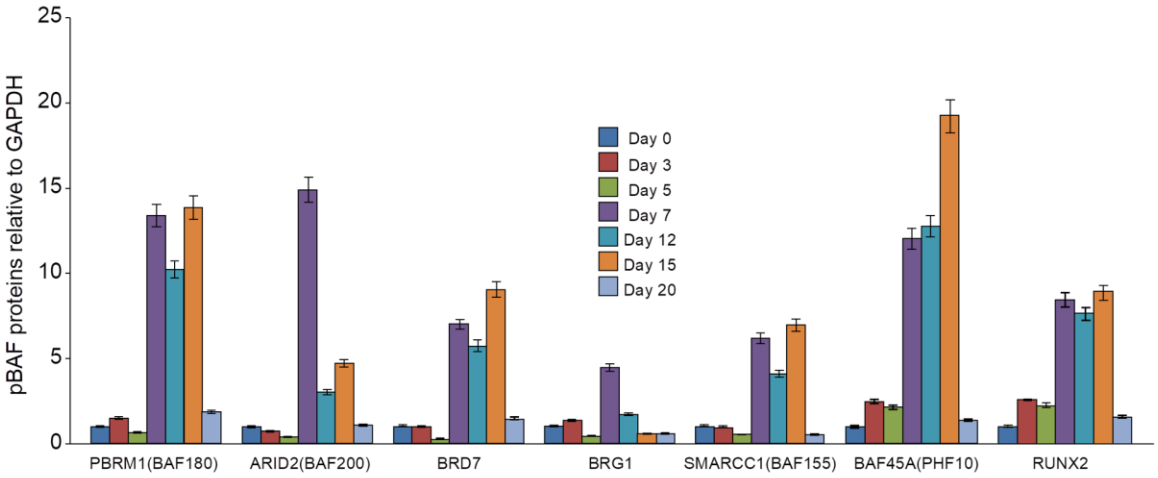
pBAF proteins relative to GAPDH
25
20
15
10
5
0
Day 0
Day 3
Day 5
Day 7
Day 12
Day 15
Day 20
PBRM1(BAF180)
ARID2(BAF200)
BRD7
BRG1
SMARCC1(BAF155)
BAF45A(PHF10)
RUNX2

B.

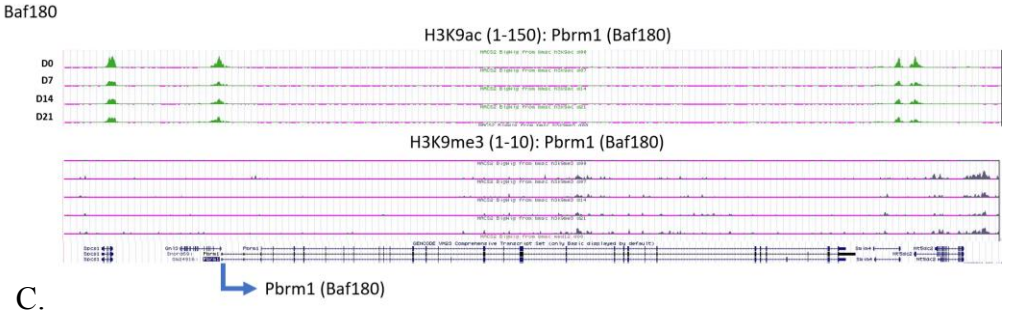
Baf180
H3K9ac (1-150): Pbrm1 (Baf180)
D0
D7
D14
D21
H3K9me3 (1-10): Pbrm1 (Baf180)
Pbrm1 (Baf180)

C.

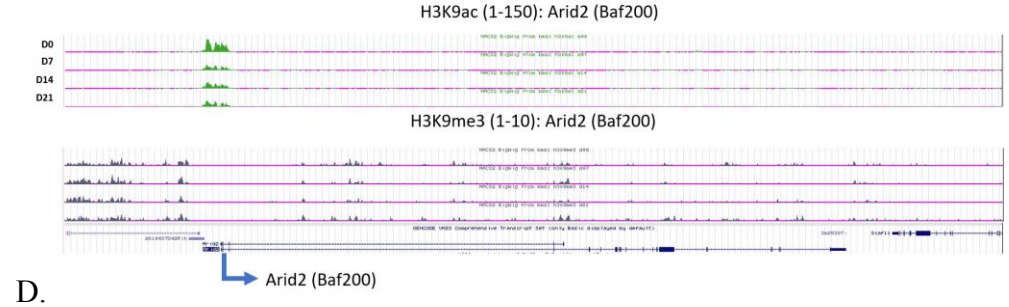
Baf200
H3K9ac (1-150): Arid2 (Baf200)
D0
D7
D14
D21
H3K9me3 (1-10): Arid2 (Baf200)
Arid2 (Baf200)

D.

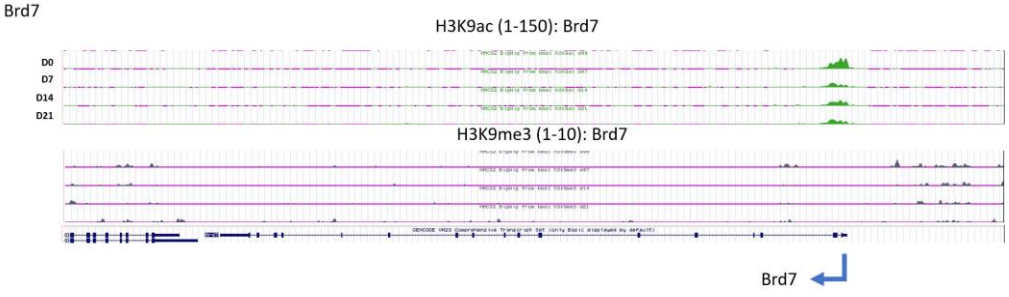
Brd7
H3K9ac (1-150): Brd7
D0
D7
D14
D21
H3K9me3 (1-10): Brd7
Brd7

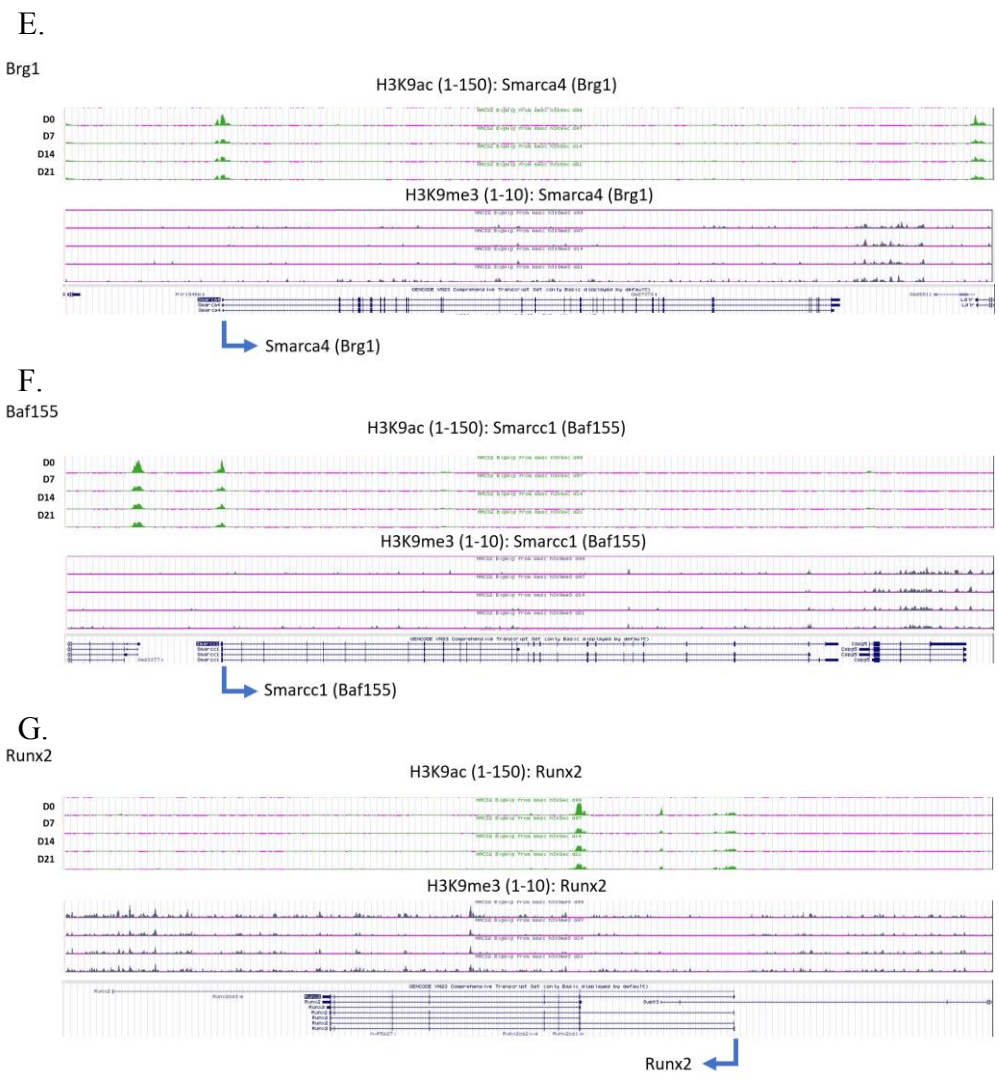

Figure 3. Osteogenic differentiation promotes activation of PBAF sub-complex genes. (A.) Protein expression levels representing western blot analysis of BAF180, BAF200, BRD7, BRG1, BAF155, BAF45A, and RUNX2. Samples were harvested at days 0, 3, 5, 7, 12, 15, and 20 during osteogenic differentiation. (B.-G.) ChIP-seq analysis of histone modifications at the gene loci of Baf45 homologs. Peaks representing the active chromatin mark H3K9ac and peaks representing the repressive chromatin mark H3K9me3 at (B.) Baf180, (C.) Baf200, (D.) Brd7, (E.) Brg1, (F.) Baf155, and (G.) Runx2 gene bodies.

A.

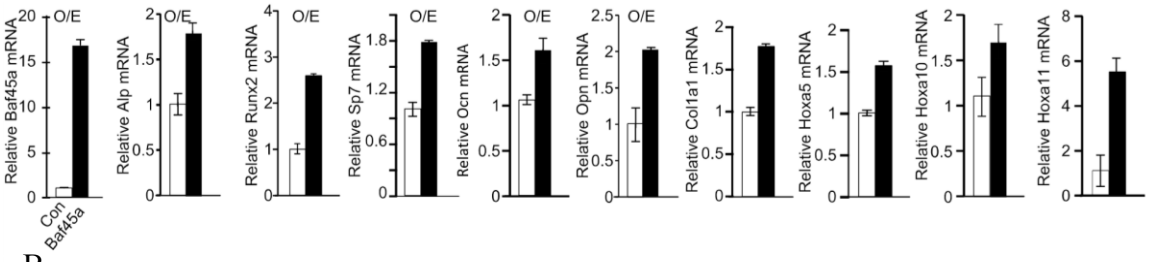
Relative Baf45a mRNA
Relative Alp mRNA
Relative Runx2 mRNA
Relative Sp7 mRNA
Relative Ocn mRNA
Relative Opn mRNA
Relative Col1a1 mRNA
Relative Hoxa5 mRNA
Relative Hoxa10 mRNA
Relative Hoxa11 mRNA
O/E
Con
Baf45a

B.

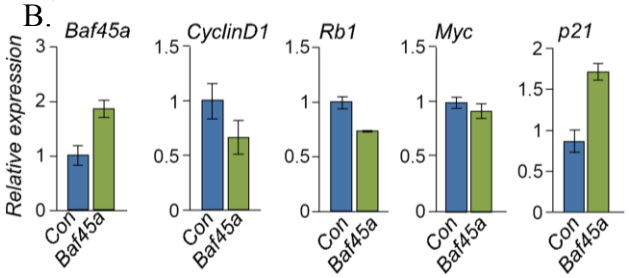
Relative expression
Baf45a
CyclinD1
Rb1
Myc
p21
Con
Baf45a

C.

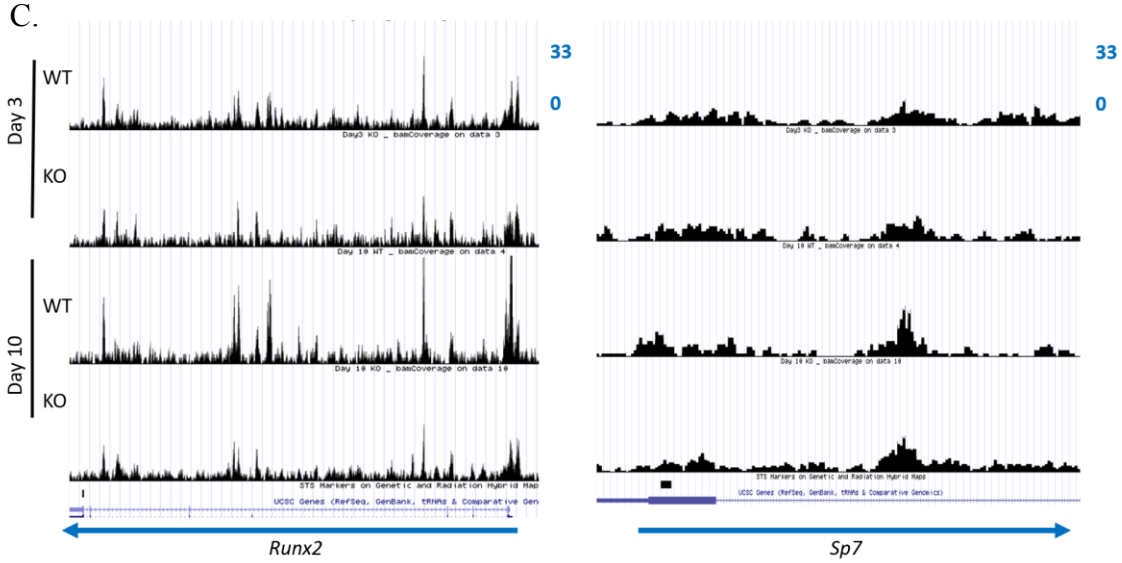
Day 3
Day 10
WT
KO
33
0
Runx2
Sp7

D.

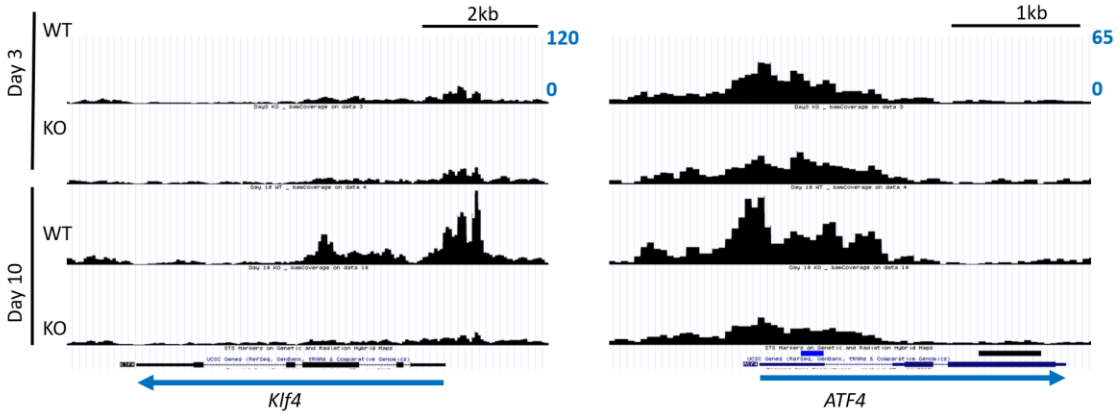
2kb
120
0
WT
KO
Day 3
WT
KO
Day 10
Klf4
1kb
65
0
ATF4

E.

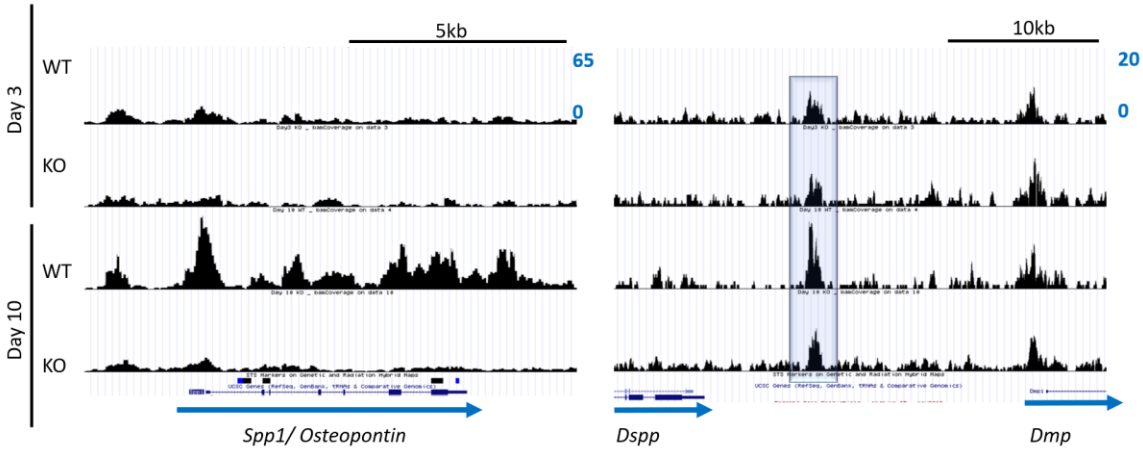
5kb
65
0
WT
KO
Day 3
WT
KO
Day 10
Spp1/ Osteopontin
10kb
20
0
Dspp
Dmp

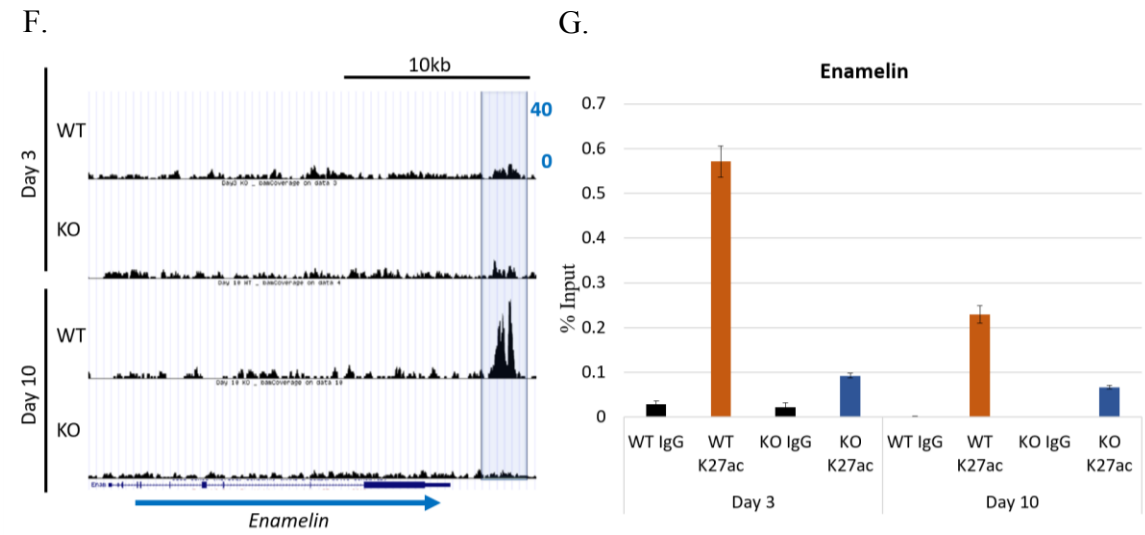

Figure 4. Baf45 expression levels lead to changes in the gene expression profiles in osteoblasts. (A-B.) Baf45a was transiently overexpressed in MC3T3-E1 osteoblast cells. RNA expression was assessed and normalized to (Gapdh). (C-F.) Baf45aflox/flox was deleted in primary calvarial osteoblasts via 4-hydroxytamoxifen inducible Cag-Cre genetic background. The cells were then subjected to osteogenic differentiation. Osteoblasts were harvested on day 3 and day 10 of differentiation. (C-F.) ATAC-seq was performed on WT and Baf45a knockout osteoblasts. Chromatin accessibility at the gene loci of (C.) osteogenic genes Runx2 and Sp7, (D.) differentiation genes Klf4 and Atf4, and (E.) tooth and bone related genes Spp1, Dmp1, Dspp, and (F.) Enam. (G.) ChIP-QPCR analysis was performed in calvarial osteoblasts. ChIP was performed using the anti-H3K27ac antibodies to probe for the Enam downstream enhancer region (F.).

A.

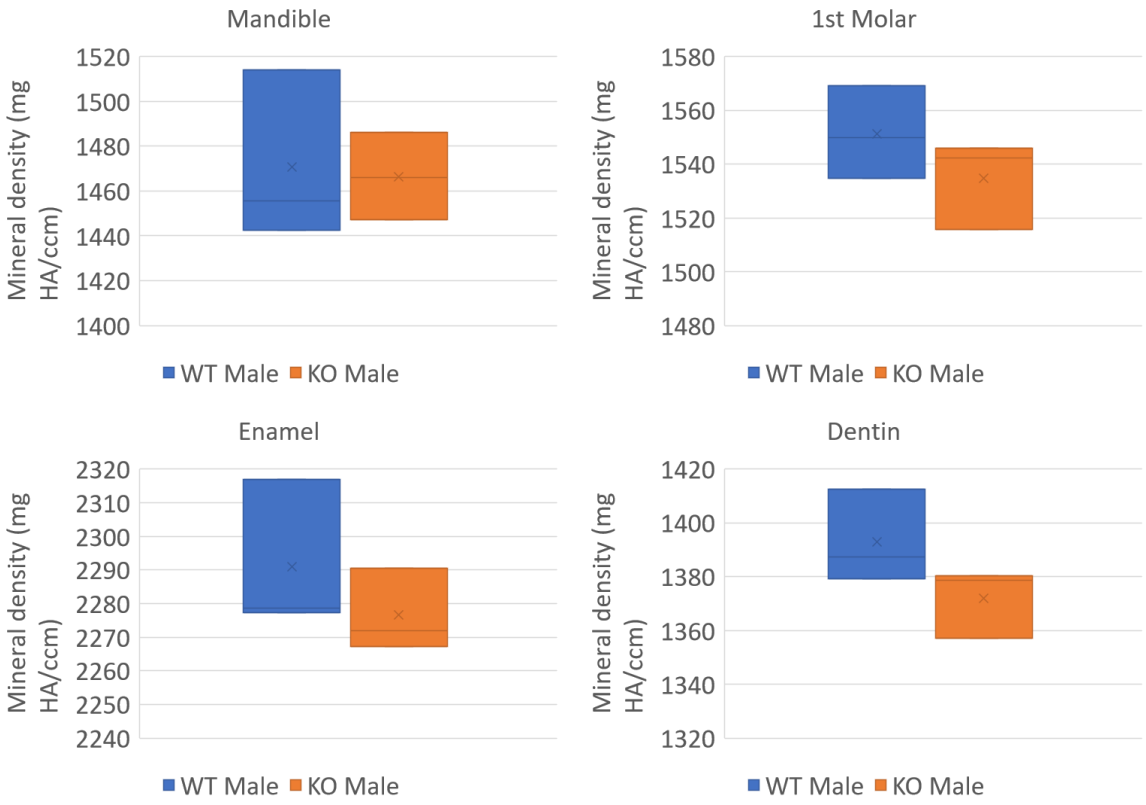
Mandible
Mineral density (mg HA/ccm)
1520
1500
1480
1460
1440
1420
1400
WT Male
KO Male
1st Molar
Mineral density (mg HA/ccm)
1580
1560
1540
1520
1500
1480
WT Male
KO Male
Enamel
Mineral density (mg HA/ccm)
2320
2310
2300
2290
2280
2270
2260
2250
2240
WT Male
KO Male
Dentin
Mineral density (mg HA/ccm)
1420
1400
1380
1360
1340
1320
WT Male
KO Male

B.

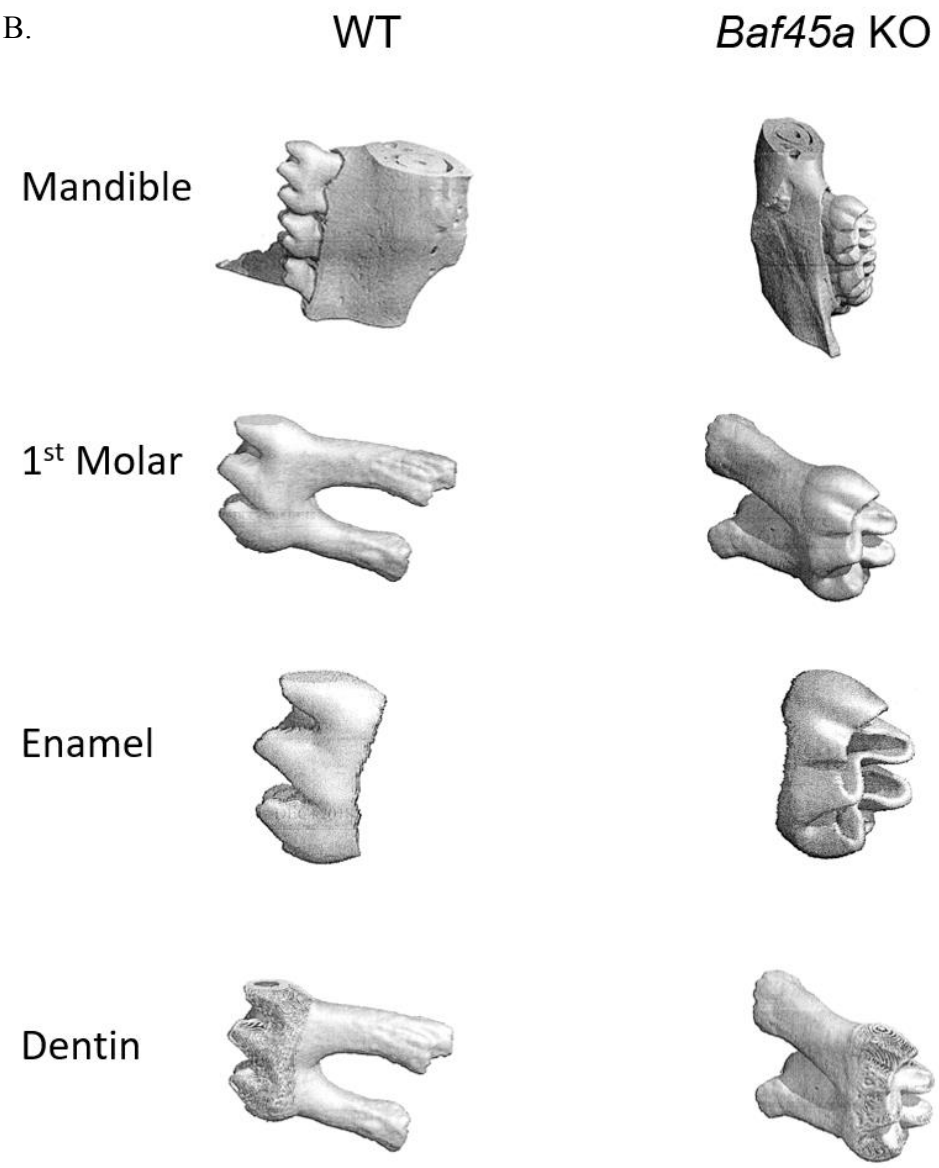

C.

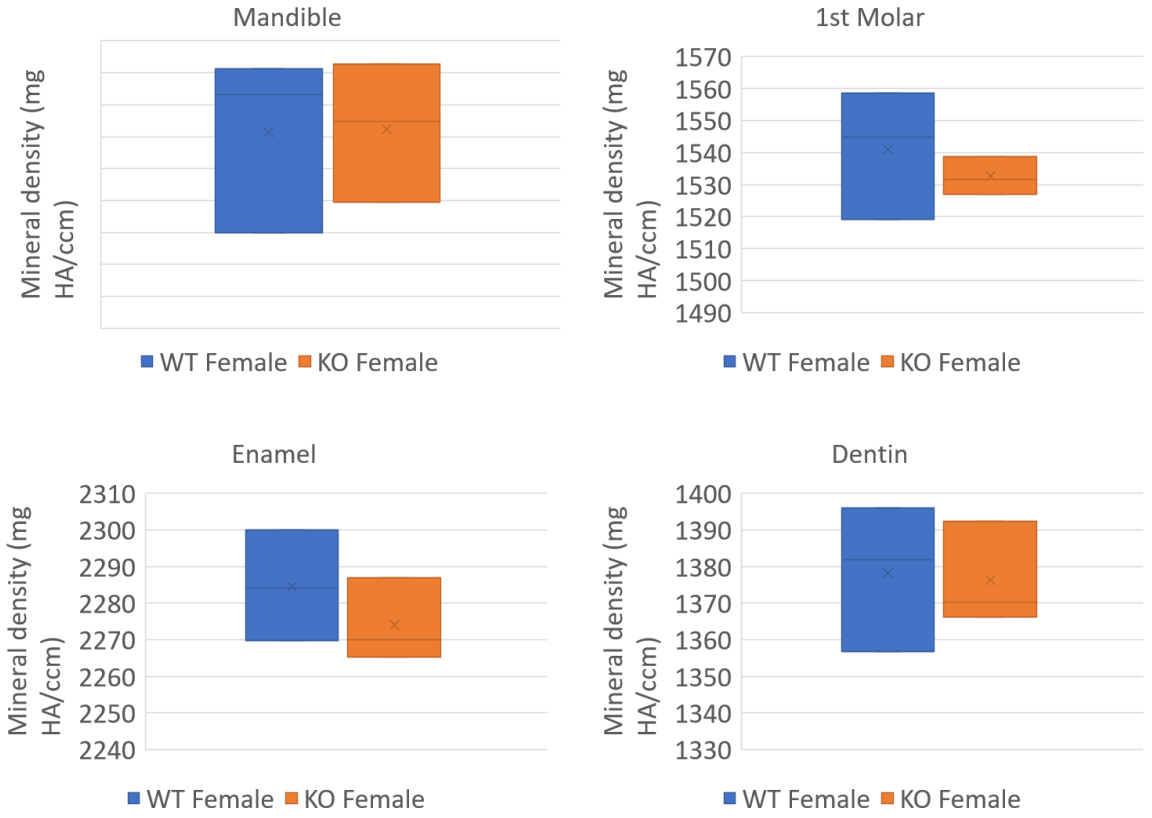
Mandible
Mineral density (mg HA/ccm)
WT Female
KO Female
1st Molar
1570
1560
1550
1540
1530
1520
1510
1500
1490
Enamel
2310
2300
2290
2280
2270
2260
2250
2240
Dentin
1400
1390
1380
1370
1360
1350
1340
1330

D.

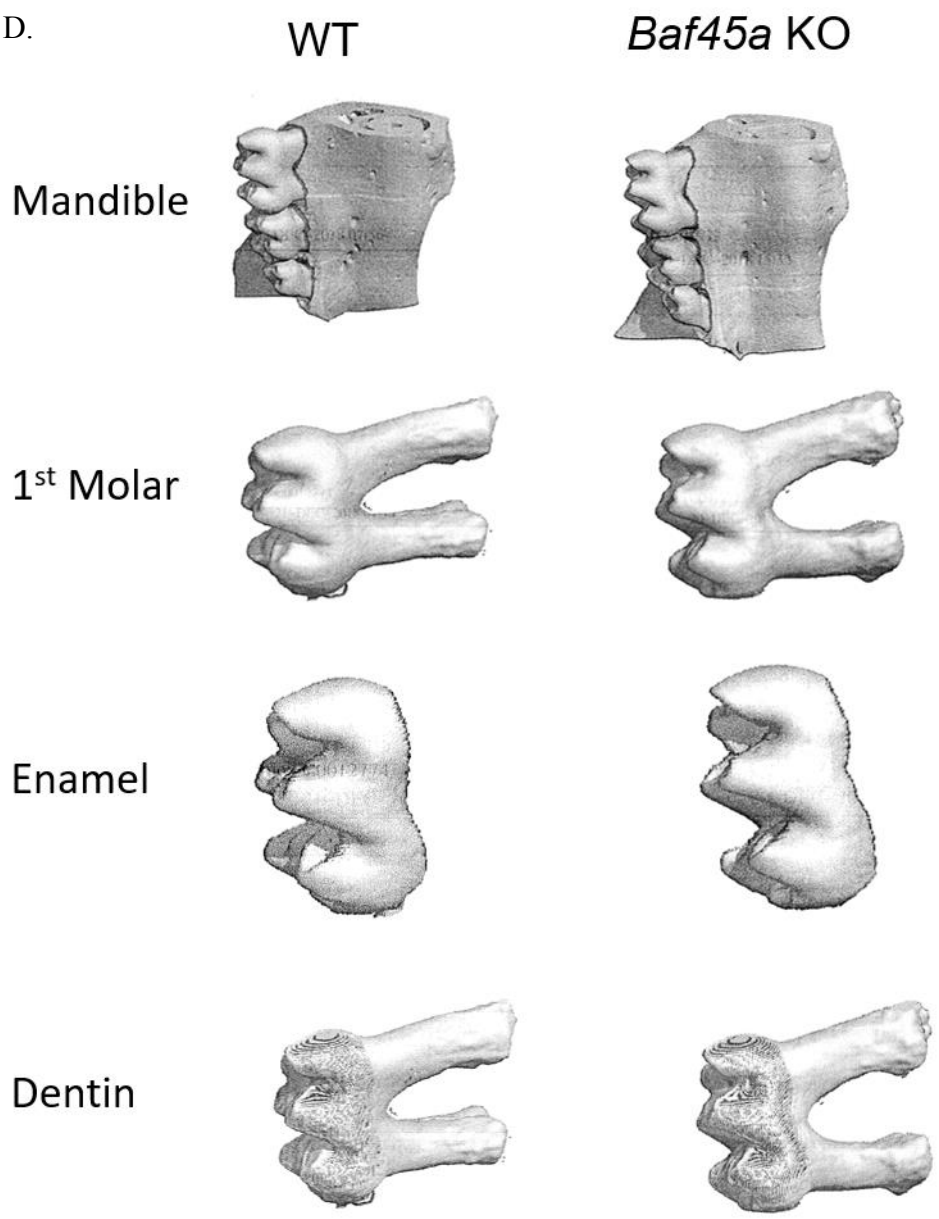

Figure 5. MicroCT analysis of mineralized tissue in 2-month old BAF45A knock out mice compared to wild type. Baf45aflox/flox was deleted at embryonic day E9.5 via a Prrx1-Cre genetic background in mice. (A and C.) Bone volume of the whole molar, the outer enamel layer, the inner dentin layer, and the whole mandible from WT and BAF45A KO mice, (A.) males (n=3) and (C.) females (n=3) at 2-months. (B. and D.) representative images of the first mandible from these mice.

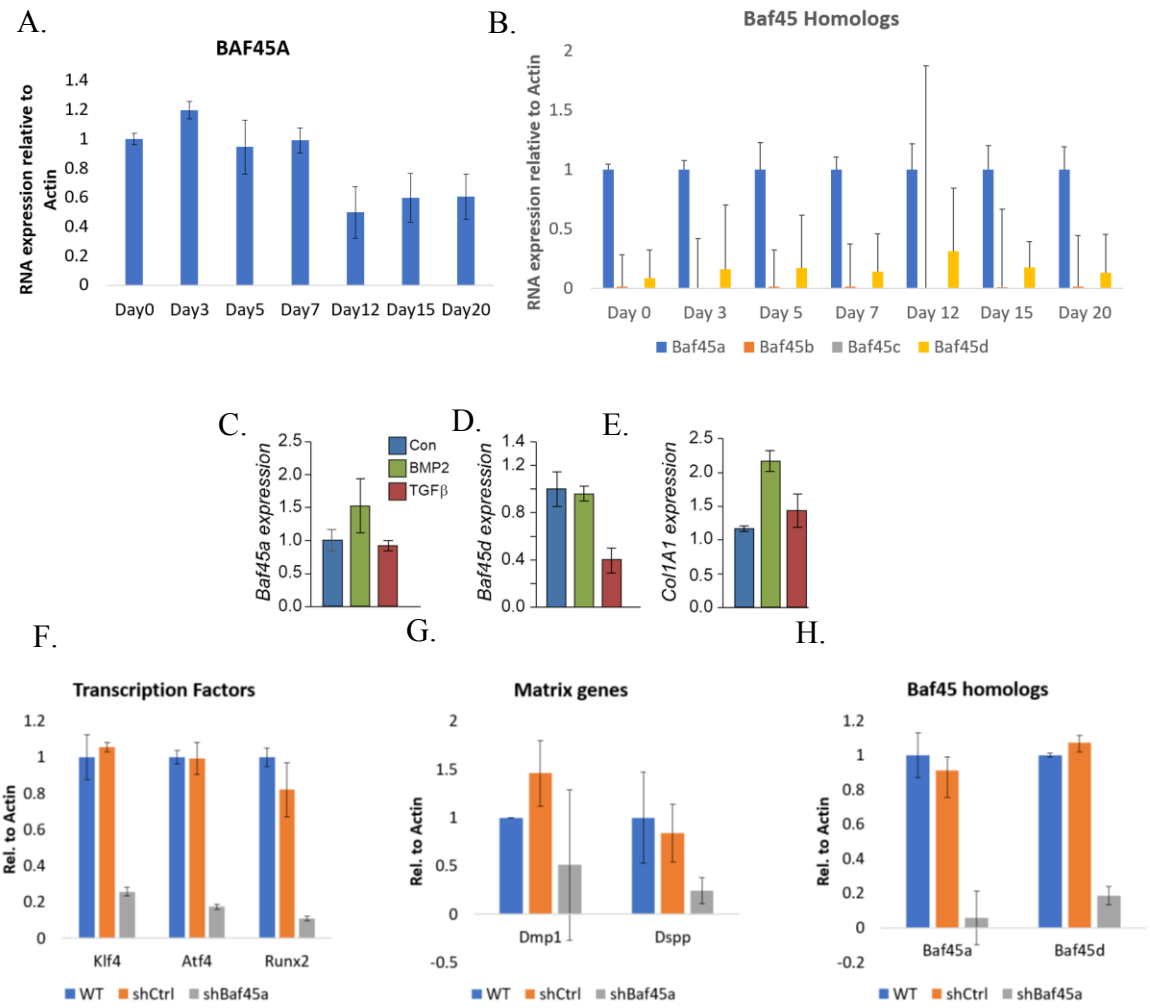

Figure 6. Baf45a is an important factor in odontoblasts. (A-B.) OD21 odontoblast cells were subjected to odontogenic differentiation. (A.) RNA expression was assessed for Baf45a during differentiation. Relative expression was normalized to beta-actin. (B.) Relative RNA expression of Baf45 homologs to Baf45a. (C-E.) OD21 cells were treated with osteogenic factors BMP2 or TGF-beta. RNA expression was assessed by QPCR for (C.) Baf45a, (D.) Baf45d, and (E.) Col1a1. (F-H.) OD21 cells were depleted of Baf45a by shRNA knockdown. QPCR analysis to assess RNA expression of (F.) transcription factors, (G.) odontogenic matrix genes, and (H.) Baf45a and Baf45d.

A. Genes altered in shBaf45a Odontoblasts

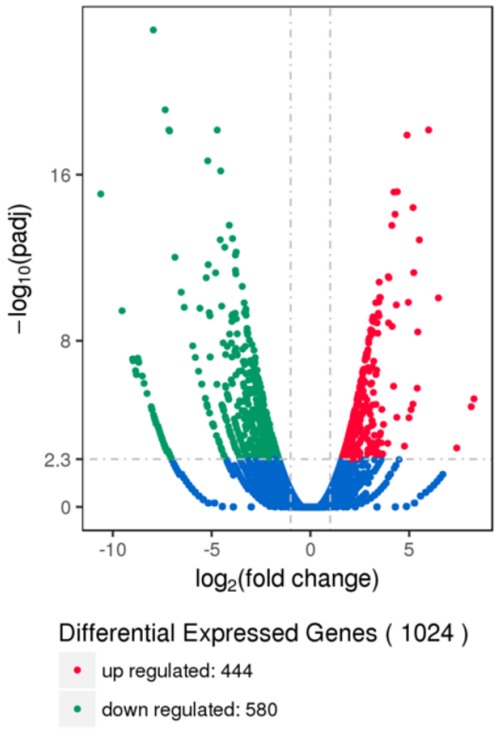

B.

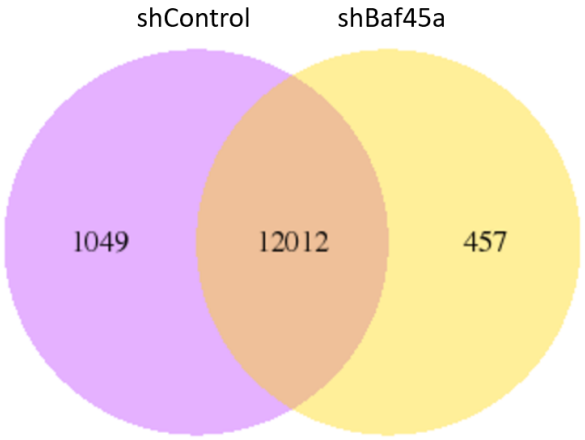

C. Gene ontology

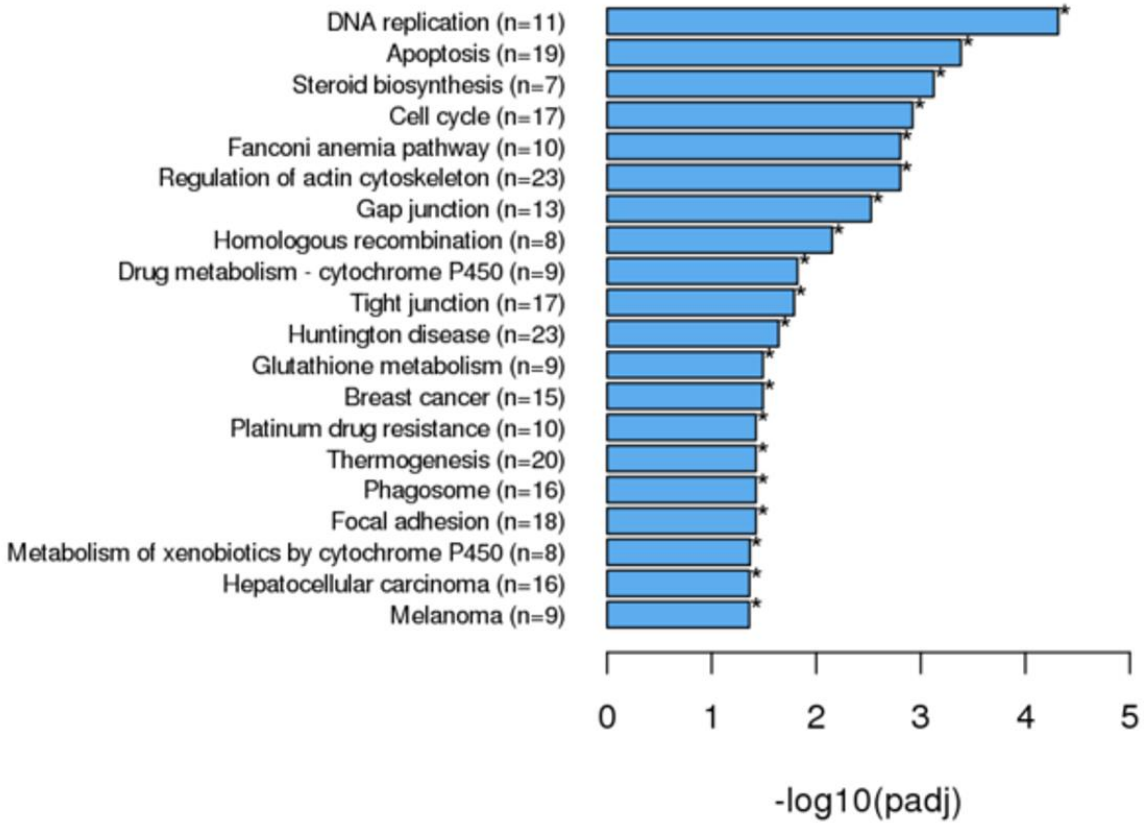

D.

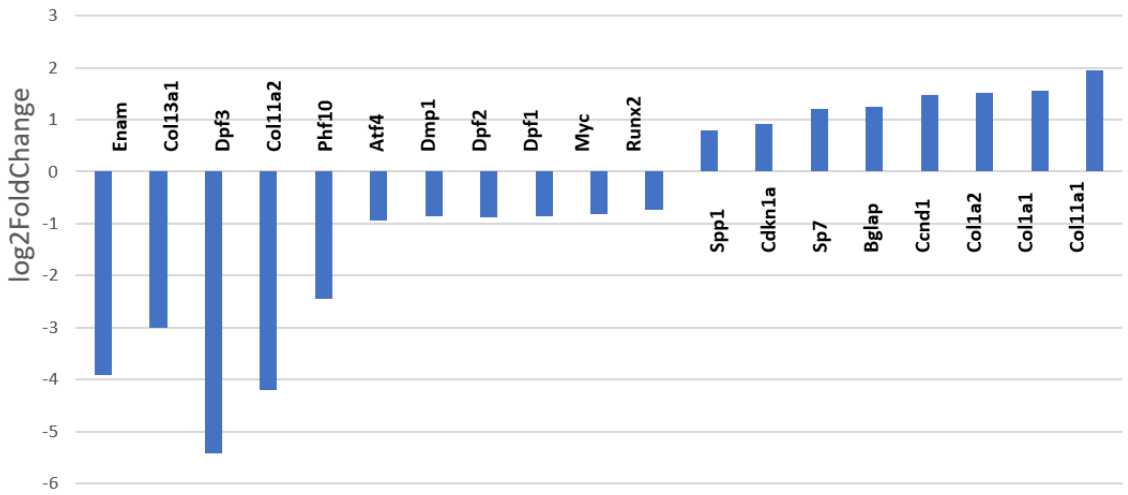

Figure 7. Baf45a depletion in odontoblast cells leads to global gene expression changes. (A.) Global gene expression changes in OD21 cells depleted of Baf45a by shRNA compared to control shRNA. Genes expressed with a 2-fold increase (red) and decrease (green) are expressed by a volcano plot. (B.) Venn diagram displaying gene expression overlap and differences between cells transduced with control shRNA (purple) and cells transduced with Baf45a shRNA (yellow). (C.) Gene ontology of the global gene expression profile changes in cells after Baf45a knockdown. (D.) Differences in transcript levels in Baf45a depleted OD21 cells compared to control OD21 cells. Data representing Log 2-fold changes in transcript reads.

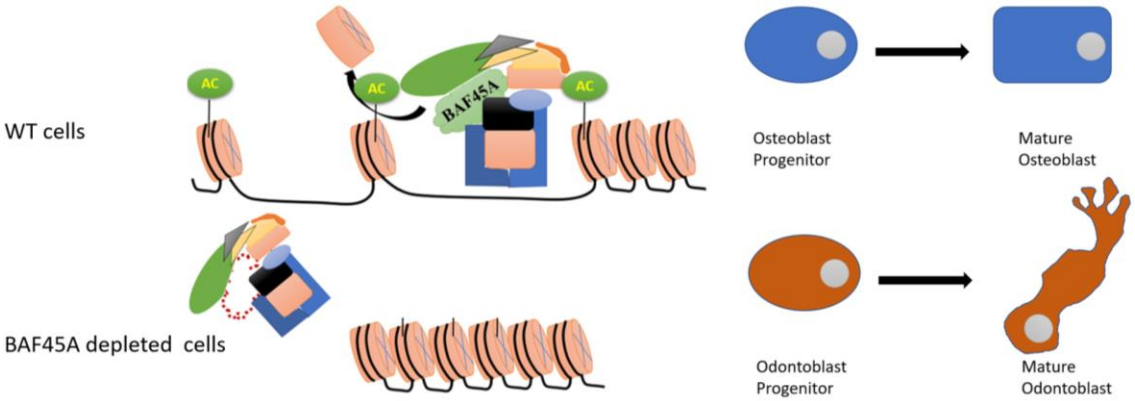

Figure 8. BAF45 regulates BAF complex function in mineralized tissues. BAF45A is an integral subunit of the mammalian Swi/Snf chromatin remodeling complex and promotes chromatin accessibility in osteoblasts. Depletion or complete knockout of Baf45a in osteoblasts and odontoblasts alters global gene expression, respectively. Further biochemical assessment of BAF45A function in the PBAF sub-complex will provide a greater understanding of chromatin remodeling in mineralized tissues.

CHAPTER 10
CONCLUSION

BAF Complex Assembly and Craniofacial Development

Mutations identified in subunits of the BAF complex have been associated with developmental anomalies described as BAF-opathies which include Coffin–Siris and Nicolaides–Baraitser syndromes (CSS and NCBRS) [1]. Symptoms of these disorders are highlighted by neurological delays and relative coarseness of craniofacial features. BAF-opathy studies have focused on some of the ubiquitously expressed subunits like BAF47, BAF155, and BAF170, as well as some that are frequently mutated like BAF60 [2-5]. Although no mutations in Baf45a have been identified that leads to BAF-opathies, chromosomal deletions that remove Baf45a and neighboring genes have been shown to cause similar features as CSS and NCBRS patients.

In chapter 10 of this dissertation, we targeted Baf45a for deletion using a Prrx1-cre driver and saw a modest change in mineralization [6]. Our objectives was to target craniofacial bone development using this model [6]. However, Prrx1-cre may be more suitable for targeting cells of the long bone derived from the mesenchyme [6]. To target craniofacial development, we need to target neural crest cells. Thus, we began breeding mice to target Baf45a in these cells using the Wnt1-cre driver [6]. By doing so, this sets up future work to interrogate the loss of Baf45a as a cause for uveal melanoma and brain

abnormalities compared to the loss of neighboring genes within the Chr 6q27 region near the Baf45a gene locus [7, 8]. Combining these studies with molecular approaches to interrogate mechanisms of Baf45a will provide information about potential pathogenesis and therapeutic strategies.

Recent studies have focused on the assembly of BAF complexes and the resulting permutations that mediate tissue specific gene expression [9]. BAF45a interacts with BAF200 within the PBAF complex. Understanding the biochemical functions and signaling events that mediate this specific assembly's activity would give insight into BAF45A function [9]. Mass spectrometry experiments specifically targeting the PBAF complex through pulling down HA-tagged BAF45a and HA-tagged BAF200, would identify non-BAF complex binding partners of this module and any post-translational modifications made to these subunits [9]. Furthermore, we could determine if BAF45a binds directly to the DNA and has a specific sequence binding motif. Similar experiments have been performed in HEK293T cells [9]. However, by performing these assays in osteoblasts and odontoblasts during differentiation, the specific mechanisms of Baf45a could be uncovered. Combining these assays with single-cell ATAC-seq, we will be able to pinpoint spatiotemporal regulation by Baf45a and the PBAF complex during the development of mineralized tissues. These findings could guide future approaches to generate specific mutations in mice and other models for in vivo studies of the PBAF complex.

Signaling Events Mediates Complex Chromatin Regulation

Chromatin regulation is dynamically orchestrated between activating and repressive modulators [10]. As it relates to this dissertation, chromatin accessibility and H3K4 methylation are both tightly associated with gene activation [11]. Like BAF complexes, there is much to be learned about the mechanisms of various SET1-MLL complex assemblies in promoting region specific gene expression [12-16]. The SET1-MLL complex promotes H3K4me3 at gene promoters and H3K4me1 at enhancers and super-enhancers. It has been shown that enhancer methylation is carried out by Mll3 and Mll4 containing complexes, both requiring Ash2l and Dpy30 [12-16]. Other characteristics of super-enhancers include the cooperative association of high levels of chromatin activators and tissue specific transcription factors [17, 18]. Depletion of any of these factors at super-enhancers lead to collapse of these complexes. We hypothesized that elevated Dpy30 expression levels promote super-enhancer activity in Myc-dependent cancers. It remains possible that targeting Dpy30 by genetic and pharmacological means in our studies leads to the to the collapse of tumor specific super-enhancers.

Cooperative binding of complexes at super-enhancers form a hub of activation. Some factors that facilitate this process have the biophysical property of undergoing liquid-liquid phase separation. Proteins that have this ability form liquid like droplets mediated by low complexity, prion-like domains (PLD), which lack well defined protein motif structure [19]. The catalytic, methyltransferase subunits of the Set1-Mll complex evolutionarily contain predicted prion-like domains including Set1 in Saccharomyces cerevisiae, Trr in Drosophila melanogaster, and Mll3 and Mll4 in mammals [20]. Future experiments include performing in vitro phase separation assays with wild type and PLD

mutant Set1 proteins to characterize residues important for droplet formation. Coupling this with in vivo imagining and genomic assays will further characterize mechanisms of the Set1-Mll complex in regulating developmental and cancer specific enhancer activity.

The series of molecular events that lead to dramatic alterations in gene expression include signaling cues from external stimuli. The translocation of the Golgi trafficking protein BIG1 to the nucleus of HepG2 hepatocyte carcinoma cells upon serum starvation and activation of the AMPK signaling pathway suggests a role for gene regulations [21, 22]. BIG1 binding to Dpy30 has been described by multiple structural studies, although BIG1 nuclear mechanisms have not been well defined [23]. BIG1 may promote expression in a subset of genes through the Set1-Mll complex downstream of AMPK signaling. Dpy30 and Big1 potentially interact with other gene regulators like the NURF chromatin remodeling complex or AKAP family of RNA-Binding proteins [23]. Alternatively, BIG1 could function to sequester Dpy30 away from the Set1-Mll complex to suppress gene expression by acting as a tumor suppressor in tumor cells. Taken together, this dissertation dissects the mechanisms that underly cancer cell manipulation of the canonical function of proteins that function in the secretory pathway and in chromatin regulation. In addition, these studies highlight the need to investigate complex interactions within the cells that were previously thought to be unlikely. Finally, this research aims to unravel mechanisms of chromatin remodeling in a tissue specific manner that will provide insight into gene regulation in diseases associated with development and aging.

References

1. Aref-Eshghi, E., et al., *BAFopathies' DNA methylation epi-signatures demonstrate diagnostic utility and functional continuum of Coffin-Siris and Nicolaides-Baraitser syndromes.* 2018. **9**(1): p. 4885.
2. Kosho, T. and N. Okamoto, *Genotype-phenotype correlation of Coffin-Siris syndrome caused by mutations in SMARCB1, SMARCA4, SMARCE1, and ARID1A.* Am J Med Genet C Semin Med Genet, 2014. **166c**(3): p. 262-75.
3. Kosho, T., et al., *Clinical correlations of mutations affecting six components of the SWI/SNF complex: detailed description of 21 patients and a review of the literature.* Am J Med Genet A, 2013. **161a**(6): p. 1221-37.
4. Tsurusaki, Y., et al., *Mutations affecting components of the SWI/SNF complex cause Coffin-Siris syndrome.* Nat Genet, 2012. **44**(4): p. 376-8.
5. Wieczorek, D., et al., *A comprehensive molecular study on Coffin-Siris and Nicolaides-Baraitser syndromes identifies a broad molecular and clinical spectrum converging on altered chromatin remodeling.* Hum Mol Genet, 2013. **22**(25): p. 5121-35.
6. Elefteriou, F. and X. Yang, *Genetic mouse models for bone studies--strengths and limitations.* Bone, 2011. **49**(6): p. 1242-54.
7. Anbunathan, H., et al., *Integrative Copy Number Analysis of Uveal Melanoma Reveals Novel Candidate Genes Involved in Tumorigenesis Including a Tumor Suppressor Role for PHF10/BAF45a.* 2019. **25**(16): p. 5156-5166.
8. Peddibhotla, S., et al., *Delineation of candidate genes responsible for structural brain abnormalities in patients with terminal deletions of chromosome 6q27.* Eur J Hum Genet, 2015. **23**(1): p. 54-60.
9. Mashtalir, N., et al., *Modular Organization and Assembly of SWI/SNF Family Chromatin Remodeling Complexes.* Cell, 2018. **175**(5): p. 1272-1288.e20.
10. Mills, A.A., *Throwing the cancer switch: reciprocal roles of polycomb and trithorax proteins.* Nat Rev Cancer, 2010. **10**(10): p. 669-82.
11. Yang, Z., et al., *Hijacking a key chromatin modulator creates epigenetic vulnerability for MYC-driven cancer.* J Clin Invest, 2018. **128**(8): p. 3605-3618.
12. FEBS Lett.
13. Ernst, P. and C.R. Vakoc, *WRAD: enabler of the SET1-family of H3K4 methyltransferases.* Brief Funct Genomics, 2012. **11**(3): p. 217-26.
14. Rao, R.C. and Y. Dou, *Hijacked in cancer: the KMT2 (MLL) family of methyltransferases.* Nat Rev Cancer, 2015. **15**(6): p. 334-46.
15. Shilatifard, A., *The COMPASS family of histone H3K4 methylases: mechanisms of regulation in development and disease pathogenesis.* Annu Rev Biochem, 2012. **81**: p. 65-95.
16. Shilatifard, A., *Molecular implementation and physiological roles for histone H3 lysine 4 (H3K4) methylation.* Curr Opin Cell Biol, 2008. **20**(3): p. 341-8.
17. Hnisz, D., et al., *Super-enhancers in the control of cell identity and disease.* Cell, 2013. **155**(4): p. 934-47.
18. Hnisz, D., et al., *Convergence of developmental and oncogenic signaling pathways at transcriptional super-enhancers.* Mol Cell, 2015. **58**(2): p. 362-70.
19. Burke, K.A., et al., *Residue-by-Residue View of In Vitro FUS Granules that Bind the C-Terminal Domain of RNA Polymerase II.* Mol Cell, 2015. **60**(2): p. 231-41.

20. Alberti, S., et al., *A systematic survey identifies prions and illuminates sequence features of prionogenic proteins.* Cell, 2009. **137**(1): p. 146-58.
21. Citterio, C., et al., *Effect of protein kinase A on accumulation of brefeldin A-inhibited guanine nucleotide-exchange protein 1 (BIG1) in HepG2 cell nuclei.* Proc Natl Acad Sci U S A, 2006. **103**(8): p. 2683-8.
22. Padilla, P.I., et al., *Nuclear localization and molecular partners of BIG1, a brefeldin A-inhibited guanine nucleotide-exchange protein for ADP-ribosylation factors.* Proc Natl Acad Sci U S A, 2004. **101**(9): p. 2752-7.
23. Tremblay, V., et al., *Molecular basis for DPY-30 association to COMPASS-like and NURF complexes.* Structure, 2014. **22**(12): p. 1821-1830.

LIST OF REFERENCES

1. Chisolm, D.A. and A.S. Weinmann, *Connections Between Metabolism and Epigenetics in Programming Cellular Differentiation.* Annu Rev Immunol, 2018. **36**: p. 221-246.
2. Yadav, T. and J.P. Quivy, *Chromatin plasticity: A versatile landscape that underlies cell fate and identity.* 2018. **361**(6409): p. 1332-1336.
3. Daigle, S.R., et al., *Selective killing of mixed lineage leukemia cells by a potent small-molecule DOT1L inhibitor.* Cancer Cell, 2011. **20**(1): p. 53-65.
4. Dawson, M.A. and T. Kouzarides, *Cancer epigenetics: from mechanism to therapy.* Cell, 2012. **150**(1): p. 12-27.
5. Dawson, M.A., et al., *Inhibition of BET recruitment to chromatin as an effective treatment for MLL-fusion leukaemia.* Nature, 2011. **478**(7370): p. 529-33.
6. Delmore, J.E., et al., *BET bromodomain inhibition as a therapeutic strategy to target c-Myc.* Cell, 2011. **146**(6): p. 904-17.
7. Filippakopoulos, P., et al., *Selective inhibition of BET bromodomains.* Nature, 2010. **468**(7327): p. 1067-73.
8. Mertz, J.A., et al., *Targeting MYC dependence in cancer by inhibiting BET bromodomains.* Proc Natl Acad Sci U S A, 2011. **108**(40): p. 16669-74.
9. Schenk, T., et al., *Inhibition of the LSD1 (KDM1A) demethylase reactivates the all-trans-retinoic acid differentiation pathway in acute myeloid leukemia.* Nat Med, 2012. **18**(4): p. 605-11.

10. Zuber, J., et al., *RNAi screen identifies Brd4 as a therapeutic target in acute myeloid leukaemia.* Nature, 2011. **478**(7370): p. 524-8.

11. Ho, L. and G.R. Crabtree, *Chromatin remodelling during development.* Nature, 2010. **463**(7280): p. 474-84.

12. Kadoch, C. and G.R. Crabtree, *Mammalian SWI/SNF chromatin remodeling complexes and cancer: Mechanistic insights gained from human genomics.* Sci Adv, 2015. **1**(5): p. e1500447.

13. Kadoch, C., et al., *Dynamics of BAF-Polycomb complex opposition on heterochromatin in normal and oncogenic states.* Nat Genet, 2017. **49**(2): p. 213-222.

14. Wang, G.G., C.D. Allis, and P. Chi, *Chromatin remodeling and cancer, Part II: ATP-dependent chromatin remodeling.* Trends Mol Med, 2007. **13**(9): p. 373-80.

15. Rao, R.C. and Y. Dou, *Hijacked in cancer: the KMT2 (MLL) family of methyltransferases.* Nat Rev Cancer, 2015. **15**(6): p. 334-46.

16. Lovén, J., et al., *Selective inhibition of tumor oncogenes by disruption of super-enhancers.* Cell, 2013. **153**(2): p. 320-34.

17. Clapier, C.R., et al., *Mechanisms of action and regulation of ATP-dependent chromatin-remodelling complexes.* Nat Rev Mol Cell Biol, 2017. **18**(7): p. 407-422.

18. Bauer, D.E., et al., *An erythroid enhancer of BCL11A subject to genetic variation determines fetal hemoglobin level.* Science, 2013. **342**(6155): p. 253-7.

19. Choi, J., et al., *The SWI/SNF chromatin remodeling complex regulates germinal center formation by repressing Blimp-1 expression.* Proc Natl Acad Sci U S A, 2015. **112**(7): p. E718-27.

20. Narayanan, R. and T.C. Tuoc, *Roles of chromatin remodeling BAF complex in neural differentiation and reprogramming.* Cell Tissue Res, 2014. **356**(3): p. 575-84.

21. Sokpor, G., et al., *Chromatin Remodeling BAF (SWI/SNF) Complexes in Neural Development and Disorders.* Front Mol Neurosci, 2017. **10**: p. 243.

22. Godfrey, T.C., et al., *Epigenetic remodeling and modification to preserve skeletogenesis in vivo.* Connect Tissue Res, 2018. **59**(sup1): p. 52-54.

23. Nguyen, K.H., et al., *SWI/SNF-Mediated Lineage Determination in Mesenchymal Stem Cells Confers Resistance to Osteoporosis.* Stem Cells, 2015. **33**(10): p. 3028-38.

24. Pico, M.J., et al., *Glucocorticoid receptor-mediated cis-repression of osteogenic genes requires BRM-SWI/SNF.* Bone Rep, 2016. **5**: p. 222-227.

25. Sepulveda, H., A. Villagra, and M. Montecino, *Tet-Mediated DNA Demethylation Is Required for SWI/SNF-Dependent Chromatin Remodeling and Histone-Modifying Activities That Trigger Expression of the Sp7 Osteoblast Master Gene during Mesenchymal Lineage Commitment.* Mol Cell Biol, 2017. **37**(20).

26. Seth-Vollenweider, T., et al., *Novel mechanism of negative regulation of 1,25-dihydroxyvitamin D3-induced 25-hydroxyvitamin D3 24-hydroxylase (Cyp24a1) Transcription: epigenetic modification involving cross-talk between protein-*

arginine methyltransferase 5 and the SWI/SNF complex. J Biol Chem, 2014. **289**(49): p. 33958-70.

27. Jiang, H., et al., *Role for Dpy-30 in ES cell-fate specification by regulation of H3K4 methylation within bivalent domains.* Cell, 2011. **144**(4): p. 513-25.
28. Shilatifard, A., *The COMPASS family of histone H3K4 methylases: mechanisms of regulation in development and disease pathogenesis.* Annu Rev Biochem, 2012. **81**: p. 65-95.
29. Shilatifard, A., *Molecular implementation and physiological roles for histone H3 lysine 4 (H3K4) methylation.* Curr Opin Cell Biol, 2008. **20**(3): p. 341-8.
30. Ari, G., S. Cherukuri, and A. Namasivayam, *Epigenetics and Periodontitis: A Contemporary Review.* J Clin Diagn Res, 2016. **10**(11): p. Ze07-ze09.
31. Tremblay, V., et al., *Molecular basis for DPY-30 association to COMPASS-like and NURF complexes.* Structure, 2014. **22**(12): p. 1821-1830.
32. Citterio, C., et al., *Effect of protein kinase A on accumulation of brefeldin A-inhibited guanine nucleotide-exchange protein 1 (BIG1) in HepG2 cell nuclei.* Proc Natl Acad Sci U S A, 2006. **103**(8): p. 2683-8.
33. Padilla, P.I., et al., *Nuclear localization and molecular partners of BIG1, a brefeldin A-inhibited guanine nucleotide-exchange protein for ADP-ribosylation factors.* Proc Natl Acad Sci U S A, 2004. **101**(9): p. 2752-7.
34. Lowery, J., et al., *The Sec7 guanine nucleotide exchange factor GBF1 regulates membrane recruitment of BIG1 and BIG2 guanine nucleotide exchange factors to the trans-Golgi network (TGN).* J Biol Chem, 2013. **288**(16): p. 11532-45.

35. Xia, B., et al., *Modulation of cell adhesion and migration by the histone methyltransferase subunit mDpy-30 and its interacting proteins.* PLoS One, 2010. **5**(7): p. e11771.

36. Mazaki, Y., Y. Nishimura, and H. Sabe, *GBF1 bears a novel phosphatidylinositol-phosphate binding module, BP3K, to link PI3Kγ activity with Arf1 activation involved in GPCR-mediated neutrophil chemotaxis and superoxide production.* Mol Biol Cell, 2012. **23**(13): p. 2457-67.

37. Niu, T.K., et al., *Dynamics of GBF1, a Brefeldin A-sensitive Arf1 exchange factor at the Golgi.* Mol Biol Cell, 2005. **16**(3): p. 1213-22.

38. Peyroche, A., et al., *The ARF exchange factors Gea1p and Gea2p regulate Golgi structure and function in yeast.* J Cell Sci, 2001. **114**(Pt 12): p. 2241-53.

39. Szul, T., et al., *Dissecting the role of the ARF guanine nucleotide exchange factor GBF1 in Golgi biogenesis and protein trafficking.* J Cell Sci, 2007. **120**(Pt 22): p. 3929-40.

40. Spang, A., *Retrograde traffic from the Golgi to the endoplasmic reticulum.* Cold Spring Harb Perspect Biol, 2013. **5**(6).

41. Szul, T., et al., *The Garz Sec7 domain guanine nucleotide exchange factor for Arf regulates salivary gland development in Drosophila.* Cell Logist, 2011. **1**(2): p. 69-76.

42. Szul, T. and E. Sztul, *COPII and COPI traffic at the ER-Golgi interface.* Physiology (Bethesda), 2011. **26**(5): p. 348-64.

43. Wright, J., R.A. Kahn, and E. Sztul, *Regulating the large Sec7 ARF guanine nucleotide exchange factors: the when, where and how of activation.* Cell Mol Life Sci, 2014. **71**(18): p. 3419-38.

44. Donaldson, J.G. and C.L. Jackson, *ARF family G proteins and their regulators: roles in membrane transport, development and disease.* Nat Rev Mol Cell Biol, 2011. **12**(6): p. 362-75.

45. Chun, J., et al., *Characterization of class I and II ADP-ribosylation factors (Arfs) in live cells: GDP-bound class II Arfs associate with the ER-Golgi intermediate compartment independently of GBF1.* Mol Biol Cell, 2008. **19**(8): p. 3488-500.

46. Vigil, D., et al., *Ras superfamily GEFs and GAPs: validated and tractable targets for cancer therapy?* Nat Rev Cancer, 2010. **10**(12): p. 842-57.

47. Rainero, E., et al., *Ligand-Occupied Integrin Internalization Links Nutrient Signaling to Invasive Migration.* Cell Rep, 2015. **10**(3): p. 398-413.

48. Béraud-Dufour, S., et al., *A glutamic finger in the guanine nucleotide exchange factor ARNO displaces Mg2+ and the beta-phosphate to destabilize GDP on ARF1.* Embo j, 1998. **17**(13): p. 3651-9.

49. Renault, L., B. Guibert, and J. Cherfils, *Structural snapshots of the mechanism and inhibition of a guanine nucleotide exchange factor.* Nature, 2003. **426**(6966): p. 525-30.

50. Robineau, S., M. Chabre, and B. Antonny, *Binding site of brefeldin A at the interface between the small G protein ADP-ribosylation factor 1 (ARF1) and the nucleotide-exchange factor Sec7 domain.* Proc Natl Acad Sci U S A, 2000. **97**(18): p. 9913-8.

51. Bhatt, J.M., et al., *Oligomerization of the Sec7 domain Arf guanine nucleotide exchange factor GBF1 is dispensable for Golgi localization and function but regulates degradation.* Am J Physiol Cell Physiol, 2016. **310**(6): p. C456-69.

52. Miyamoto, T., et al., *AMP-activated protein kinase phosphorylates Golgi-specific brefeldin A resistance factor 1 at Thr1337 to induce disassembly of Golgi apparatus.* J Biol Chem, 2008. **283**(7): p. 4430-8.

53. Morohashi, Y., et al., *Phosphorylation and membrane dissociation of the ARF exchange factor GBF1 in mitosis.* Biochem J, 2010. **427**(3): p. 401-12.

54. Jang, S.Y., S.W. Jang, and J. Ko, *Regulation of ADP-ribosylation factor 4 expression by small leucine zipper protein and involvement in breast cancer cell migration.* Cancer Lett, 2012. **314**(2): p. 185-97.

55. Rahmatpanah, F.B., et al., *Differential DNA methylation patterns of small B-cell lymphoma subclasses with different clinical behavior.* Leukemia, 2006. **20**(10): p. 1855-62.

56. Keller, S. and M.H.H. Schmidt, *EGFR and EGFRvIII Promote Angiogenesis and Cell Invasion in Glioblastoma: Combination Therapies for an Effective Treatment.* Int J Mol Sci, 2017. **18**(6).

57. Cuddapah, V.A., et al., *A neurocentric perspective on glioma invasion.* Nat Rev Neurosci, 2014. **15**(7): p. 455-65.

58. Wang, J., et al., *Activation of Rab8 guanine nucleotide exchange factor Rabin8 by ERK1/2 in response to EGF signaling.* Proc Natl Acad Sci U S A, 2015. **112**(1): p. 148-53.

59. Mao, L., et al., *AMPK phosphorylates GBF1 for mitotic Golgi disassembly.* J Cell Sci, 2013. **126**(Pt 6): p. 1498-505.

60. Kim, S.W., et al., *ADP-ribosylation factor 4 small GTPase mediates epidermal growth factor receptor-dependent phospholipase D2 activation.* J Biol Chem, 2003. **278**(4): p. 2661-8.

61. Boulay, P.L., et al., *ADP-ribosylation factor 1 controls the activation of the phosphatidylinositol 3-kinase pathway to regulate epidermal growth factor-dependent growth and migration of breast cancer cells.* J Biol Chem, 2008. **283**(52): p. 36425-34.

62. Walton, K. and A. Leier, *Regulating the regulators: role of phosphorylation in modulating the function of the GBF1/BIG family of Sec7 ARF-GEFs.* 2020.

63. Busby, T., et al., *The Arf activator GBF1 localizes to plasma membrane sites involved in cell adhesion and motility.* Cell Logist, 2017. **7**(2): p. e1308900.

64. Meissner, J.M., et al., *The ARF guanine nucleotide exchange factor GBF1 is targeted to Golgi membranes through a PIP-binding domain.* J Cell Sci, 2018. **131**(3).

65. Belov, G.A., et al., *Poliovirus replication requires the N-terminus but not the catalytic Sec7 domain of ArfGEF GBF1.* Cell Microbiol, 2010. **12**(10): p. 1463-79.

66. Humphrey, S.J., et al., *Dynamic adipocyte phosphoproteome reveals that Akt directly regulates mTORC2.* Cell Metab, 2013. **17**(6): p. 1009-20.

67. Sharma, K., et al., *Ultradeep human phosphoproteome reveals a distinct regulatory nature of Tyr and Ser/Thr-based signaling.* Cell Rep, 2014. **8**(5): p. 1583-94.

68. Yi, T., et al., *Quantitative phosphoproteomic analysis reveals system-wide signaling pathways downstream of SDF-1/CXCR4 in breast cancer stem cells.* Proc Natl Acad Sci U S A, 2014. **111**(21): p. E2182-90.

69. Barna, M., et al., *Suppression of Myc oncogenic activity by ribosomal protein haploinsufficiency.* Nature, 2008. **456**(7224): p. 971-5.

70. Gandin, V., et al., *Eukaryotic initiation factor 6 is rate-limiting in translation, growth and transformation.* Nature, 2008. **455**(7213): p. 684-8.

71. Luo, J., N.L. Solimini, and S.J. Elledge, *Principles of cancer therapy: oncogene and non-oncogene addiction.* Cell, 2009. **136**(5): p. 823-37.

72. Miluzio, A., et al., *Impairment of cytoplasmic eIF6 activity restricts lymphomagenesis and tumor progression without affecting normal growth.* Cancer Cell, 2011. **19**(6): p. 765-75.

73. Truitt, M.L., et al., *Differential Requirements for eIF4E Dose in Normal Development and Cancer.* Cell, 2015. **162**(1): p. 59-71.

74. Kouzarides, T., *Chromatin modifications and their function.* Cell, 2007. **128**(4): p. 693-705.

75. Martin, C. and Y. Zhang, *The diverse functions of histone lysine methylation.* Nat Rev Mol Cell Biol, 2005. **6**(11): p. 838-49.

76. Dou, Y., et al., *Regulation of MLL1 H3K4 methyltransferase activity by its core components.* Nat Struct Mol Biol, 2006. **13**(8): p. 713-9.

77. Ernst, P. and C.R. Vakoc, *WRAD: enabler of the SET1-family of H3K4 methyltransferases.* Brief Funct Genomics, 2012. **11**(3): p. 217-26.

78. Je, E.M., et al., *Mutational and expressional analysis of MLL genes in gastric and colorectal cancers with microsatellite instability.* Neoplasma, 2013. **60**(2): p. 188-95.

79. Kim, J.H., et al., *UTX and MLL4 coordinately regulate transcriptional programs for cell proliferation and invasiveness in breast cancer cells.* Cancer Res, 2014. **74**(6): p. 1705-17.

80. Kim, J.Y., et al., *A role for WDR5 in integrating threonine 11 phosphorylation to lysine 4 methylation on histone H3 during androgen signaling and in prostate cancer.* Mol Cell, 2014. **54**(4): p. 613-25.

81. Lin, D.C., et al., *Genomic and molecular characterization of esophageal squamous cell carcinoma.* 2014. **46**(5): p. 467-73.

82. Lüscher-Firzlaff, J., et al., *The human trithorax protein hASH2 functions as an oncoprotein.* Cancer Res, 2008. **68**(3): p. 749-58.

83. Okosun, J., et al., *Integrated genomic analysis identifies recurrent mutations and evolution patterns driving the initiation and progression of follicular lymphoma.* Nat Genet, 2014. **46**(2): p. 176-181.

84. Parsons, D.W., et al., *The genetic landscape of the childhood cancer medulloblastoma.* Science, 2011. **331**(6016): p. 435-9.

85. Rabello Ddo, A., et al., *Altered expression of MLL methyltransferase family genes in breast cancer.* Int J Oncol, 2013. **43**(2): p. 653-60.

86. Song, Y., et al., *Identification of genomic alterations in oesophageal squamous cell cancer.* Nature, 2014. **509**(7498): p. 91-5.

87. Watanabe, Y., et al., *Frequent alteration of MLL3 frameshift mutations in microsatellite deficient colorectal cancer.* PLoS One, 2011. **6**(8): p. e23320.

88. Ziemin-van der Poel, S., et al., *Identification of a gene, MLL, that spans the breakpoint in 11q23 translocations associated with human leukemias.* Proc Natl Acad Sci U S A, 1991. **88**(23): p. 10735-9.

89. Gu, Y., et al., *The t(4;11) chromosome translocation of human acute leukemias fuses the ALL-1 gene, related to Drosophila trithorax, to the AF-4 gene.* Cell, 1992. **71**(4): p. 701-8.

90. Tkachuk, D.C., S. Kohler, and M.L. Cleary, *Involvement of a homolog of Drosophila trithorax by 11q23 chromosomal translocations in acute leukemias.* Cell, 1992. **71**(4): p. 691-700.

91. Simboeck, E., et al., *DPY30 regulates pathways in cellular senescence through ID protein expression.* Embo j, 2013. **32**(16): p. 2217-30.

92. Yang, Z., et al., *The DPY30 subunit in SET1/MLL complexes regulates the proliferation and differentiation of hematopoietic progenitor cells.* Blood, 2014. **124**(13): p. 2025-33.

93. Yang, Z. and K. Shah, *Dpy30 is critical for maintaining the identity and function of adult hematopoietic stem cells.* 2016. **213**(11): p. 2349-2364.

94. FEBS Lett.

95. Cao, F., et al., *An Ash2L/RbBP5 heterodimer stimulates the MLL1 methyltransferase activity through coordinated substrate interactions with the MLL1 SET domain.* PLoS One, 2010. **5**(11): p. e14102.

96. Chen, Y., et al., *Structure of the SPRY domain of human Ash2L and its interactions with RbBP5 and DPY30.* Cell Res, 2012. **22**(3): p. 598-602.

97. South, P.F., et al., *A conserved interaction between the SDI domain of Bre2 and the Dpy-30 domain of Sdc1 is required for histone methylation and gene expression.* J Biol Chem, 2010. **285**(1): p. 595-607.

98. Zhang, H., et al., *Structural implications of Dpy30 oligomerization for MLL/SET1 COMPASS H3K4 trimethylation.* Protein Cell, 2015. **6**(2): p. 147-51.

99. Sarvan, S., et al., *Crystal structure of the trithorax group protein ASH2L reveals a forkhead-like DNA binding domain.* Nat Struct Mol Biol, 2011. **18**(7): p. 857-9.

100. Jiang, H., et al., *Regulation of transcription by the MLL2 complex and MLL complex-associated AKAP95.* Nat Struct Mol Biol, 2013. **20**(10): p. 1156-63.

101. Thiel, A.T., et al., *MLL-AF9-induced leukemogenesis requires coexpression of the wild-type Mll allele.* Cancer Cell, 2010. **17**(2): p. 148-59.

102. Ullius, A., et al., *The interaction of MYC with the trithorax protein ASH2L promotes gene transcription by regulating H3K27 modification.* Nucleic Acids Res, 2014. **42**(11): p. 6901-20.

103. Mungamuri, S.K., S. Wang, and J.J. Manfredi, *Ash2L enables P53-dependent apoptosis by favoring stable transcription pre-initiation complex formation on its pro-apoptotic target promoters.* 2015. **34**(19): p. 2461-70.

104. Yang, Z., et al., *Physical Interactions and Functional Coordination between the Core Subunits of Set1/Mll Complexes and the Reprogramming Factors.* PLoS One, 2015. **10**(12): p. e0145336.

105. van Nuland, R., et al., *Quantitative dissection and stoichiometry determination of the human SET1/MLL histone methyltransferase complexes.* Mol Cell Biol, 2013. **33**(10): p. 2067-77.

106. Yang, Z., et al., *Hijacking a key chromatin modulator creates epigenetic vulnerability for MYC-driven cancer.* J Clin Invest, 2018. **128**(8): p. 3605-3618.

107. Takahashi, Y.H., et al., *Structural analysis of the core COMPASS family of histone H3K4 methylases from yeast to human.* Proc Natl Acad Sci U S A, 2011. **108**(51): p. 20526-31.

108. Calo, E. and J. Wysocka, *Modification of enhancer chromatin: what, how, and why?* Mol Cell, 2013. **49**(5): p. 825-37.

109. Heintzman, N.D., et al., *Distinct and predictive chromatin signatures of transcriptional promoters and enhancers in the human genome.* Nat Genet, 2007. **39**(3): p. 311-8.

110. Pekowska, A., et al., *H3K4 tri-methylation provides an epigenetic signature of active enhancers.* Embo j, 2011. **30**(20): p. 4198-210.

111. Chapuy, B., et al., *Discovery and characterization of super-enhancer-associated dependencies in diffuse large B cell lymphoma.* Cancer Cell, 2013. **24**(6): p. 777-90.

112. Chipumuro, E., et al., *CDK7 inhibition suppresses super-enhancer-linked oncogenic transcription in MYCN-driven cancer.* Cell, 2014. **159**(5): p. 1126-1139.

113. Hnisz, D., et al., *Super-enhancers in the control of cell identity and disease.* Cell, 2013. **155**(4): p. 934-47.

114. Hnisz, D., et al., *Convergence of developmental and oncogenic signaling pathways at transcriptional super-enhancers.* Mol Cell, 2015. **58**(2): p. 362-70.

115. Whyte, W.A., et al., *Master transcription factors and mediator establish super-enhancers at key cell identity genes.* Cell, 2013. **153**(2): p. 307-19.

116. Alfert, A., N. Moreno, and K. Kerl, *The BAF complex in development and disease.* Epigenetics Chromatin, 2019. **12**(1): p. 19.

117. Aoyagi, S. and J.J. Hayes, *hSWI/SNF-catalyzed nucleosome sliding does not occur solely via a twist-diffusion mechanism.* Mol Cell Biol, 2002. **22**(21): p. 7484-90.

118. Mellor, J., *The dynamics of chromatin remodeling at promoters.* Mol Cell, 2005. **19**(2): p. 147-57.

119. Lequieu, J., D.C. Schwartz, and J.J. de Pablo, *In silico evidence for sequence-dependent nucleosome sliding.* Proc Natl Acad Sci U S A, 2017. **114**(44): p. E9197-e9205.

120. Mashtalir, N., et al., *Modular Organization and Assembly of SWI/SNF Family Chromatin Remodeling Complexes.* Cell, 2018. **175**(5): p. 1272-1288.e20.

121. Krasteva, V., G.R. Crabtree, and J.A. Lessard, *The BAF45a/PHF10 subunit of SWI/SNF-like chromatin remodeling complexes is essential for hematopoietic stem cell maintenance.* Exp Hematol, 2017. **48**: p. 58-71.e15.

122. Allen, M.D., et al., *The SWI/SNF Subunit INI1 Contains an N-Terminal Winged Helix DNA Binding Domain that Is a Target for Mutations in Schwannomatosis.* Structure, 2015. **23**(7): p. 1344-9.

123. Lessard, J., et al., *An essential switch in subunit composition of a chromatin remodeling complex during neural development.* Neuron, 2007. **55**(2): p. 201-15.

124. Wu, J.I., et al., *Regulation of dendritic development by neuron-specific chromatin remodeling complexes.* Neuron, 2007. **56**(1): p. 94-108.

125. Yoo, A.S. and G.R. Crabtree, *ATP-dependent chromatin remodeling in neural development.* Curr Opin Neurobiol, 2009. **19**(2): p. 120-6.

126. Shidlovskii, Y.V., et al., *A novel multidomain transcription coactivator SAYP can also repress transcription in heterochromatin.* Embo j, 2005. **24**(1): p. 97-107.

127. Brechalov, A.V., S.G. Georgieva, and N.V. Soshnikova, *Mammalian cells contain two functionally distinct PBAF complexes incorporating different isoforms of PHF10 signature subunit.* Cell Cycle, 2014. **13**(12): p. 1970-9.

128. Tatarskiy, V.V., et al., *Stability of the PHF10 subunit of PBAF signature module is regulated by phosphorylation: role of β-TrCP.* Sci Rep, 2017. **7**(1): p. 5645.

129. Panov, V.V., et al., *Transcription co-activator SAYP mediates the action of STAT activator.* Nucleic Acids Res, 2012. **40**(6): p. 2445-53.

130. Vorobyeva, N.E., et al., *SAYP and Brahma are important for 'repressive' and 'transient' Pol II pausing.* Nucleic Acids Res, 2012. **40**(15): p. 7319-31.

131. Wei, M., et al., *A novel plant homeodomain finger 10-mediated antiapoptotic mechanism involving repression of caspase-3 in gastric cancer cells.* Mol Cancer Ther, 2010. **9**(6): p. 1764-74.

132. Godfrey, T.C., et al., *The microRNA-23a cluster regulates the developmental HoxA cluster function during osteoblast differentiation.* 2018. **293**(45): p. 17646-17660.

133. Li, C., et al., *MicroRNA-409-3p regulates cell proliferation and apoptosis by targeting PHF10 in gastric cancer.* Cancer Lett, 2012. **320**(2): p. 189-97.

134. Anbunathan, H., et al., *Integrative Copy Number Analysis of Uveal Melanoma Reveals Novel Candidate Genes Involved in Tumorigenesis Including a Tumor Suppressor Role for PHF10/BAF45a.* 2019. **25**(16): p. 5156-5166.

135. Bradfield, J.P., et al., *A genome-wide meta-analysis of six type 1 diabetes cohorts identifies multiple associated loci.* PLoS Genet, 2011. **7**(9): p. e1002293.

136. Conti, V., et al., *Periventricular heterotopia in 6q terminal deletion syndrome: role of the C6orf70 gene.* Brain, 2013. **136**(Pt 11): p. 3378-94.

137. Mehrotra, S., et al., *Genetic and functional evaluation of the role of DLL1 in susceptibility to visceral leishmaniasis in India.* Infect Genet Evol, 2012. **12**(6): p. 1195-201.

138. Peddibhotla, S., et al., *Delineation of candidate genes responsible for structural brain abnormalities in patients with terminal deletions of chromosome 6q27.* Eur J Hum Genet, 2015. **23**(1): p. 54-60.

Appendix

INSTITUTIONAL ANIMAL CARE AND USE COMMITTEE APPROVAL

Contact Detail Close

Date 12-Nov-2019

From UAB, Office of IACUC

To Hassan, Quamarul

CC Wildman, Benjamin

BCC

Contact Type Email

Subject IACUC Approval for Modification of Animal Protocol Number (APN): IACUC-21319

Message DO NOT Reply or Reply All to this email!

Protocol PI: Quamarul Hassan
Title: An Epigenetic Axis in Bone Formation
Sponsor: National Institute of Arthritis & Musculoskeletal & Skin Diseases/NIH/DHHS
Animal Project Number (APN): IACUC-21319

On 11/12/2019, the UAB Institutional Animal Care and Use Committee (IACUC) approved the proposed modification: Personnel: Theodore Busby. The sponsor for this project may require notification of modification(s) approved by the IACUC, but not included in the original grant proposal/experimental plan; please inform the sponsor if necessary.
Approval from the IACUC must be obtained before implementing any changes or modifications in the approved animal use. Refer to APN IACUC-21319 when ordering animals or in any correspondence with the IACUC or Animal Resources Program (ARP) offices regarding this study. If you have concerns or questions regarding this notice, please call the IACUC office at (205) 934-7692.

IACUC Office
University of Alabama at Birmingham
CH19 Suite 403
933 19th Street South
Birmingham, Alabama 35294-2041
Voice: 205-934-7692
FAX: 205-934-1188
www.uab.edu/iacuc

Posted by Tolliver, Lynn

Attachments Modification Approval Notice